KWAME NKRUMAH UNIVERSITY OF SCIENCE AND TECHNOLOGY, KUMASI

Long -Term Vegetation Dynamics over the Bani River Basin as Impacted by Climate Change and Land Use

by

Souleymane Sidi TRAORE

(BSc. Geography, MSc. Natural Resources Management)

A Thesis submitted to the Department of Civil Engineering

College of Engineering

in partial fulfilment of the requirement for the degree of

DOCTOR OF PHILOSOPHY

in

Climate Change and Land Use

April, 2015

CERTIFICATION

I hereby declare that this submission is my own work towards the PhD and that, to the best of my knowledge, it contains no material previously published by another person, nor material which has been accepted for the award of any other degree of the University, except where due acknowledgment has been made in text.

Souleymane Sidi TRAORE — April 29, 2015

(PG6687611) Signature Date

Certified by: April 29, 2015

Prof. Eric Kwabena FORKUO

(Principal Supervisor) Signature Date

Certified by: April 29, 2015

Dr. Tobias LANDMANN

(Co- Supervisor) Signature Date

Certified by:

Prof. Yaw Adubofour TUFFOUR

(Head of Department) Signature Date

ABSTRACT

This study investigated the long-term trends in vegetation and rainfall and the extent and rate of vegetation change over the Bani river Basin at multiple spatial and temporal scales in relation to local and regional drivers. Monthly 8-km Normalized Difference Vegetation Index (NDVI) time-series data from 1982 to 2011 was derived from 10-day Satellite Pour l'Observation de la Terre vegetation product (SPOT-VGT) at 1-km (1998-2011) and 15-day GIMMS (Global Inventories Monitoring and Modelling Systems) at 8-km satellite data (1982-2006). Gridded rainfall data at 8-km grid resolution was created from 40 meteorological stations and complemented with Tropical Rainfall Measurement Mission (TRMM) data. A Mann Kendall (MK) trend analysis was used to determine the trend for each dataset using monthly and annual time-series. This analysis produced some indicators like Kendall's tau, p-value and Theil-Sen. The p-value estimator (p-value less than 0.07) was used in this study to show the significance of the trend. Trend analysis revealed that within the study area vegetation greening trends are mostly associated with areas where natural vegetation is still well represented. From the results 934 pixels (49% of the study area) showed a positive trend while 155 pixels (8% of the study area) showed a negative trend significant at p-value less than 0.07. During the same period rainfall had increased by about 17 mm, translating into a positive trend for almost the entire study area. Vegetation productivity in the study area is dependent on rainfall which varies greatly temporally and spatially. The linear Pearson correlation was used to estimate the relationship between NDVI and rainfall for every pixel at monthly interval for the growing season data. Comparing their long-term mean the result showed a good correlation between the two datasets with an R value of 0.98. Four (4) reference areas were used to explain and cross verify representative areas that exhibit either entirely negative MK-trends or entirely positive MK-trends over the monitoring period. These reference areas were selected based on their trend in rainfall and NDVI and their NDVI long-term departure. Free 30-meter Landsat images were acquired for the four reference areas for the following three intervals: 1984 and 1986, 1999 and 2000 and 2009 and 2010. Land Use/Land Cover (LULC) change was then quantified and the rate of land conversion was determined. LULC variables included urban, Cropland and natural vegetation (Shrublands, Steppe, Open Trees and Closed Trees). For the entire period, the class 'Natural Vegetation' decreased between 22.83% and 63.47% from its initial area for areas (1) and (2), while the

decrease was 8.35% for area (3) and 13.39% for area (4). The class ‘Cropland’ increased for 564.86% in area (3); 62.17% in area (4); 35.79% in area (2) and 16.22% in area (1). To investigate whether there is a relationship between NDVI, rainfall and LULC change, LULC variables were correlated with long-term trend in rainfall and NDVI. The results showed there is a positive correlation between increases in rainfall and some land cover classes, while some classes such as settlements were negatively correlated with vegetation productivity trends. Croplands and Natural Vegetation were positively correlated (r=0.89) with rainfall while settlements have a negative correlation with NDVI time series trends (r=-0.57). Despite the fact that rainfall is the major determinant of vegetation cover dynamics in the study area, it appears that other human-induced factors such as urbanisation have negatively influenced the change in vegetation cover. The results provide spatially explicit and temporally good and rich information of vegetation productivity dynamics and its drivers at landscape scale. This is an important input for assessing the impact of climate change on vegetation for biophysical modelling. It also improves our knowledge of the drivers of vegetation productivity changes. The study suggests that NDVI can be useful for general vegetation cover monitoring and planning. Future studies need to also look at the effect of vegetation cover change in regard to other landscape components such as specifically population density and soil degradation.

TABLE OF CONTENTS

LIST OF TABLES

LIST OF FIGURES

LIST OF ABBREVIATIONS AND ACRONYMS

AVHRR:	Advanced Very High Resolution Radiometer
CAMS:	Climate Assessment and Monitoring System
CILSS:	Permanent Interstate Committee for drought control in the Sahel (in French: Comité permanent Inter-Etat de Lutte contre la Sécheresse dans le Sahel)
CO_2:	Carbone dioxide
CoV:	Coefficient of Variation
EEA:	European Environmental Agency
ENSO:	El-Niño Southern Oscillation
ESA:	European Space Agency
ETM+:	Enhanced Thematic Mapper Plus
FAO:	Food and Agricultural Organisation
GCPs:	Ground Control Points
GEM:	Global Environment Monitoring
GIMMS:	Global Inventory Monitoring and Modelling Systems
GLC2000:	Global Land Cover of 2000
GOFC-GOLD:	Global Observation of Forest and Land Cover Dynamics
GPCC:	Global Precipitation Climatological Centre
HDF:	Hierarchical Data Format
IDW:	Inverse Distance Waiting
IGBP:	International Geosphere-Biosphere Programme
IPCC:	Intergovernmental Panel on Climate Change
ITCZ:	Inter Tropical Convergence Zone

JRC: Joint Research Centre

LCCS: Land Cover Classification System

LEO: Low-Earth Orbiting

LULC: Land Use / Land Cover

MCV: Maximum Value Compositing

MERIS / FR: Medium Resolution Imaging Spectrometer / Fine Resolution

MK: Mann Kendall

MODIS: Moderate Resolution Imaging Spectroradiometer

MSS: Multi Spectral Scanner

NDVI: Normalized Difference Vegetation Index

NOAA: National Oceanic and Atmospheric Administration

OLS: Ordinary Least Squares

PIRL/PIRT: Project Inventories of Ligneous / Terrestrial Resources

RF: Rainfall

RMS: Root Mean Square

ROI: Region of Interest

SPOT – VGT: Satellite Pour l'Observation de la Terre – Vegetation product

STD: Standard Deviation

TM: Thematic Mapper

TRMM/PR/TMI: Tropical Rainfall Measurement Mission /Precipitation Radar/ TRMM Microwave Imager

UMD: University of Maryland

UN: United Nations

UNEP:	United Nation Environment Programme
US	United States of America
VIRS:	Visible and Infrared Scanner
WA:	West Africa
WAM:	West African Monsoon
WMO:	World Meteorological Organisation

DEDICATION

To my parents, Sidi and Adidiatou,

Wife Fatoumata,

Children Mariam and Sidi junior…

ACKNOWLEDGEMENTS

My sincerest gratitude goes to the Almighty God for his Love, Grace and Mercies bestowed upon me throughout my entire life and education career.

The financial support provided by the German Ministry of Education (BMBF) for this research is gratefully acknowledged. This scholarship was granted through the WASCAL PhD Programme on Climate Change and Adapted Land Use, through the Graduate Research Programme on Climate Change and Land Use (GRP CCLU). I value this immense contribution and express my gratitude to all involved for that.

Writing a thesis in a foreign language is a particular challenge and requires correction and advice from several people especially my supervisor Dr Eric K. FORKUO. He devoted a significant portion of his time for reading my work. I offer to him my sincerest gratitude for his support and his generous guidance throughout this thesis.

I feel great pleasure and honour to express my sincere thanks to Dr Tobias LANDMANN, the co-supervisor of this thesis, for his continuous technical and scientific guidance, patience, motivation and enthusiasm. He guided me in all facets of my research from the proposal to the final write-up.

I am very grateful to my mentor, Mr P.C. Sibiry TRAORE who gave me great amount of advice, help and support throughout the whole thesis. I extend my gratitude to the head of SotubaGIS Dr Cheick H. DIAKITE and his team for their fruitful encouragement and their support in this research. I also acknowledge encouragement and support from Dr Mamadou K. Ndiaye, Mr Makan Sissoko and many anonymous persons.

My special thanks go to my jury members for their willingness to review and evaluate my thesis. Their critical comments and suggestions helped to improve the standard of this PhD thesis. I address a special mention to Prof Alfred A. Duker for his willingness to review the final version of this thesis.

Finally I would like to extend my gratitude to my colleagues and friends (first Batch Wascal-CCLU), my parents, brothers and sisters, my children and wife. I would not have gone so far without their support and encouragement.

1. INTRODUCTION

1.1. Background

West African (WA) countries are experiencing rapid changes, specifically climate-driven related but also those caused by human-induced activities. These countries are endowed with diverse, yet fragile environment. For centuries, humans have been a trivial force in the environmental equation, but this changed dramatically in the 20th century, particularly in the last 50 years. As West Africans enter the 21st century, environmental changes are predicted to accelerate, with unknown and potentially serious implications for both its people and the environment (Tappan and Cushing, 2004), which includes changes in water bodies and vegetation cover.

According to Salim *et al* (2008), vegetation cover is the most important parameter, used frequently in human environmental assessments and it is also used as a proxy (variable) in geosphere, biosphere and atmosphere interaction models. Moreover, this variable plays an important role in global climate models and assessments. The amount of vegetation controls the partitioning of incoming solar energy and the sensible and latent heat fluxes. This inevitably will affect the amounts of vegetation locally and globally in a long-term. This in turn will again affect the vegetation growth feedback mechanism (Qi *et al.*, 1995). Vegetation has special characteristics due to its distinct annual and seasonal changes; thus its productivity and vitality is often used as a proxy to assess climate and/or human activity effects, within the context of global and local environment change models studies.

Considerable attention has been given to the use of Normalized Difference Vegetation Index (NDVI) to assess the impact of climate change using the National Oceanic and Atmospheric Administration – Advanced Very High Resolution Radiometer (NOAA-AVHRR) NDVI images.

In a series of papers, (e.g. Anyamba and Turker, 2005; Herrmann *et al.,* 2005; Vlek *et al.,* 2008) the authors used and analysed NOAA-AVHRR NDVI using time-series analysis, they concluded that there is as consistent trend of increasing vegetation 'greenness' (chlorophyll activity) in much of the Sahelian region, semi-arid region stretching approximately 5000 km across Northern Africa from the Atlantic Ocean in the West to near the Red Sea in the East and extending roughly from 12˚N to 18˚N (Anyamba and Tucker, 2005). Increasing rainfall in recent years emerges as the dominant causative factor in the dynamics of this vegetation 'greenness' (Ahmedou *et al.*, 2008; Lacaze and Toulouse, 2011). However, other factors such as Land Use / Land Cover (LULC) changes and mass migrations of people, fire regime, atmospheric CO_2 may also contribute. This point is not well explored and needs further elaboration so that the main drivers of vegetation change in this particular area in West Africa can be better explained. This research analyses NDVI time-series over 30-year period and rainfall dynamics (inter-annual and inter-seasonal variability) and hot spots studies with high resolution satellite which could be the appropriate tool to help explain long-term vegetation cover dynamics and trend in West Africa.

1.2. Problem Statement

While many regions of the world are subject to dramatic fluctuations in climate, the West Africa savannah area is characterised by severe and persistent rainfall deficit that is known to have lasted for more than three decades (Ekpoh and Nsa, 2011). The reduction of annual precipitation amounts, from 20 to 40% according to Nicholson *et al.,* (2000) is largely due to a general decline in the number of rainfall events. Within the same period, LULC changes are rapidly causing a decline in natural vegetation. Research results indicated that large tracts of natural savannah, woodland were converted to cultivated lands and specifically, grazing lands. The conversion process also caused a decline in the quantity of the animal fodder. On the other hand, the total

woodland area reduced due to the expansion of farmland (as a result of increasing human population, and an increasing demand for food). Also, extensive wood harvesting to meet the local people needs for charcoal and other domestic uses have contributed to the changes in the forest cover. The sustainable management of the environment poses a challenge as imbalance between natural resources (arable land, water quantity and quality, vegetation, *etc*) and increased needs of a rapidly growing population deepens.

1.3. Aims and Objectives

This study seeks to verify and explain spatial and temporal vegetation pattern in the Bani River Basin by analysing 30 years of remote sensing data. The specific objectives of this study are to:

- Investigate whether change in vegetation is related to NDVI dynamics and change,
- Investigate whether precipitation in the region is related to changes in NDVI over the time,
- Identify the main effects of climatic change in relation to vegetation cover dynamics.

1.4. Limitation

Other than precipitation there are different physical and human phenomena that affect the growth of natural vegetation and crops. Among other things temperature, potential evaporation, type of soil, the level of soil erosion, slope and aspect, and economic activities affect vegetation dynamics. For example available temperature data have been found unsuitable for this study and also because of the limited scope of this thesis all other factors other than precipitation are excluded.

1.5. Organisation of the thesis

This thesis is divided into ten chapters. Chapter 1 provides the overall scope and objectives of the study. In Chapter 2 key background literature pertaining to the characteristics and importance of long-term vegetation dynamics as well as the use of space borne data to monitor vegetation is reviewed. Chapter 3 presents a detailed description of the study area, its specifications and importance in the context of climate change. Chapter 4 focuses on the research methods including a detailed description of the datasets used, pre-processing and processing methods. The results are presented in Chapter 5 to 9. These chapters include comparison of results with previous studies and evaluation of the findings. The conclusion and recommendations are presented in Chapter 10.

2. LONG -TERM VEGETATION DYNAMICS, CLIMATE CHANGE AND LAND USE

2.1. Introduction

This Chapter provides a broad overview of different concepts regarding this research. The long-term environmental is the first to be reviewed. Thereafter the fundamental concept of climate change and its characteristics and the global vegetation characteristics, Land Use / Land Cover (LULC) changes and their drivers are reviewed as well as the use of remote sensing based data for vegetation cover monitoring.

2.2. Long-Term Environmental Monitoring

The change in environment is known as a persistent feature occurring all over the world. From a few millennia ago, dense vegetation, as well big mammals dominated the North Africa region, known to this day as the Sahara Desert (Maley, 1980). Frequently asked questions are: how will the change affect precipitation? Will the desert spread or shrink? How will human life or livelihood be affected by such changes? These questions can only be answered through the use of information obtained over a long period through long-term environmental research (Pickett, 1989; South African Environmental Observatory Network, 2004).

In spite of the importance of long-term monitoring of the natural environment, it is often regarded as a low-grade, adding little to our understanding of the functioning of the environmental systems (Burt, 1994). The objective of long-term ecological monitoring is to examine and document changes in essential assets of biological communities. Monitoring of the vegetation structure and dynamics has to be done in a scientifically accurate way (e.g. use of

remote sensing), while being cost-effective and widely understandable. The methods of environmental monitoring can be limited by the cost, training requirements and poor repeatability. Therefore, it is essential to identify an appropriate group of rapid, repeatable and cost effective methods that reflect various processes and functions (Havtad and Herrick, 2003).

The past has an influence on the present and future course of an ecosystem. Long-term studies document the effects of the past conditions on continuous processes. Therefore the aim of long-term studies is to document the changing environmental influences and conditions before being lost to the historical record (Pickett, 1989; Burt, 1994).

Method used to gather information for the management decisions on seasonal or annual time frame are called short-term monitoring and provide data on vegetation status at specific sites. Methods used to gather information that create a 'trend-record' are called long-term monitoring. Short and long-term monitoring programmes can be integrated in order to achieve management objectives (Havstad and Herrick, 2003). Short-term studies are often misleading and without long-term data there is a lack of interpretation. Thus long-term datasets are fundamental for testing most theoretical constructs of concepts central to environmental studies, but most of these concepts are not usually selected either because they are suited for studies limited in time and space or they are likely to confirm the theoretical construct. There is consequently an unacknowledged excess of unanswered questions in environmental sciences, and hypotheses of which the validity is known. Most scientists are only interested in new and intriguing ideas and not in supporting long-term testing (Broodryk, 2010). The problem is that concepts are accepted and rejected with little experimental foundation. In addition, the need to examine spatial and temporal validity, or the application of a process, structure or mechanism, once recognized, has

barely any support among environmentalist. Most scientists have been working on long-term programmes of abiotic rather than biotic factors. This may be because numerous parameters address social needs (weather and climate) and the greater ease in standardising methods in abiotic research (Franklin, 1989). Just as long-term studies are vital to environmental sciences, they are also important to identify and resolve social issues, such as the sustained productivity of forests, agricultural land and fisheries.

2.3. Climate Change Characteristics

Climate is described in terms of the variability of relevant atmospheric variables such as temperature, precipitation, wind, snowfall, humidity, clouds, including extreme or occasional ones, over a long period in a particular region. The classical period for performing the statistics used to define climate corresponds to at least 3 decades, and it is designated by "climate normal period" (WMO, 2011). As a consequence, the 30-year period proposed by the World Meteorological Organisation (WMO) should be considered more as an indicator than a norm that must be followed in all cases. This definition of the climate as representative of conditions over several decades should, of course, not mask the fact that climate can change rapidly. Climate can thus be viewed as a synthesis or aggregate of weather in a particular area and for a long time (Goosse *et al.*, 2010). This includes the region's general pattern of weather conditions, seasons and weather extremes like hurricanes, droughts, or rainy periods. Two of the most important factors determining an area's climate are air temperature and precipitation (Goosse *et al.*, 2010).

It is also important to take into account the fact that the state of the atmosphere used in the definition of the climate given above is influenced by multiple processes involving also the ocean, the sea ice, the vegetation, etc. Climate is thus defined in a wider sense as the statistical

description of the climate system (Goosse *et al.,* 2010). This includes the analyses of the behaviour of its five major components: the atmosphere; the gaseous envelope surrounding the earth, the hydrosphere; liquid water, i.e. ocean, lakes, underground water, etc., the cryosphere; solid water, i.e. sea ice, glaciers, ice sheets, etc., the land surface and the biosphere (all the living organisms) and of the interactions between them (Solomon *et al.,* 2007).

According to Pidwirny (2006) the factors that affect climate are: the location on the earth, the local land features like mountains, the type and amount of plants like forest or grassland, altitude, latitude and its influence on solar radiation received, the variations in the earth's orbital characteristics, volcanic eruptions, the nearness of large bodies of water, prevailing winds and human activities like the burning fossil fuels, farming or cutting down forest.

The climate of a region will determine what plants will grow there, and what animals will inhabit it. The world's biomass is thus controlled by climate conditions.

2.4. Global Vegetation Characteristics

About three-fourths of the earth's surface is covered by the green biomass (Kulawardhana, 2008). However, huge variety could be observed in their characteristics which are attributed to the changing conditions of climatic as well as geo-morphological characteristics over the earth surface. The different types of vegetation communities that exist on earth could be explained in terms of biomes.

A biome is a large geographical area of distinctive plant and animal groupings, which are adapted to that particular environment. The type of the biome that could exist in a region is determined by the climate and geography of that particular region. Major biomes on earth

include deserts, forests, grasslands, tundra, and several types of aquatic environments. Figure 1 shows the distribution pattern of these biomes on earth.

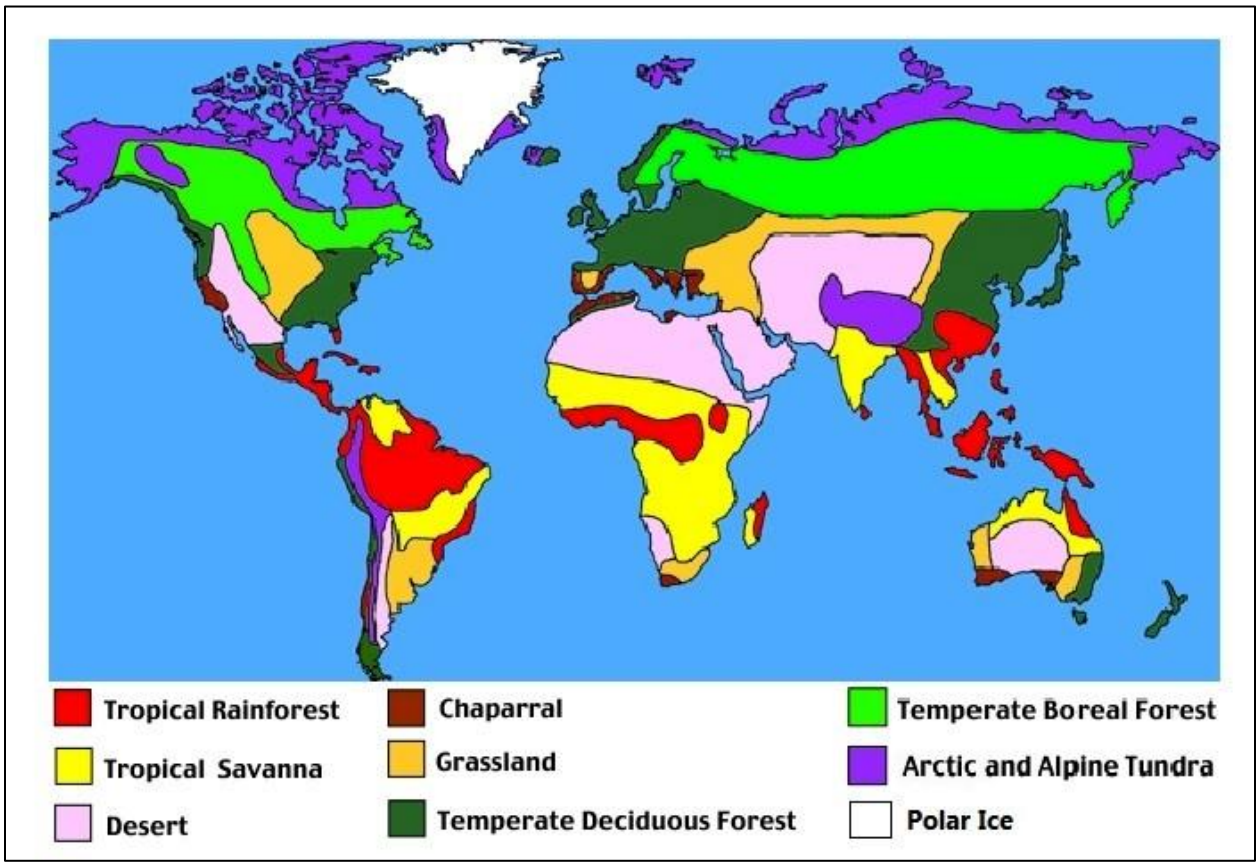

Figure 1: Distribution of the Earth's eight major terrestrial biomes, (Adapted from: De Blij and Miller, 1996).

A wide variety is found among these different biomes in terms of their vegetation and climatic characteristics. For example, tropical rain forests are characterized by greater species diversity. Tall trees contribute for more than seventy percent of plants within the forest. The temperature in a rain forest rarely gets higher than 93°F (34°C) or drops below 68 °F (20°C); average humidity is between 77 and 88%; rainfall is often more than 100 inches a year, while in a deciduous forest the average annual temperature is 50°F and the average rainfall is 30 to 60 inches a year (Kulawardhana, 2008). The climate in grasslands is humid and moist. The savannahs are

characterised by rainfall-induced seasonality, an herb as woody cover in spatial arrangement, which can be found between a tropical rainforest and desert biome. Savannahs have warm temperature all year round. Alpine biomes are found in the mountain regions all around the world. In the Alpine biomes average temperatures in summer range from 10 to 15°C and it goes below freezing in winter (Kulawardhana, 2008). The tundra is the world's coldest and driest biomes with an average annual temperatures of about -70°F (-56°C) (Kulawardhana, 2008). Each of these biomes consists of many ecosystems whose communities have adapted to small differences in climate and the environment inside the biome. Therefore it is evident that any change in climatic parameters at global as well as regional scale can have serious consequences on the distribution and even the existence of these different communities of vegetations. For example, when temperature and precipitation patterns shifts as a result of global climate change, the potential vegetation over a region or a pre defined climatic zone will no longer coincide with the actual vegetation that exists on the ground.

Although it is essential to understand the changes in the vegetation cover and their dynamics, many deficiencies have appeared in the understanding of the role of vegetation in terrestrial and atmospheric systems. Basic data regarding the extents and dynamics of vegetation are still missing or disputed (Woodwell, 1984). However, it is now recognized that a better assessment of natural or man induced changes in vegetation cover of the earth is needed to understand the role of plant communities in climatic, hydrologic and geochemical cycles (Hamilton, 1983, cited in Kulawardhana, 2008).

2.5. Land Use / Land Cover (LULC) Change Pattern

In addition to other anthropogenic factors, LULC changes are linked to climate, vegetation and weather in complex ways (Getahun, 2012). LULC changes play an important role in global environmental change. Land cover refers to the physical characteristics of the earth surface, captured in the distribution of vegetation, water, desert, ice and other physical feature of the land including those created solely by human activities such as agriculture, forestry and settlement (Shrestha, 2008). Land use is a more complicated term. Land use is the action of human activities on their environment such as agriculture, forestry and building constructions that alter land surface processes including biogeochemistry, hydrology and biodiversity (Shrestha, 2008).

LULC change can be classified into two broad categories: conversion or modification (Butt and Olson, 2002). Conversion refers to the changes from one cover or use to another, e.g. conversion of forests to pasture or to Cropland. Modification on the other hand refers to the maintenance of the broad cover or use type in the face of changes in its attributes. For example, a forest may be retained but significant alterations may be made on its structure or function. The key LULC change pathways include deforestation, desertification, wetland drainage and agricultural intensification (Butt and Olson, 2002). The pathways can be envisioned as forcing functions, which have direction (forest to pasture or pasture to Cropland), magnitude (amount of change), and pace (rates of change). LULC change reflects the complex interaction of human activities and environmental processes over time. Humans play a key role in contributing to the process and are equally affected by these LULC changes.

Whereas the major reasons for such LULC changes are positive and aim to increase the local capacity to support the human enterprise, there are also unforeseen negative impacts that can

reduce the ability of land to sustain the human enterprise (Houghton, 1994). For example, deforestation can be beneficial through sale of forest products as well as the use of cleared land to produce food for the local community. However, deforestation can result in the loss of biodiversity and impacts on the hydrological processes, leading to localized declines in rainfall, and more rapid runoff of precipitation, causing flooding and soil erosion. Deforestation can disrupt the carbon cycle and contribute to greenhouse gases, which contribute to climate change (de Sherbinin, 2002). Understanding LULC changes is therefore critical for the design of effective land management programmes.

2.6. Climatic versus Anthropogenic Driving Forces of Land Use/ Land Cover Dynamics

The LULC patterns of a region are an outcome of natural and socio–economic factors and of their utilization by man in time and space (Zubair, 2006). Driving forces also referred to as factors, can be categorized as natural and human induced. The natural factors may be mostly meteorological or geological phenomena like intense rainfall, earthquake, steep relief, soil type and climate change. Deforestation, immense agricultural and demographic pressure, as well as clearing of natural grass or bush land due to population increase are human factors. In the last few decades, conversion of grassland, woodland and forest into Cropland and grazing has risen dramatically in the tropics (Shiferaw, 2011). Significant LULC changes since the 1960s were identified in the Bani River Basin (Ruelland *et al.*, 2009).The most important changes were lost of the natural vegetation through increase in farming activities and expansion of grazing land. Vegetation covers as well as crop production show much variability across the globe depending on the types of crop, the biome and the region (Kulawardhana, 2008). Vegetation cover on the earth's surface is rapidly changing, and changes are observed in phenology and diversity.

Even though vegetation cover analysis does not directly show crop production, many studies state that there is also a decrease of crop production related to LULC change and climate variability (Crawford, 2001). LULC change and increase of greenhouse gases are two of the most interrelated factors associated with climate change and variability. They both tend to produce surface warming so that their impact to global ecosystem and society is too difficult to resist. Many studies indicated that analysing and modelling of spatial-temporal features of LULC change either globally or regionally is significantly important for better environmental management in view of sustainable development (Nellemann *et al.*, 2009; Shiferaw, 2011). According to Nellemann *et al.*, (2009) past soil erosion in Africa might have contributed to significant yield reduction (2-40% compare to the global average).

Different studies indicate that vegetation condition could affect and change the climatic zones of Africa. Changes in vegetation result in alteration of surface properties and the efficiency of ecosystem exchange of water, energy and CO_2 with the atmosphere (Nellemann *et al.*, 2009). According to WMO and the Inter governmental Panel of Climate Change (IPCC) Sub-Saharan Africa has the highest rate of land degradation (WMO, 2005). Some of the countries that have the worst rate of degradation are Rwanda and Burundi (57%), Burkina Faso (38%), Lesotho (32%), Madagascar (31%), Togo and Nigeria (28%), Niger and South Africa (27%) and Ethiopia (25%) (Bwalya, 2009 cited in TerrAfrica, 2009). Land degradation in sub-Saharan Africa is caused mainly by conversion of forests, woodlands and rangelands to crop production areas, overgrazing of rangelands; and unsustainable agricultural practices.

Sub-Saharan Africa is expected to face the largest challenges regarding food security as a result of climate change and other drivers of global change (Easterling *et al.*, 2007). Many farmers in

Africa are likely to experience net revenue losses as a result of climate change, particularly as a result of increased variability and extreme events. According to Fischer *et al.*, (2005) most climate model scenarios agree that Sudan, Nigeria, Senegal, Mali, Burkina Faso, Somalia, Ethiopia, Zimbabwe, Chad, Sierra Leone, Angola, Mozambique and Niger are likely to lose their cereal production potential by the 2080s.

2.7. The Use of Space-borne Data to Assess Vegetation Dynamics

Satellite derived NDVI is a convenient tool for monitoring vegetation cover at all scales from global to local. It enables regular detection of seasonal and inter-annual changes in vegetation activity. The NDVI has successfully served as vegetative indicator in many studies on desert encroachment and desertification (Tucker and Nicholson, 1999; Wessels *et al.,* 2004; Symeonakis and Drake, 2004), drought monitoring (Kogan, 1997; Song *et al.,* 2004), El-Nino impacts on ecosystems (Anyamba *et al.,* 2001), global phenology and bioclimatology (Tateishi and Ebata, 2004; Chen and Ravallion, 2004). These and other similar studies are motivated by the appropriation of NDVI for the analysis of vegetation cover at a wide range of spatial scales (i.e. local to regional).

Also the correlation between NDVI and above-ground biomass is well established (Tucker and Sellers, 1986). Satellite derived NDVI can serve as a general surrogate for vegetation conditions (Justice *et al.,* 1985; Tucker and Sellers, 1986). Temporal and spatial correlations between NDVI and climatic factors are investigated in many research works. Particularly, well correlations in arid regions, both spatial and temporal, which show the relationship between NDVI and rainfall (Richard and Poccard, 1998; Chen *et al.,* 2004; Weiss *et al.,* 2004; Tateishi and Ebata, 2004),as well as the relationship between NDVI and temperature, which were reported to be weaker but

also significant (Kowabata *et al.,* 2001; Schultz and Halpert, 1995). According to recent studies, precipitation has a strong effect on the inter-annual variability of vegetation activity especially in dry regions (Yang *et al.,* 1998; Richard and Poccard, 1998; Wang *et al.,* 2003; Li *et al.,* 2002).

Numerous studies have suggested a linear relationship between NDVI and climate predictors. Theoretically NDVI can be considered as a climatic indicator which depends mainly on rainfall condition. This assumption was used in various drought monitoring and drought early warning systems (Kogan, 1997; Song *et al.,* 2004). However, the relationship is linear only in a limited range of rainfall conditions. The upper thresholds for the linear relationship between NDVI and rainfall were reported to be approximately 500 mm/yr for semi-arid Botswana (Nicholson and Farrar, 1994), 700-800 mm/yr for Senegal (Li *et al.,* 2004), and 500-700 mm/yr for China (Li *et al.,* 2002). Above these limits, NDVI increases with rainfall only at a slower rate.

The response of NDVI to rainfall and temperature is dependent on vegetation types and varies by geographical region. For example, Woodland and forest vegetation shows a lesser correlation between NDVI and climatic factors (Propastin *et al.,* 2006). Shrubs and desert vegetation patterns are reported to correlate stronger with temporal and spatial variations of climatic factors (Propastin *et al.,* 2006). Vegetation patterns in steppe grassland and savannah show evidence of the highest correlation with that of rainfall and temperature (Li *et al.,* 2002; Wang *et al.,* 2001, Li *et al.,* 2004). However, Nicholson and Farrar (1994) reported that the response of NDVI to rainfall relationship is more dependent on soil types than on vegetation types in Botswana.

Many studies proved a high sensitivity of NDVI to inter-annual rainfall anomalies. Thus NDVI can be used as a good proxy for the study of inter-annual climate variability on regional and global scales or for identification of climatic signal by evaluation of land degradation (Kowabata

et al., 2001; Evans and Geerken, 2004). However, there are limits of rainfall amounts beyond which only a weak NDVI sensitivity to inter-annual rainfall anomalies can be found. This rainfall limit varies by geographical region, but generally, a minimum of 200-300 mm/y seems sufficient to induce NDVI sensitivity to rainfall anomalies (Richard and Poccard, 1998).

Vegetative cover is the best measurable indicator of environmental change and can be easily detected by remote sensing methods. Vegetation cover performance is strongly predicated on macro and micro-climatic factors, such as global temperature, rainfall distribution change and local topographic characteristics. Therefore, discrimination between different causes of change in vegetation cover, climate and human activity is difficult. The neglect of this aspect can lead to mistakes by evaluation of land conditions (Binns, 1990; Hellden, 1991). A few recent studies have developed methods for discrimination by use of satellite data time-series and time-series of climatic variables (Evans and Geerken, 2004; Li *et al.*, 2004). These methods have been based on identification of climate signal in inter-annual dynamic of vegetation activity. Once the climate signal is identified, it can be removed from the trends in vegetation activity. The remaining vegetation changes are attributed to human influence and areas considered to be experiencing a human-induced degradation of vegetation cover.

3. STUDY AREA

3.1. Physical Characteristics

3.1.1. Location and extend of the study area

The Bani River is the most important tributary of the Niger River. It is principally located in the southern part of Mali from latitudes 9˚8′10″ N to 14˚8′50″ N and longitudes 3˚8′50″ W to 8˚8′50″ W (Figure 2). With a catchment area of around 130 000 km^2 at its confluence with the Niger at Sofara, it is one of the longest rivers in West Africa (approximately 700 km). It flows into the inner Niger Delta at Mopti and is a large contributor to the annual Niger Inner delta flooding (Figure 2).

3.1.2. Rainfall

The natural resources of the area have been subjected to substantial pressure during recent decades. One reason is rainfall variability in the whole West Africa. Rainfall data showed a pronounced decline from the seconds half of the 1960s. This is the most marked short-term precipitation trend in any part of the world during the twentieth century (Hulme and Kelly, 1993; Nicholson *et al.,* 2000). Figure 3 illustrates the average rainfall time-series and the averaged Standardized Precipitation Index from 1982 to 2011 for some stations throughout the study area. The region is characterized by a single, strong North-South rainfall gradient; that has traditionally been associated with the seasonal movements of the Inter Tropical Convergence Zone (ITCZ) while inter-annual rainfall variation has been explained by the latitudinal displacement of the ITCZ (Kraus, 1977; Lamb, 1979). The ITCZ is an area of low pressure that forms where dry, mid-continental air masses from the northeast meet south-easterly humid, maritime air from the Atlantic near the earth's equator. Dry, dust-laden, cooler air from the

northeast is undercut by the wedge of warm, humid air from the Gulf of Guinea. The ITCZ moves seasonally and is controlled by the area of most intense solar heating where the surface temperatures are highest.

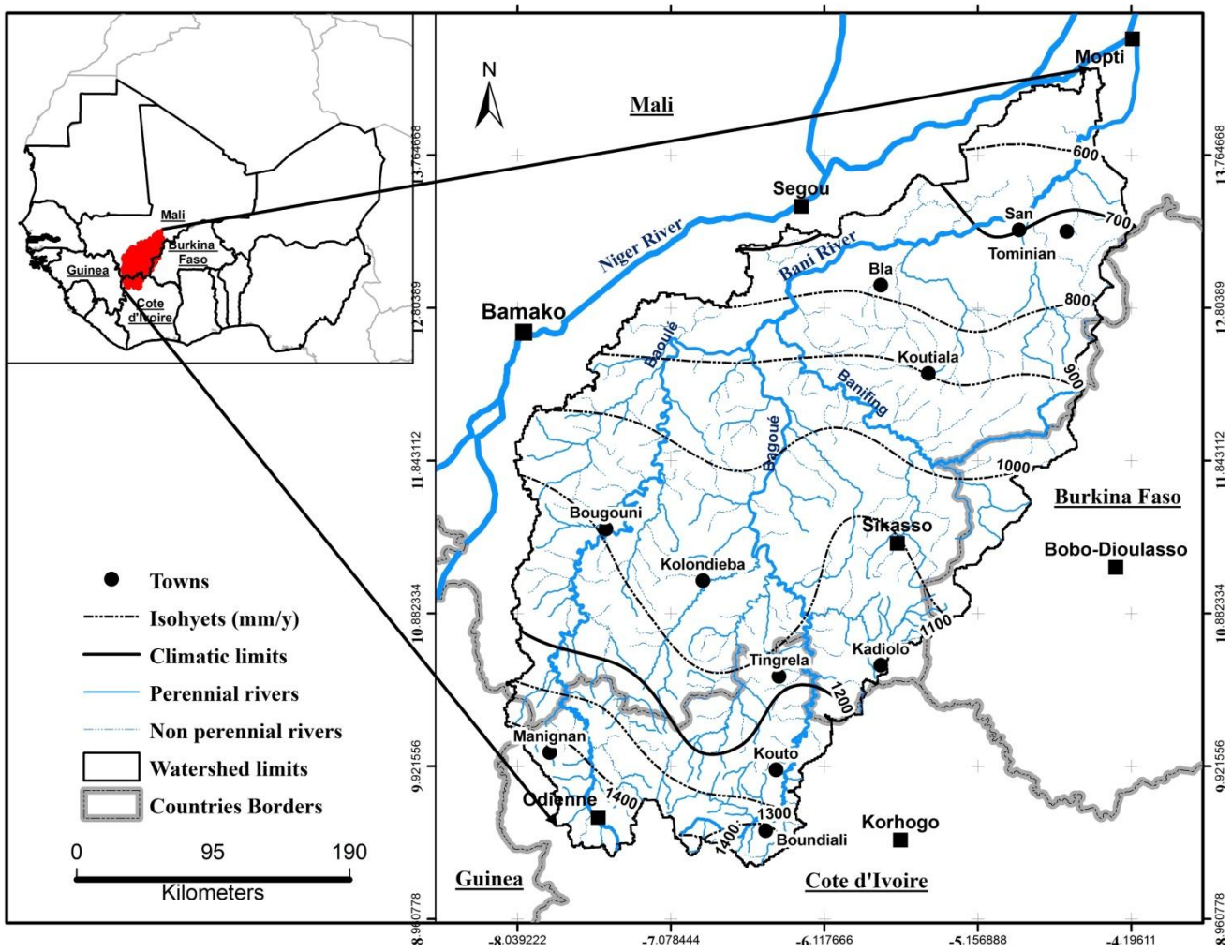

Figure 2: Map showing the Study Area

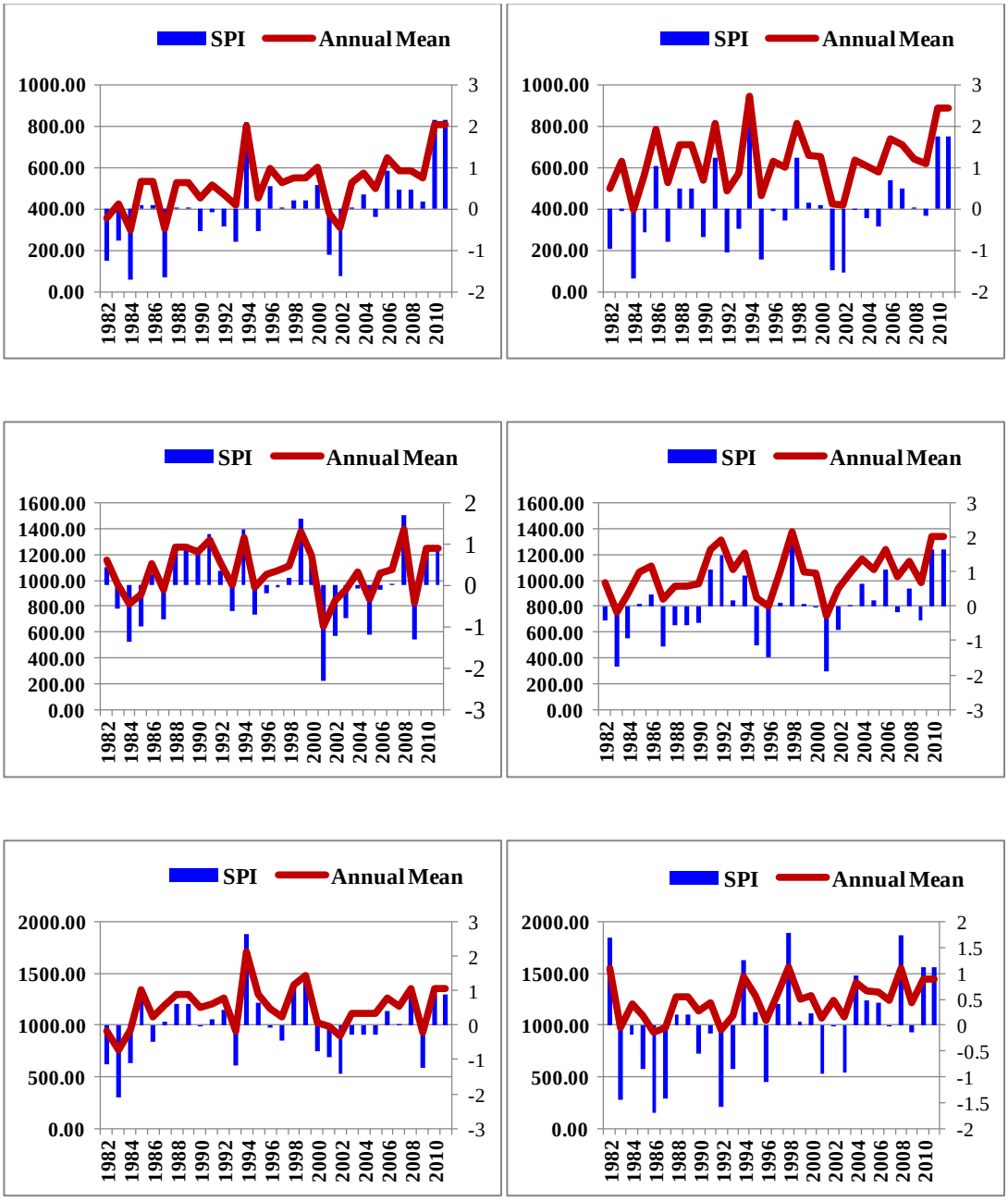

Figure 3: 30-year (1982-2011) annual rainfall and Standardized Precipitation Index SPI for Sahelian (Djenne and San), Sudanian (Bougouni and Sikasso) and Sudano-Guinean (Odienne and Boundiali).

3.1.3. Topography and drainage

The topography of the study area has low slopes (0-5%) and elevations ranging from 265m at the outlet to 702m at the highest zone. As a result the Southern parts represent the major contributor to the river flows of the basin. The Bani River has three main tributaries namely: Baoulé, Bagoé and Banifing. The Baoulé rises near Odienne in Cote d'Ivoire and passes just South of Bougouni district (Mali) and joins the Bagoé around Dioila. The Bagoé rises near Boundiali in Cote d'Ivoire and passes through the districts of Korhogo (Cote d'Ivoire), and Kadiolo, Kolondieba, Sikasso and joins the Baoulé in Dioila district (Mali). After this junction, the Baoulé-Bagoé flows around 20 km and is joined by the Banifing between Dioila and Bla districts. The Banifing flows from Banfora (Burkina Faso) and drains the regions around Yorosso, Koutiala and Sikasso.

3.1.4. Soils

Soils are one of the most valuable natural resource for society since they produce food, fibre and fodder, which are basic to our existence. In the Bani River Basin, soils are mainly ferralitic and lessivated with high sand and clay content. Sandy hillwash is often found at the surface while basal gravelis found in deeper layers of the profile. In the basement, the aquifers are found in two types of fissured formation: in the South-West, they have low permeability and a base layer of Birrimian mica-schists and metamorphic rocks (60%). In the North-East, they are made of Infracambrian sandstone (40%) so that the downstream area of the basin has higher permeability and might provide better support for groundwater flows (Brunet-Moret *et al.,* 1986).

3.2. Agroclimatic Characteristics

Three climatic zones, as seen in Figure 4, can be identified in the Basin in the Basin (Ruelland *et al.*, 2008a):

The first is the Sahel zone which has less than 800 mm rainfall per year. It is characterised by a single rainy season (June to September) and a total absence of rainfall between November and April. The type of vegetation found is arboraceous and/or scrubland steppe, with small trees or shrubs. In general, the grass cover is patchy and essentially made up of annual species, which are occasionally touched by bushfires.

The second zone is the Sudanian, which has a rainfall between 800-1200 mm per year. This zone is characterised by a rainy season that increases in duration as one approaches the tropics (May to October with a maximum in July-August), has the abundance of grasslands. The height of the herbaceous cover ranges from 20cm to 1.5m. It consists particularly of Andropogons and Pennisetum, which are regularly affected by bushfires. Beside these grasslands, other vegetation formations such as shrubs, open woodlands savannas, clear forests, gallery forests, Croplands or fallow lands can be found.

The third zone is the Sudano-Guinean, with a total annual rainfall greater than 1200 mm and characterised by rainfall almost all year round but heavier from March to October, with a maximum in August-September. The Sudano-Guinea zone is constituted by a varied mosaic of different types of vegetation including those just mentioned as well as groves or wood islands of a height of 3m to 8m. The clear forests are made up of trees whose crowns almost join and below which land cover and herbaceous cover are very sparse. The wooded savannas and open

woodland savannas are formed of dense trees or sparse trees and high grass (especially of the Andropogons species) that are easily affected by bushfires. The gallery forests are located along the perennial rivers and in the permanently humid valleys or gullies.

3.3. Problem of Land Degradation

Human activity is generally organized around water resources, topography, pedology and the axes of communication. In this catchment, the population is considered as agro-pastoral (Collet, 2010). Most of the agricultural areas are located in the Northern area of the basin where the hydrographical network is highly developed and a main road runs from Segou to Mopti (see Figure 4). In this area agriculture is mainly traditional, located around rivers and with typical crops like millet, sorghum, cotton, cassava and peanuts. In the South, the vegetation is denser and there are very few cultivated areas (Figure 4). Here, agricultural areas are rapidly expanding due to demographic pressure. Recent remote sensing studies (Ruelland et *al.,* 2008b; 2009) showed that Sahelian and Sudano-Sahelian areas have been suffering from the rapid extension of Croplands and pastureland for 40 years now; this is a result of Mali's growing population. The population increased by nearly 3.6% per year according to the report of the last census (RGPH, 2009). Deforestation has also increased as wood and charcoal remain the prime energy sources (Ruelland *et al.,* 2011). Other land-cover changes caused by the growing population have been observed. For example soil degradation has sometimes led to increase in erosion (Ruelland *et al.,* 2011) and woodland has been replaced by pasture in dry season.

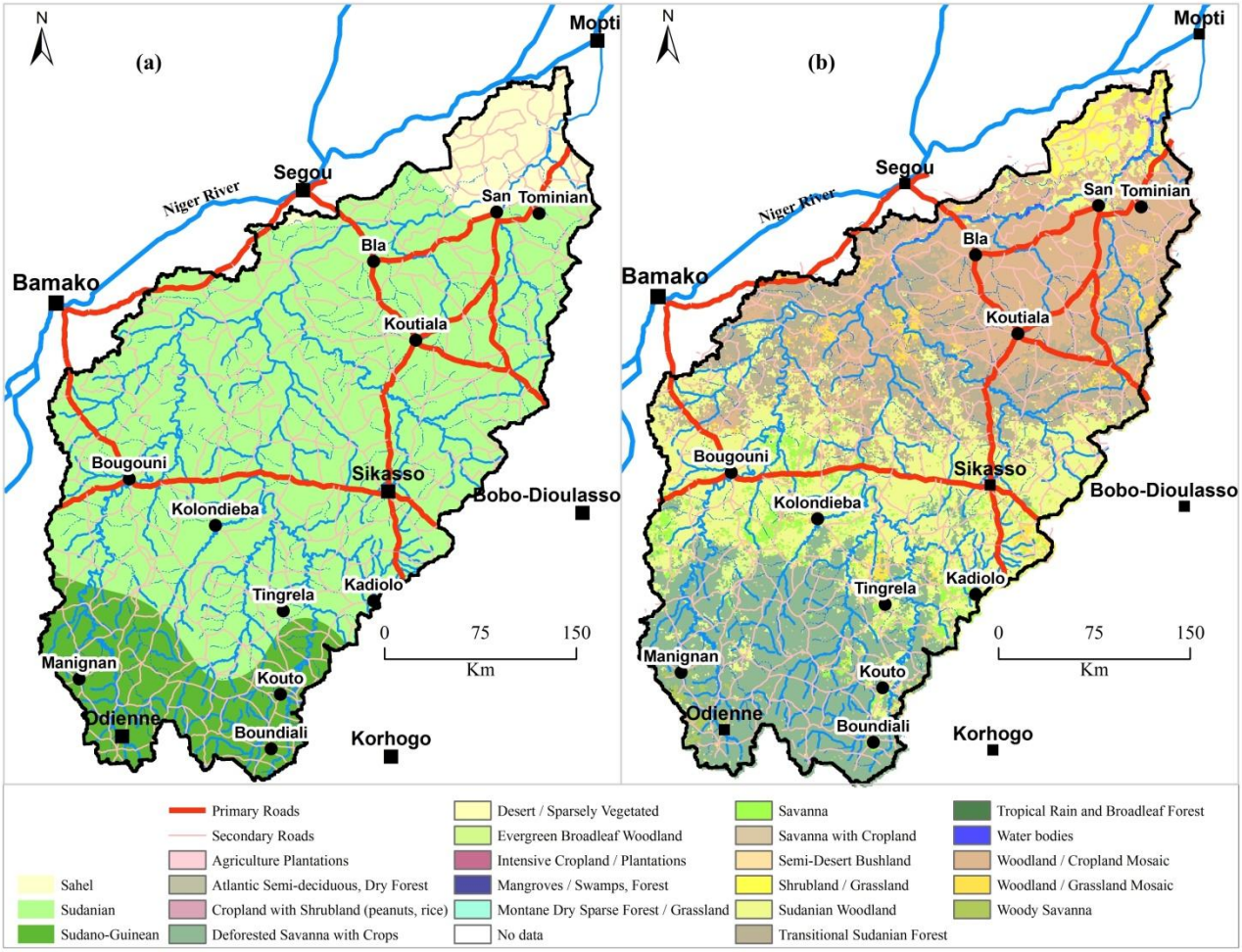

Figure 4: (a) Climatic zone and (b) Land Cover map of Bani river Basin extracted from the West Africa Land cover map at 1-km resolution using the SPOT 4 satellite (Mayaux *et al.* 2003).

4. MATERIALS AND METHODS

4.1.Introduction

The methodology of the study could be presented in two (2) major steps. These include the description of the datasets used and their pre-processing in the first step and the data analysis in the second step. The next sections give the details about the whole process.

4.2. Data used in the study and their pre-processing

This study used rainfall data from meteorological station as well as satellite data from multiple sensors. The pre-processing concerned the assessment of gauge rainfall data and updating for missing value, the generation of time-series for both Normalised Difference Vegetation Index (NDVI) and Rainfall (RF) and geometric correction of Landsat data collected.

4.2.1. Climate data and their preparation

The climatic data used in this study are monthly rainfall from rain gauge stations throughout the basin. These data have been completed using satellite rainfall estimate from Tropical Rainfall Measurement Mission (TRMM 3B43) product. The details are as follows in the section below.

4.2.1.1. Gauge rainfall data

Rainfall data were retrieved from the annual statistics by the National meteorological services of Mali, Burkina Faso and Cote d'Ivoire. These data contain monthly mean records of 40 meteorological stations in or around the study area during the period from 1982 to 2001.

The monthly rainfall is used for the analysis (monthly mean rainfall total amount in mm). The quality of the data was assessed and missing values were either replaced by the long-term mean for the missing month or value from the nearest station. The climate stations are irregularly distributed over the study area but represent most broad land cover classes. The mean characteristics of the climate stations are shown in Table 1.

Table 1: Geographical characteristics for the meteorological stations used in the study (1982-2001 growing season mean rainfall)

Stations	Country	Longitude (dd.)	Latitude (dd.)	Altitude (m)	Mean rainfall (mm)
Bouguni	ML	-7.5	11.42	361	1075.87
Segou*	ML	-6.15	13.4	288	618.57
Kadiolo	ML	-5.77	10.55	348	1044.18
N'tarla	ML	-5.75	12.7	327	794.07
Sikasso	ML	-5.68	11.35	379	1054.41
Koutiala	ML	-5.47	12.4	360	818.85
San	ML	-4.9	13.28	291	638.86
Dioila	ML	-6.8	12.48	318	779.65
Djenne	ML	-4.57	13.9	270	524.29
Yanfolila*	ML	-8.15	11.18	364	1117.15
Mahou	ML	-4.63	12.13	340	832.19
Ke-Macina*	ML	-5.37	13.95	278	513.89
Kalana*	ML	-8.2	10.78	393	1055.6
Beleko	ML	-6.42	12.48	305	742.38
Kimparana	ML	-4.93	12.83	308	718.71
Sofara*	ML	-4.23	14.02	273	542.46
Dionkele N.*	BF	-4.82	11.77	342	917.80
Kignan	ML	-6.02	11.85	347	886.92
Bobola Z.	ML	-4.98	12.53	321	805.35
Fana	ML	-6.95	12.78	334	763.52
Misseni	ML	-6.08	10.32	343	1060.66
Cinzana	ML	-5.97	13.25	284	643.77
Manakoro	ML	-7.45	10.45	359	1074.66
Kolondieba	ML	-6.9	11.1	331	1029.16
Konobougou*	ML	-6.76	12.92	330	721.79
Bla	ML	-5.77	12.95	292	685.06

Klela	ML	-5.67	11.7	319	914.77
Loumana*	BF	-5.35	10.58	322	1083.35
Odienne	CI	-7.57	9.5	423	1240.05
Samo R.*	BF	-4.93	11.4	363	1012.01
Kourouma*	BF	-4.8	11.62	340	965.09
Dogo B.	ML	-7.33	11.88	375	994.17
Tansila*	BF	-4.38	12.42	439	857.00
Koumantou	ML	-6.85	11.42	347	985.34
Boundiali	CI	-6.47	9.52	403	1172.72
Farako	ML	-5.48	11.22	424	1050.44
Filamena	ML	-7.95	10.5	417	1298.01
Tengrela	CI	-6.4	10.48	376	1044.55
Kouto	CI	-6.42	9.9	368	1078.31
Minignan	CI	-7.83	10	398	1178.47

* Stations outside the catchment in a buffer of 20 km, ML=Mali, BF= Burkina Faso, CI= Cote d'Ivoire.

4.2.1.2.Gridded rainfall data

Mean monthly rainfall data from the TRMM was used in this study. The TRMM instrument orbits at an altitude of around 400-km with an inclination of 35° and an orbital period of around 92.5 minutes, completing approximately sixteen orbits each day (Fleming *et al.*, 2011). The primary objective of TRMM is to measure rainfall and energy exchange over the tropical and subtropical regions of the world, in particular covering the oceans and unsampled land areas (Kummerow *et al.*, 1998, 2000). TRMM provides a variety of products to meet the needs of different users. The level 3 products, which are space-time grids representing average rates of rainfall over different time scales, and the TRMM (e.g. Huffman *et al.*, 1995; Kummerow *et al.*, 2000; Huffman *et al.*, 2007) is used in this work. It is a time-series of monthly average rainfall (in mm^{-1}, product code 3B43), inferred from data provided by multiple satellites in addition to TRMM, as well as rain gauge data provided by the Global Precipitation Climatological Centre (GPCC), produced by the German Weather Service and the Climate Assessment and Monitoring

System (CAMS) produced by the NOAA. The satellite data is provided by two types of sensors: (1) passive microwave data collected by various Low-Earth Orbiting (LEO) satellites, including TRMM, the United States (US) Defence Meteorological Satellite Program satellites, and the NOAA satellite series; and (2) infrared data collected by an international constellation of geosynchronous satellites (Kummerow *et al.,* 2000). The TRMM satellite itself has multiple sensors, the most important being the TRMM precipitation radar (TRMM-PR), the passive TRMM microwave imager (TMI), and the visible and infrared scanner (VIRS). Each of these provides products in its own right for the scientific community. However, the interest of this study is only in the 3B43 product because it has been found to be more representatives (e.g. Nicholson *et al.,* 2003, Fleming *et al.,* 2011). The 3B43 data is provided as Hierarchical Data Format (HDF) on a 0.25° (c.27.8-km) grid resolution that covers the globe between latitudes 50°N to 50°S. Improving the TRMM products is an ongoing process with superior versions of the various products released when appropriate (e.g. Shige *et al.,* 2006).

4.2.1.3. Generation of rainfall times-series for the study period

Since the rain-gauge datasets were not available for the stations used up to the year 2000 because of many problems, (i.e. political crisis in Cote d'Ivoire since 2002), the satellite estimated rainfall was used to complete the rainfall time-series for this study. The monthly rainfall data (mm) obtained from the TRMM instrument were compared to the *in situ* rain-gauge measurement for the overlapping time period 1998 to 2002 for 40 meteorological stations. The correlation coefficient (r) of the rainfall between the TRMM and rain-gauge data obtained for each month is significant (greater than 0.5) for all the stations. This indicates a strong correlation

between the two datasets. The rainfall data for the period 2002-2011 were generated using the following regression equation developed by Almazroui, (2011):

$$RF_{Estimated} = c_{RF} + m_{RF} \times (RF_{TRMM}) \quad (1)$$

Where $RF_{.Estimated}$ is the rainfall to be estimated, $m_{.RF}$ is the slope, $c_{.RF}$ is a constant and RF_{TRMM} is the detected rainfall. The results showed a good linear relationship between gauge rainfall and TRMM data with a correlation coefficient up to 0.8 for all the stations used in this analysis.

4.2.1.4.Preparation of gridded rainfall data

Rainfall data have been used to interpolate a 0.07˚ gridded (8-km) monthly rainfall time-series for the period from 1982 to 2012. The Inverse Distance Weighting (IDW) method was used in this study. This method which was found to be the most accurate for the area (Ruelland *et al.,* 2008b) estimates values at unsampled points by the weighted average of observed data at surrounding points. This then can be defined as a distance reverse function of each point from neighbouring points (Teegavarupu and Chandramouli, 2005). That means by using a linear combination of values at a known sampled point, values at un-sampled points can be calculated. IDW relies on the theory that the unknown value of a point is more influenced by closer points than by points further away (Ly *et al.*, 2011). The weight λi can be computed by:

$$\lambda i = \frac{\frac{1}{|Di|^d}}{\sum_{i=1}^{ns} \frac{1}{|Di|^d}}, \; d > 0 \quad (2)$$

Di is the distance between sampled and un-sampled points. The *d* parameter is specified as a geometric form for the weight while other specifications are possible. This specification implies that if the power d is larger than 1, then the distance-decay effect will be more than proportional to an increase in distance, and vice versa. Thus small power *d* tends to give estimated values as averages of observed values in the neighbourhood, while large power d tends to give larger weights to the nearest points and increasingly down-weights points further away (Lu and Wong, 2008). Using a power value of 2 for daily and monthly time steps, 3 for hourly and 1 for yearly would appear to minimize the interpolation errors (Dirks *et al.,* 1998). Furthermore, the power ***d*** is usually set to 2, following Lloyd (2005) and hence inverse square distances are used in the estimation. Consequently a power value of 2 was adopted for IDW and the gridded rainfall data were made by interpolation based on the longitude and latitude in this study.

4.2.2. Satellite data

The satellite data collected and used in this study are the 15-day Global Inventory Monitoring and Modelling Systems (GIMMS), the 10-day Satellite pour l'Observation de la Terre Vegetation Product (SPOT-VGT) and 30 m resolution Landsat imageries.

4.2.2.1. Data of coarse resolution

The most recent studies of changes in vegetation activity at global or regional scales have been based on the use of data time-series from AVHRR launched by the NOAA in 1981. The sensor has given a continuous spatial cover of the entire earth area on a regular frequency. The coarse spatial resolution (1-16 km) and fine temporal frequency have made products from NOAA AVHRR indispensable for use in environmental studies on regional to global scale. AVHRR derived data have been successfully used for monitoring vegetation activity and environmental

changes (Xu *et al.,* 2012), detection of droughts (Bayarjargal *et al* 2006; Bajgiran *et al.,* 2008), desertification and land degradation studies (Hountondji *et al.,* 2006; Fensholt *et al.,* 2013), estimation of El-Nino Southern Oscillation (ENSO) and impact on vegetation cover (Anyamba and Tucker, 2001; Erasmi *et al.,* 2014). This study used a 15-day GIMMS NDVI dataset 8-km grid resolution derived from the NOAA AVHRR sensor, and a 10-day SPOT VGT NDVI 1-km grid resolution. Satellite data used and their characteristics are shown in Table 2.

Table 2: Satellite data used in the study and their characteristics

Satellite system	**Sensor**	**Spatial Resolution**	**Temporal Resolution**	**Equatorial Crossing**	**Time-period Acquisition date**	**Field of View**
NOAA	AVHRR	8 000m	15 day	~9 AM- ~6PM	1982-2006	±55.4˚
SPOT	VEGETATION	1 000m	10 day	10:30 AM	1998-2011	±101˚
Landsat	TM	30m	16 days	9:30 AM -10AM	2009/2010	
	ETM+	30m	16 days	10AM - 10:15AM	1999/2000	
	TM	30m	16 days	9:30 AM -10AM	1984/1986	

For the purpose of this study monthly averages NDVI values were computed from the 15-day GIMMS and 10-day VGT composites to match the monthly temporal resolution for rainfall dataset. Monthly data sets were generated using a Maximum Value Composite (MVC) procedure, which selects the maximum NDVI value for every pixel (Holben, 1986). This procedure is used to reduce noise signal in NDVI data due to clouds or other atmospheric factors. The raw data of the two datasets are converted into the -1 to +1 range using the following formulae:

$$NDVI(GIMMS) = raw/10000 \quad (3)$$

and

$$NDVI(SPOT - VGT) = (\mathrm{RAW} \times 0.004) - 0.1 \quad (4)$$

4.2.2.2. Fine resolution data

The Landsat sensor was specifically designed for studies such as land cover mapping. Essentially detection of changes in land cover involves the ability to quantify temporal differences using multi-temporal data sets. One of the major applications of remotely sensed data obtained from earth orbiting satellites is change detection because of repetitive coverage, fine spatial resolution, and consistent image quality. For this purpose datasets from two Landsat sensors have been used. The Landsat Thematic Mapper (TM) sensor launched in 1982 is an upgrade of the Multispectral Scanner Subsystem (MSS) on which efforts were made to incorporate improvements into a new instrument. The TM instrument is therefore based on the same technical principal as the MSS, but with a more complex design as it provides finer spatial resolution, improved geometric reliability, greater radiometric detail and more detailed spectral information. The MSS has four broadly defined spectral regions whereas the TM has seven, customized to record radiation of interest to specific investigations (Campbell, 1996). On the other hand Landsat Enhanced Thematic Mapper Plus (ETM+) sensor carried by Landsat 7, launched in 1999, is an offshoot of the TM. The ETM+ sensor offers several enhancements over the Landsat 4 and 5 TM sensors, including increased spectral information content, improved geodetic accuracy, reduced noise, reliable calibration, the addition of a panchromatic band, and improved spatial resolution of the thermal band. The same resolution as the TM bands 1-5 and 7 apply for the ETM+ (Masek *et al.,* 2001).

These imageries were used to check out changes in surface features over the last three decades. Concerning the information extraction from the Landsat data, this study was mainly interested in identification of changes in spatial patterns of LULC in the study area. Pre-processing of the Landsat dataset included common procedures of satellite data treatment such as radiometric and geometric correction, rectification and co-registration of all images.

4.2.2.3. Generation of NDVI time-series data

Following the concept of Yin *et al* (2012) and Song *et al* (2010), a correlation analysis to test the linear relationship between different datasets is conducted. SPOT VGT time-series data have been spatially resampled to meet the coarser 8-km resolution of GIMMS NDVI time-series by spatial averaging. Next representative land cover classes are selected using the Global Land Cover 2000 (GLC) map. These land cover classes were: Shrublands, Cropland, Woodland, Forest and Savannah. Thirdly the pixel-wise linear correlation coefficient (r) between monthly VGT and GIMMS for selected pixels is then calculated for the overlapping period of 1999-2006. Lastly a 30-year time-series dataset is generated using GIMMS 1982-2000 and VGT 2001-2011 (Zhang *et al.*, 2013).

4.2.2.4.The Global Land Cover 2000 and Globcover 2009 data

Land cover maps created by Global Land Cover project, whose aims to create a better land cover product for the whole globe (Latifovic *et al.*, 2004), show the different types of vegetation as well as the surfaces without vegetation to be found in Africa and elsewhere. The dataset used for this map were acquired from near to daily SPOT 4 satellite observations. The period of observation for the map used in this study covers the interval between November 1999 and December 2000 (Fritz *et al.*, 2003; Fritz and Belward, 2004; Mayaux *et al.*, 2003). The

vegetation and non-vegetation classification for this map was based on the Land Cover Classification System (LCCS) of the Food and Agricultural Organisation **(**FAO**)** (Di Gregorio, 2005). Each class is specifically connected with one land cover type falling into the following categories: forests, woodlands, shrublands, grasslands, agricultural lands, bare soil, cities and water bodies. These classification results are used in many ecological applications (Defries and Townshend, 1999; Kerr and Ostrovsky, 2003; Lu and Weng, 2007). Global land cover 2000 (Bartholome and Belward, 2005) is a vegetation classification map with a 1-km resolution. In order to respond to the dynamics of land cover in a changing environment, other maps of this kind have been published, using different methods and satellite data from different sensors (Herold *et al.*, 2008). These maps are: International Geosphere-Biosphere Programme (IGBP**)** Discover (Loveland *et al.*, 2000), the Moderate Resolution Imaging Spectroradiometer (MODIS**)** land cover product (Friedl *et al.*, 2002) and University of Maryland (UMD**)** land cover product (Hansen and Reed, 2000). This global product originally contains 20 land cover classes and was reclassified into 7 classes (Figure 5): Forest, Woodland, Savannah, Shrublands, Grassland, Cropland, and Water bodies are considered.

Globcover land cover product is the result of the European Space Agency (ESA) Globcover project. The objective is the generation of a land cover map of the world using an automated processing chain from the 300-m Medium Resolution Imaging Spectrometer (MERIS) time-series. This project was started in April 2005 by an international consortium and based on abundant feedbacks and comments from ESA internal assessment and a large group of partners and end users: Joint Research Centre (JRC**),** Food and Agricultural Organisation **(**FAO**),** European Environment Agency **(**EEA**),** United Nation Environment Programme **(**UNEP**)**, Global Observation of Forest and Land Cover Dynamics (GOFC-GOLD) and IGBP. The Globcover

global land cover dataset 2009 contains different land cover classes at 300m ground resolution. The land cover map is derived by an automatic and regionally-tuned classification of a time-series of global MERIS Fine Resolution (FR) mosaics for the year 2009. The global land cover map counts 22 land cover classes defined with the United Nations (UN) Land Cover Classification System (LCCS**)**. The quality of the Globcover product is highly dependent on the reference land cover database used for the labelling process and on the number of valid observations available as input (Globcover 2009).

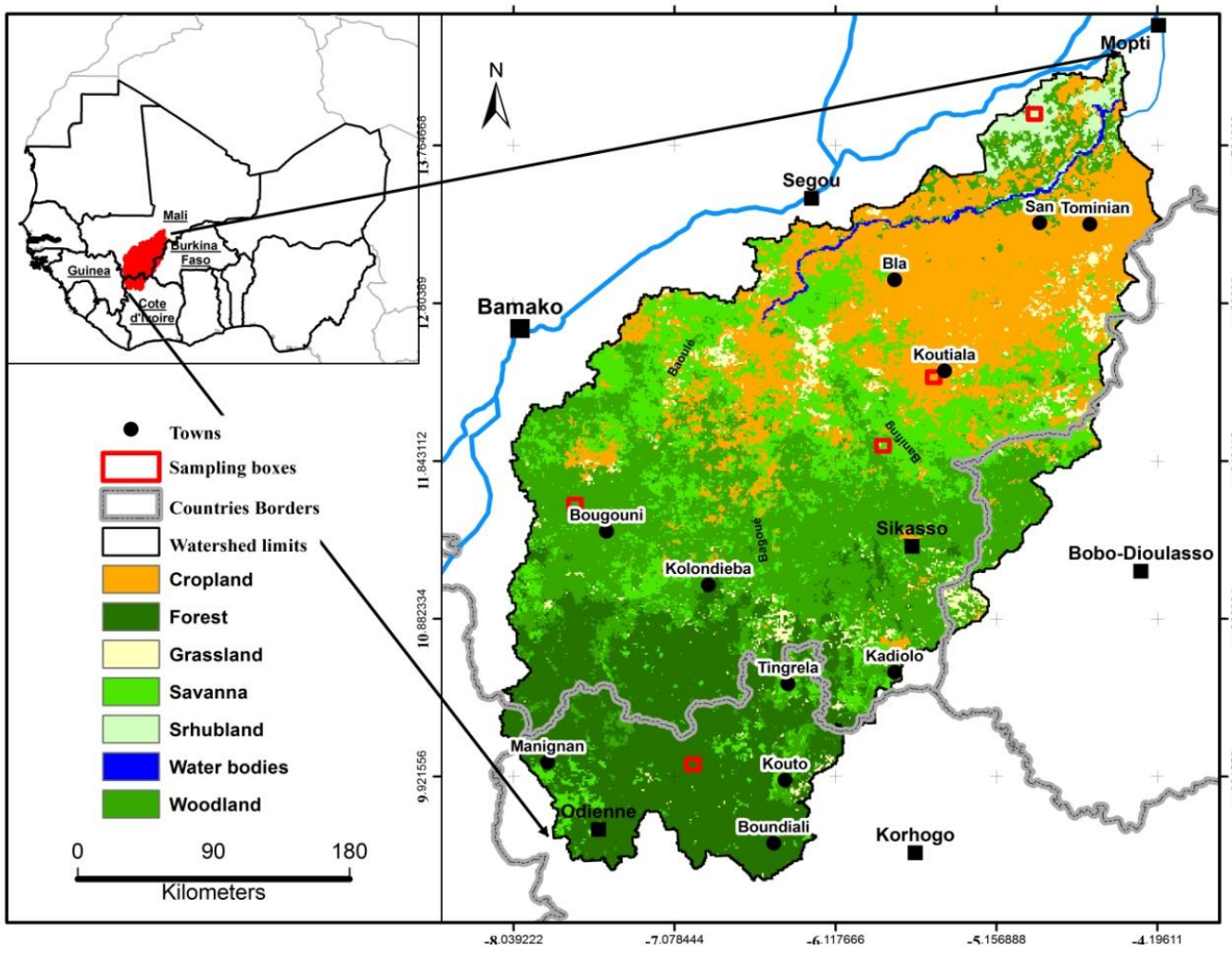

Figure 5: Land Cover map of the Bani River Basin. In red boxes: samples extraction area for NDVI comparison (extracted from GLC-2000 map, Mayaux *et al.* 2003 modified by sstraore for this study).

4.2.2.5. Ground truth

During November 2013 to January 2014 corresponding to the end of harvest period in the study area, the field data collections were conducted. The first (in November) was allotted to preparatory field work (reconnaissance survey), while the second (in January) was the major one. By using a Trimble Juno SB Global Positioning receiver (±3-meter positioning accuracy in real time), 20 grounds control points (GCPs) per reference site were collected. Although the dates of field work did not coincide with the dates of images acquisition (the field work was conducted in December and January 2014 and the images were acquired in November –December for the respective periods) the collected data were used to determine the major LULC for the area and to classify the images. The training sites were distributed throughout the study area taking into account the main categories.

4.2.2.6. Ancillary data

Ancillary data were used to support the classification. LULC maps from the Project Inventories of Ligneous / Terrestrial Resources (PIRL/PIRT) of Mali produced between 1984 and 1990 using Landsat TM and SPOT data were scanned and geo referenced. These maps of 1/200,000 scale, which were generated using topographic maps, SPOT imagery and reference data from ground survey contain helpful information for land survey and image classification for the area. High resolution Google imagery, expert and local knowledge were also used to support the image processing.

4.3. Methodology of data analysis

In this section data analysis procedure of the study could be presented in three (3) major steps. These include the analysis of vegetation distribution, variability and change in space and time, the investigation of the relationship between NDVI and rainfall and the linkage of vegetation productivity change to climate and anthropogenic activities.

4.3.1. Analysis of vegetation distribution, variability and change in space and time

This section assessed vegetation distribution and variability using analysis of variance, the departure from the long-term mean and the Mann Kendall trend. The details are presented as follows.

4.3.1.1. Simple methods of descriptive statistic

The analysis of spatial and temporal variability in vegetation cover was based on the use of variables of descriptive statistic. This statistical methods and variables are widely used and published. The following statistical variables and statistical measures were used: NDVI Mean, NDVI Standard deviation and NDVI Coefficient of Variation. The NDVI Mean represents the average value of each pixel during the study period. The NDVI Standard deviation (STD) is the root mean square (RMS) deviation of the NDVI time-series values from their arithmetic mean. It is a measure of statistical dispersion, measuring the spread of NDVI values. The NDVI Coefficient of Variation (CoV) represents the dispersion of NDVI values relative to the mean value. A positive change in the value of a pixel-level CoV over time relates to increased dispersion of values, not increased NDVI; similarly a negative CoV dispersion means decreasing

dispersion of NDVI around mean values not decreasing NDVI. The trends in CoV may reflect land cover change.

4.3.1.2.NDVI departure

Long-term time-series image data provides an opportunity to assess quantitatively and qualitatively the vegetation cover status in the past and present. Moreover trends can be used to map and assess the ecosystem processes (Nemani and Steve, 1997). An average of 30-year NDVI data is computed for each image pixel and departure from its average is then calculated for each participating year in order to evaluate a yearly vegetation growth rate or greenness visually and statistically. The departure from average is calculated using the algorithm developed by Burgan *et al.*, 1996.

$$NDVI_{dep} = NDVI_i - NDVI_{av} \times 100 \qquad (5)$$

Where $NDVI_{dep}$ is the NDVI departure for a particular year; $NDVI_i$ is the Annual NDVI integral for year ***i*** $NDVI_{av}$ is the NDVI average for the period.

4.3.1.3. Calculation of time-trends

Ordinary Least Squares (OLS) regression is the most common method applied for trend analysis in long image time-series. However four basic assumptions affecting the validity of trends summarized by OLS regression are often violated: i) all the Y-values should be independent of each other; ii) the residuals should be random with zero mean and iii) the variance of the residuals should be equal for all values of X (De Beurs, 2005). Since time-series of biophysical parameters are temporally correlated, OLS regression retrieved trends are not reliable.

The approach used in this study relies on Mann-Kendall monotonic trend tests, which have been applied in a few previous studies of time-series of remotely sensed data (De Beurs and Henebry, 2004a; De Beurs and Henebry, 2004b; De Beurs and Henebry, 2005a; De Beurs and Henebry, 2005b). There are two advantages of using this test. First, it is a non-parametric test and does not require the data to be normally distributed. Second, the test has low sensitivity in abrupt breaks due to inhomogeneous time-series (Tabari *et al.*, 2011). Any data reported as non-detects are included by assigning them a common value that is smaller than the smallest measured value in the data set. According to this test, the null hypothesis *H0* assumes that there is no trend (the data is independent and randomly ordered) and this is tested against the alternative hypothesis H1, which assumes that there is a trend (Oznos and Bayizit, 2003).

The basic principle of Mann-Kendall (MK) tests for trend is to examine the sign of all pair wise differences of observed values (Libiseller and Grimvall, 2002). A Univariate form of such tests was first published by Mann (1945), and the theory of multivariate MK tests is due to Hoeffding (1948), Kendall (1975), and Dietz and Killeen (1981). During the past two decades, applications in the environmental sciences have given rise to several new MK tests. Hirsch and Slack (1984) published a test for detection of trends in serially dependent environmental data collected over several seasons.

The MK statistic for monotonic trend in a time series $\{Z_k, k= 1, 2....n\}$ of data is defined as:

$$T = \sum_{j<i} \text{sgn}(Zi - Zj) \qquad (6)$$

Where

$$\mathrm{sgn}(x) = \begin{cases} 1, if \cdots x > 0 \\ 0, if \cdots x = 0 \\ -1, if \cdots x < 0 \end{cases} \quad (7)$$

If no ties are present and the values of Z_1, Z_2.....Zn are randomly ordered, this statistic test has expectation zero and variance:

$$Var(T) = \frac{n(n-1)(2n+5)}{18} \quad (8)$$

Furthermore T is approximately normal if n is large (n >10) – (Kendall, 1975).

Finally the null trend hypothesis can be rejected at α% confidence level if T (in absolute value) is greater than a corresponding threshold, which value is $z \cdot \sqrt{\text{Var}}$ (T), retrieved from the standard normal distribution table. The level of significance is represented by α and Z and the Z-scores and are represented as follow: Z= ±2.576 where α = 0.001, Z= ±1.960 where α =0.05 and Z= ±1.645 where to α =0.1.

Besides the Z statistic, the test delivers the p-values of the trend statistic, which yields an estimated probability that the observed trend could have occurred by chance. It expresses the trend significance. The lower the p-value, the higher is the likelihood that there is a trend in the data. In this work, a threshold for the p-value of 0.07 was used to map exclusively strong significance trends.

The Theil-Sen method is also used to estimate the trend strength in NDVI time-series. This procedure calculates the linear trend at each pixel using all pair wise combinations of images in

time and takes the median of all slopes to create a slope image for each of the greenness parameters (Hoaglin *et al.*, 2000). The Theil-Sen slope represents the overall trend of the series and is not affected by outlier values, as long as the number of outliers is less than 0.29 times the total number of observations in the series (Hoaglin *et al.*, 2000). For example, a conversion of forest to urban land cover within one 8-km by 8-km pixel grid would register as potential change if dominant (in this case decreasing) trends of NDVI values have persisted for at least 29% (~8 out of 26 observations) of total observations in the time-series (Neeti *et al.*, 2012).

4.3.2. Investigating the relation between NDVI and rainfall

This section investigates the relationship between NDVI and rainfall. The interannual anomalies between them were also compared. The subsequent sections provide detail analysis.

4.3.2.1.NDVI and Rainfall Greening anomalies

Measurements from different distributions, describing different variables and populations, can be standardised (or normalised) in order to provide a way of comparing them that includes consideration of their respective distributions. This is carried out by transforming the original observations into Z-scores which are expressed as standardized deviations from their mean. The z-score distributions always have a mean of 0 and a standard deviation equal to 1 (Abdi, 2007).

The z-score, also called the standard score, the normal score, the standard normal variate, the standard normal deviate or the standardized score is a dimensionless quantity. It is derived by subtracting the population mean from an individual raw score and then dividing the difference by the population standard deviation (Snedecor and Cochran, 1980; Hammond and McCullagh, 1982). The z-score indicates how many standard deviations are above or below the mean. In

other words, it represents the distance between the raw score and the population mean in units of the standard deviation. When the raw score is below the mean Z is negative and positive when above the mean. The standard score is:

$$z = \frac{x - \mu}{\sigma} \qquad (9)$$

Where **x** is a raw score to be standardised

σ is the standard deviation of the population, and

μ is the mean of the population

The annual variability of NDVI and rainfall as well as their spatio-temporal relationship was investigated by calculating yearly NDVI and rainfall anomalies to allow for comparative analysis expressing both variables in terms of data converted to z-scores. The z-scores were calculated on pixel basis to assess each pixel annual deviation from its long-term mean.

The anomalies (i.e. z-scores) have certain advantages over absolute values such as annual integrated NDVI and total annual rainfall. First of all and due to the standardization procedure the z-scores represent an efficient way to visually compare the spatial relationship between NDVI and rainfall. Further standard analysis of the relationship between NDVI and rainfall tend to be influenced by the presence of spatial auto-correlation (i.e. the phenomenon where locational similarity is matched by value similarity), which in essence means that they are merely expressing an underlying geographical relationship rather than a true relationship of dependence.

The z-scores methodological approach provides a very robust and valid estimate of temporal (rather than spatial and geographical transect driven) NDVI and rainfall variability.

4.3.2.2. Correlation analysis between rainfall and NDVI

NDVI time-series data for each station was extracted from 30-year NDVI time-series images. Correlation coefficient between seasonal mean NDVI and seasonal integral was calculated for each station. Generally, there is a time lag between rainfall events and response of vegetation to such event. The time interval between a precipitation event and the time when the precipitation reach a plant roots and affect growth vary from 1 to 12 weeks depending on the vegetation type (Li *et al.*, 2002). Seasonal integral rainfall has been used in this analysis in order to eliminate the time lag.

4.3.3. Linking change in vegetation productivity to climate and LULC change

Many studies have shown a strong relationship between inter-annual changes in vegetation activity and precipitation. Thus it is clear that climate signal in NDVI time-series expected to be very strong. Climate should have a substantial control on NDVI through annual precipitation. This control however should be predictable in every point of the study area where the relationship between NDVI and climate change are statistically significant. Identification and quantification of climate signals should help to discriminate between the two major factors of vegetation change being climatic and anthropogenic. A number of recent studies have already developed monitoring systems for land degradation assessment that separate the dynamics of vegetation cover driven by human activity and climate (Li *et al.*, 2004; Evans and Geerken, 2004; Wessel *et al.*, 2004 and 2007; Propastin *et al*, 2008; Landmann and Dubovyk, 2014; Zhang

et al., 2014). These monitoring system for degradation assessment using remote sensing data are not globally suitable. In this study a system of discrimination between climate and human driving forces in vegetation change has been utilised. This simple system is based on the concept of synchrony and asynchrony of time-trends in vegetation and climate factors. This concept is based on the framework developed by Propastin *et al.* (2008) (Figure 6).

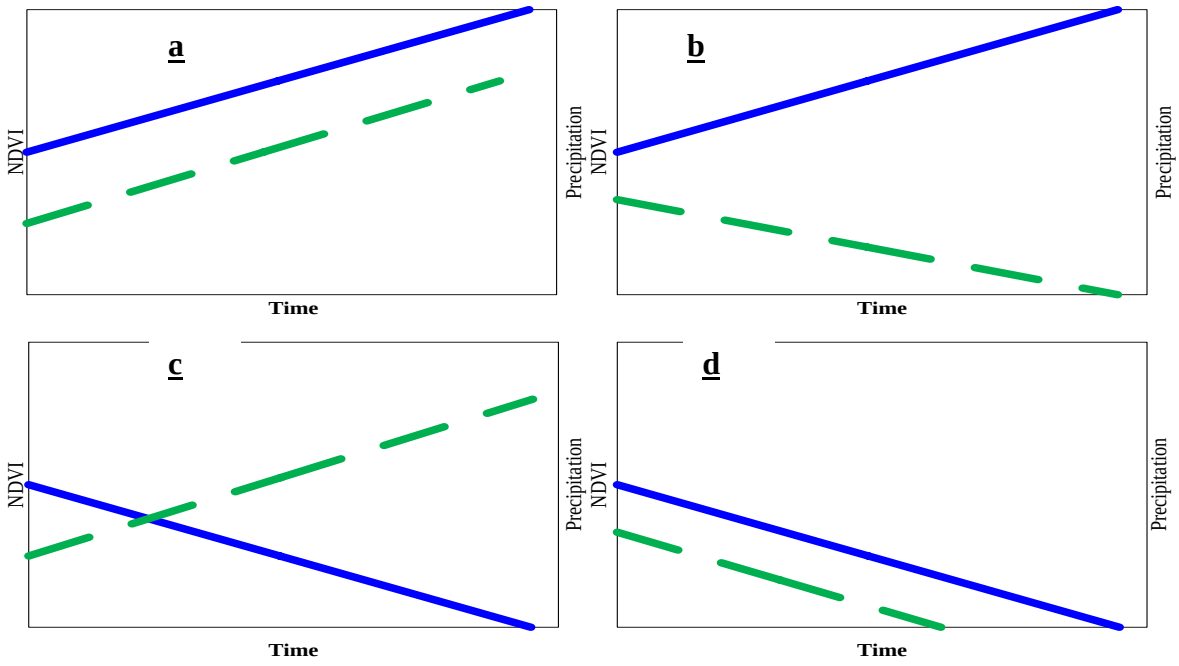

Figure 6: Scenarios described to illustrate how the combine used of NDVI and precipitation time-series may help to detect a vegetation cover being improved or degraded. A thick broken line (Green) and a thick unbroken line (blue) represent respectively NDVI and precipitation trends. (After Propastin *et al.*, 2008)

Figure 6-a displays improving vegetation cover caused by increase in precipitation; Figure 6-b degradation of vegetation cover caused by human impact; Figure 8-c recovering vegetation cover caused by human impact and Figure 6-d vegetation degradation due to climate change. In Figure 6-a, the upward trend in NDVI is synchronous to precipitation. Then, the observed improved vegetation cover will be due to increasing precipitation. In Figure 6-d, the downward trend in NDVI is synchronous to precipitation. Thus, the decreasing NDVI is driven by a decrease of

precipitation. In Figure 6-b and Figure 6-c, the trends are asynchronous. NDVI decreases even as precipitation increases for one case, and decrease of precipitation did not cause an improvement of vegetation cover for the other. This may be the cases when vegetation is recovering or degrading due to others factors than climate, probably human induced.

4.3.3.1. Identification of climate and anthropogenic signals in the vegetation time-series

Taking into account the relationship between rainfall and NDVI as the key factor for the method described earlier in Figure 6, the system will work only in an area where this relationship is strong and is statistically significant. Since this relation for this study area is weak, one cannot use this criterion for splitting climate and human-induced land degradation in the study area. This study combines analysis of long-term trend in vegetation, trend in rainfall, the NDVI coefficient of variation and its departure from the long-term mean to map vegetation productivity loss or recovery over the period (Table 3). For example, if a pixel shows positive trend in NDVI and rainfall with a positive departure from its long-term mean and low variability, this is considered to indicate a rainfall driven change vegetation cover. But if the NDVI shows positive trend and negative rainfall trend with low variability and a positive departure from long-term mean, then it could be considered as a human-impacted recovery. Contrary, if a pixel shows a negative NDVI trend and a positive trend in rainfall and negative departure from its long-term mean, this could be considered as an anthropogenic-induced degradation, whereas a negative NDVI and negative rainfall trend and a negative departure from the long-term mean would indicate climatic-induce degradation.

Table 3 : Vegetation index and Rainfall characteristics for the subset selection

Reference site #	NDVI trend ($p<0.07$)	Rainfall trend	NDVI CoV	NDVI Departure
1	-	+	15 %	Neg. (-0.22)
2	+	-	12 %	Pos. (+1.43)
3	-	-	6 %	Neg. (-2.50)
4	+	+	12 %	Pos. (+3.13)

4.3.3.2. Using Landsat data to verify land degradation/recovery for selected sites

A fundamental goal of remote sensing analysis is the classification of an image or scene (Lusch, 1999). Supervised classification is a widely used technique in satellite image processing (Forkuo and Frimpong, 2012) was used to produce LULC classes. The success of the method depends on the accuracy of training data as well as field investigation. Supervised classification is the procedure most often used for quantitative analysis of remote sensing image data (Richards and Jia, 2006). For the purpose of this study a supervised Maximum Likelihood Classification based on the spectral distances between different classes was used to quantify the change in land cover. Maximum likelihood classification is the most commonly used supervised classification method of remotely sensed imagery (Manandhar *et al.*, 2009, Forkuo and Frimpong, 2012). It uses the mean and covariance matrix of each class. Sufficient training samples for each spectral class must be available to allow reasonable estimates of the elements of the mean vector and the covariance matrix to be determined. For an N dimensional multi-spectral space, at least N+1 samples are required to avoid the covariance matrix being singular. Maximum classifier

algorithm computes these equations to classify the image based on training data for each pixel at specific location x:

$$p(x) = \sum_{i=1}^{M} p(x \mid w_i)\, p(w_i) \qquad (10)$$

Where:

p(x) = Probability of finding a pixel from any class at location x; M = Total number of class 1…M; p(x| w_i) = Probability that pixel at location x belong to class wi; p(w_i) = Probability that class wi occurs in the image.

The p (wi) is called prior probabilities since they are the probabilities with which class membership of a pixel could be guessed before classification. By comparison the p (x|wi) is posterior probabilities. Then the classification rule is: x ε wi if p(x|wi) p(wi) > p(x|wj) p(wj) for all $j \neq I$

4.3.3.3. Accuracy Assessment of the classification

Accuracy assessment was performed for the three Landsat–based LULC maps. It is important to measure the reliability of the classification. This is achieved by making comparison between the image classification and validation data, often called 'ground truth' or 'ground control' data that represents verified landscape states and conditions (Weiss and Walsh, 2008). The Overall Accuracy and Kappa coefficient are routinely used to assess the accuracy of the classifications. The Overall Accuracy is calculated by summing the number of pixels classified correctly and dividing by the total number of pixels. The Kappa coefficient (k) is defined as:

$$K = (N\sum_{k} x_{kk} - \sum_{k} x_{k\sum^{x}\sum k})(\frac{1}{N^2 - \sum_{k} x_{k\sum^{x}\sum k}}) \qquad (11)$$

With N being the total number of pixels in all the ground truth classes, X_{kk} is the sum of the confusion matrix diagonals and $X_{k\sum^{x}\sum k}$ is the sum of the ground truth pixels in a class times the sum of the classified pixels in that class summed over all classes.

At the same time, producer's accuracy and user's accuracy were used to estimate the accuracy of each individual class. The producer's accuracy results from dividing the number of correctly classified pixels in each category (on the major diagonal) by the number of training set pixels used for that category (the column total). This figure indicates how well training set pixels of the given cover type are classified (Lillesand and Kiefer, 1994). User's accuracy is computed by dividing the number of correctly classified pixels in each category by the total number of pixels that were classified in that category (the row total). This Figure is a measure of commission error and indicates the probability that a pixel classified into a given category actually represents that category on the ground (Lillesand and Kiefer, 1994). The Accuracy assessment can be affected by samples number for each class. As the samples number increases, the accuracy assessment becomes more reliable (Richard and Jia, 1999).

4.3.3.4. Change detection

After performing the classification of the images for every year, a post-classification comparison change detection algorithm was used to determine changes in LULC over three intervals, namely: date1 to date2, date2 to date3 and date1 to date3. Post-classification comparison has been proven to be the most effective approach for change detection, because each image is

separately classified, thereby minimizing the problem of normalizing for atmospheric and sensor differences between two dates (Jensen, 2005). The post-classification approach provides ‘‘from–to’’ change information, for which LULC transformations can be calculated. Cross tabulation analysis was carried out to analyze the spatial distribution of different LULC classes and LULC changes. The rate of land conversion was computed using this formula:

$$Change(\%) = \frac{AreaD2 - AreaD1}{AreaD1} \times 100 \qquad (12)$$

Change area = D2 –D1, where D1and D2 are the area of the target vegetation cover type at the beginning and the end of the study period, respectively.

5. ANALYSIS OF RAINFALL TIME-SERIES DATA

5.1. Introduction

The network of meteorological stations in the catchment is administrated by national meteorological services of Mali (Mali Meteorological Agency), Burkina Faso (General Directorate of Meteorology) and Cote d'Ivoire (Operating and Development Company of Airport, Aeronautical and Meteorological Data: SODEXAM). The number of meteorological stations in the study area is seventy (70). All of these stations, except the ones from Cote d'Ivoire, are part of the Interstate Committee for Drought Control in the Sahel (CILSS) rainfall network. The CILSS network consists of more than 650 rainfall gauges dispatched in nine (9) member countries. These gauges are managed by the national meteorological service for each country which report to the centre at the end of the rainy season for managing meteorological database.

This study used only meteorological station in the catchment or at twenty kilometres in the boundary. In line with the objectives of this work, all stations with more than three years of missing data were removed from the analysis. The quality of the data is assessed and the gaps are filled by the long-term mean for each missing month. Finally rainfall data from 40 meteorological stations (30 stations in Mali, 5 in Burkina Faso and 5 in Cote d'Ivoire) completed by the TRMM data were used and analysed. The linear relationship between gauge rainfall and TRMM data showed a good relationship between the two data with a correlation coefficient up to 0.8 for all the stations used in this analysis. Figure 7 presents this relationship for selected stations throughout the study area. From these total, 28 meteorological stations are located in the Sudanian zone, while 8 are in Sudano-Guinean zone and 4 in Sahel zone. The general

characteristics of these stations are listed the Chapter (4)**.** The spatial distribution of the stations is shown in Figure 8**.** The stations are fairly distributed but the density is lower with a mean distance of about 40 kilometres between stations.

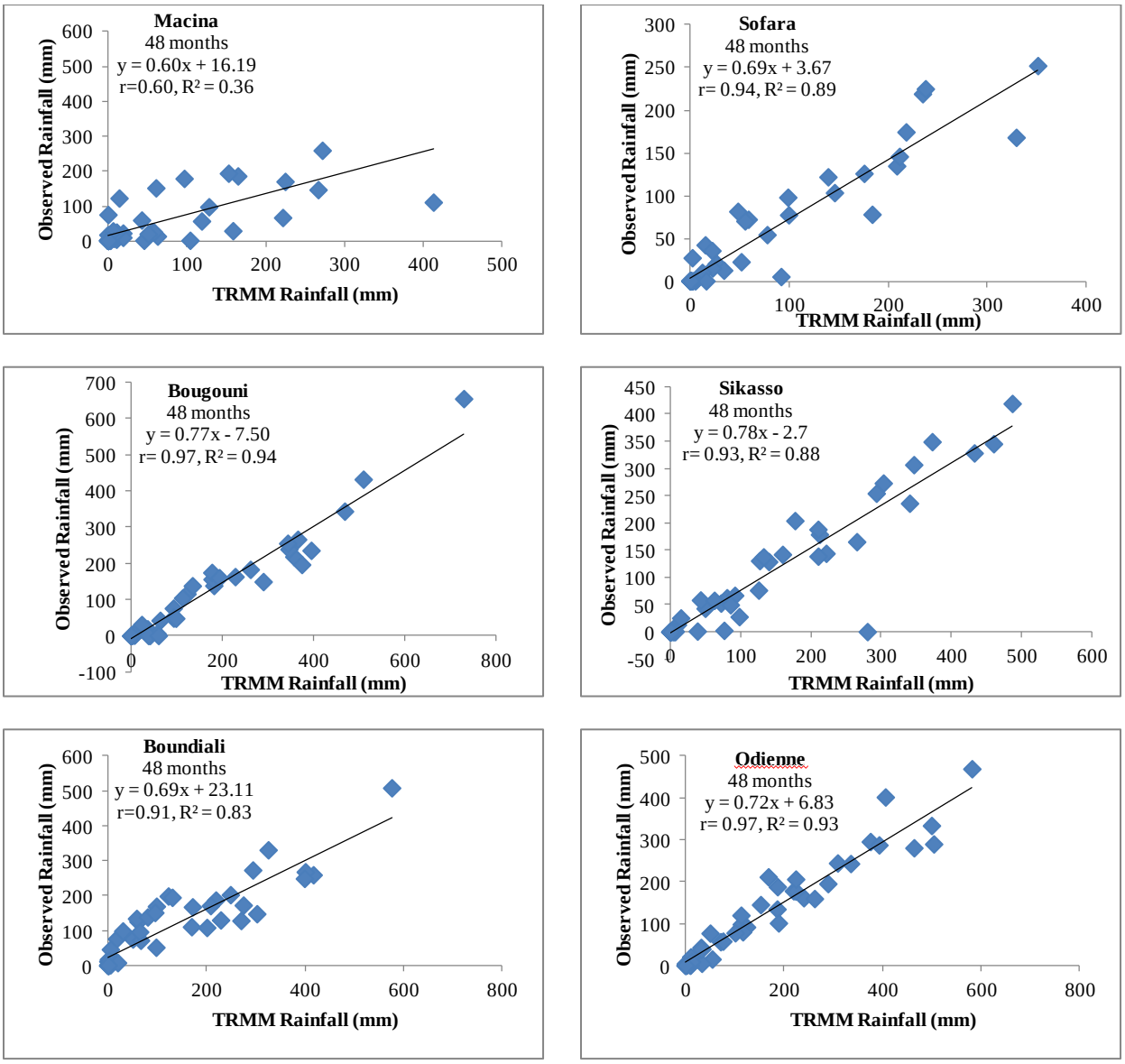

Figure 7: Regression statistics for 3 stations: Macina and Sofara (North, Sahelian zone), Bougouni and Sikasso (Centre, Sudanian zone), Boundiali and Odienne (South, Sudano-Guinean zone).

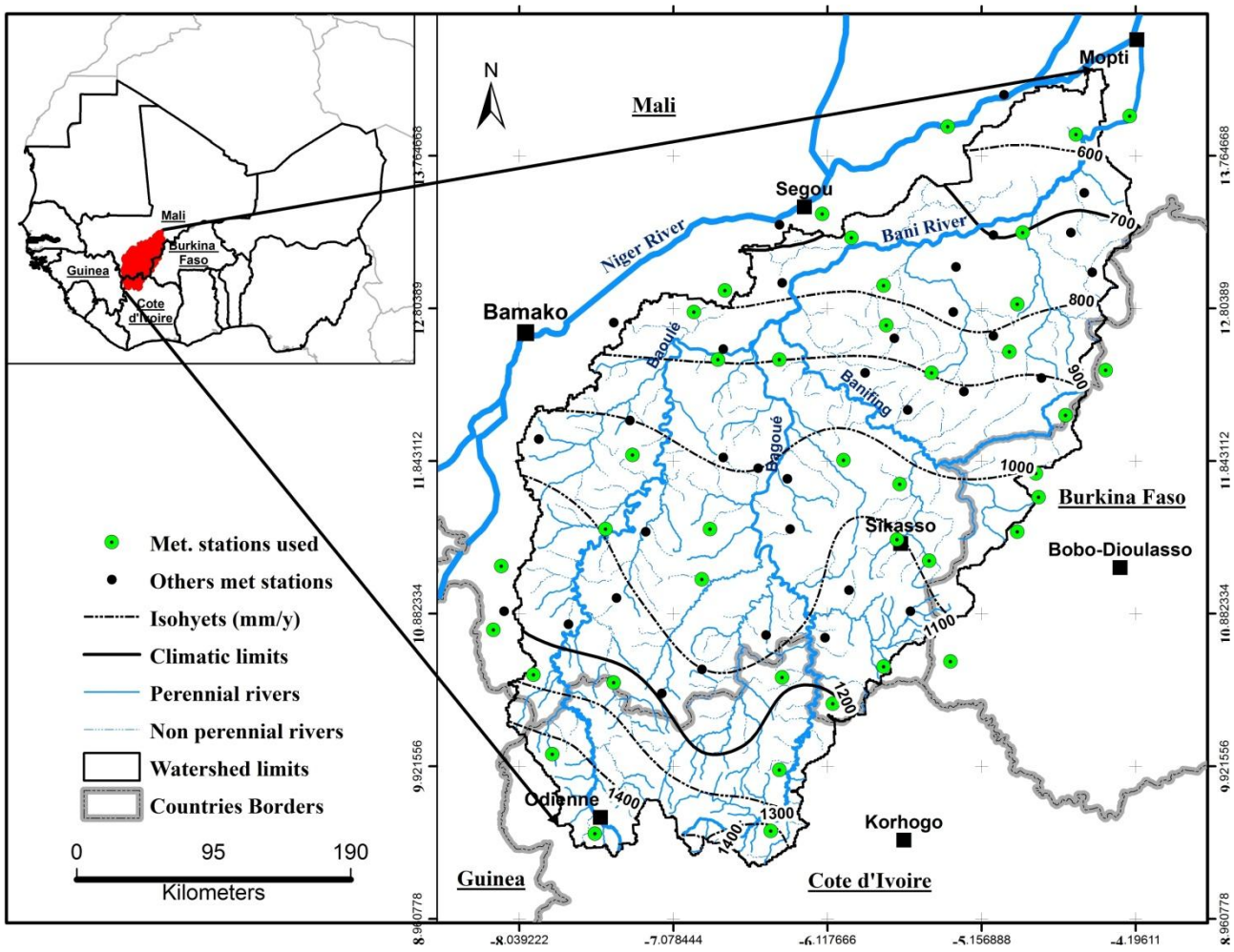

Figure 8: Map showing the distribution of the meteorological stations used in the study.

Modelling spatial pattern of mean seasonal rainfall time-series is shown in Figure 9. This result was obtained using IDW method considering the integral rainfall for the months April to October referred to AMJJASO representing the growing season. The rainfall in the study area is typically concentrated in the summer months, as a result, this study focussed only on this period. The relief has only a minor impact on the rainfall, thus, it has not been used in the modelling of the gridded rainfall series. The spatial distribution confirms the North-South gradient in the rainfall

pattern. The rainfall amount varies from less than 480 mm in the Northern area to greater 1200 mm/ season in the Southern and differs from one year to another.

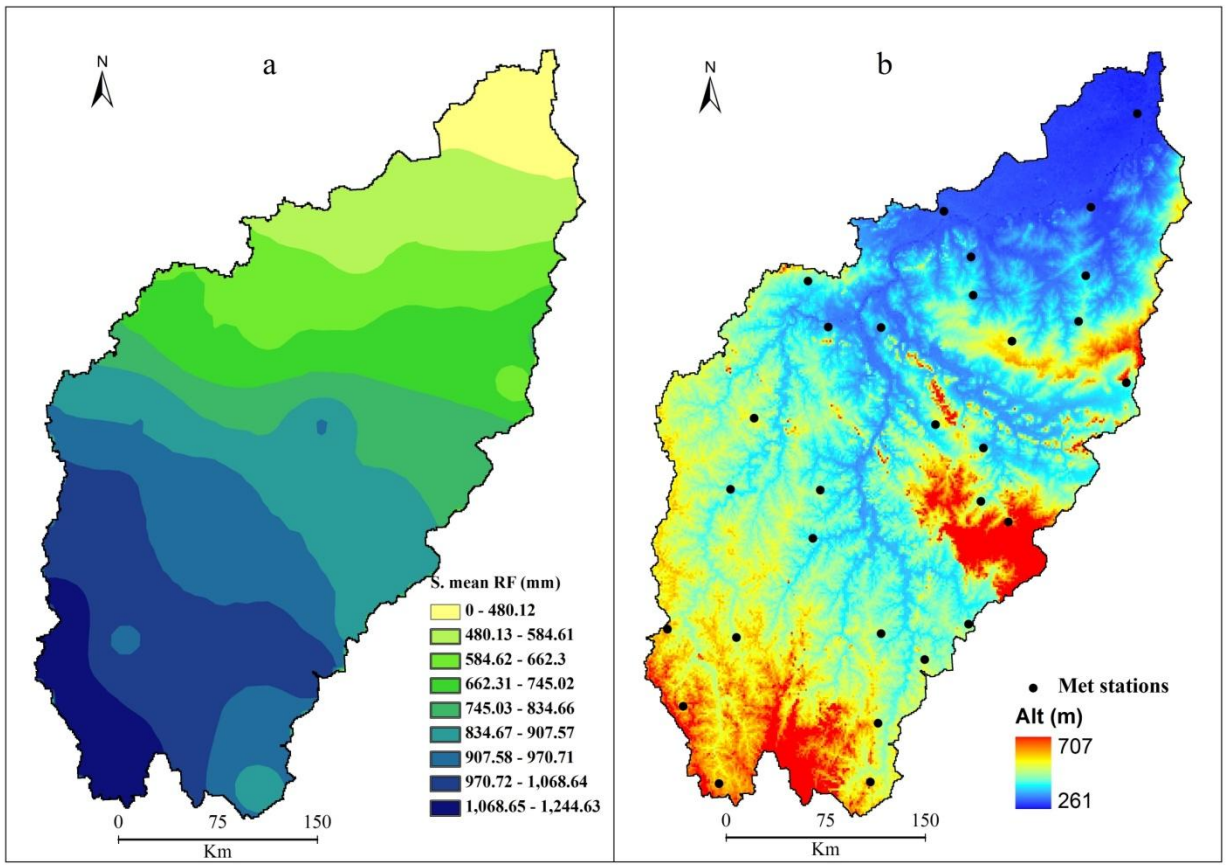

Figure 9: (a) Spatial variation of mean seasonal rainfall (1982-2011) and the Digital Elevation Model (b) for the study area.

5.2. Distribution of seasonal rainfall

The rainfall distribution (Figure 10) is characterised by an increase in the amount of precipitation and a higher amount from June to September. The contribution of each month to the seasonal rainfall is different from one climatic zone to another. For most of the stations August rainfall account for more than 25%: 35% in Sahel zone, 26% in Sudanian zone and Sudano-Guinean zone. The July, August and September rainfall are critical to the total rainfall because they

account for more than 70% in the Sahel to 50% in Sudano-Guinean zone. The contribution of April and May are low in Sahel, 1 to 5% and about 7% in Sudano-Guinean zone.

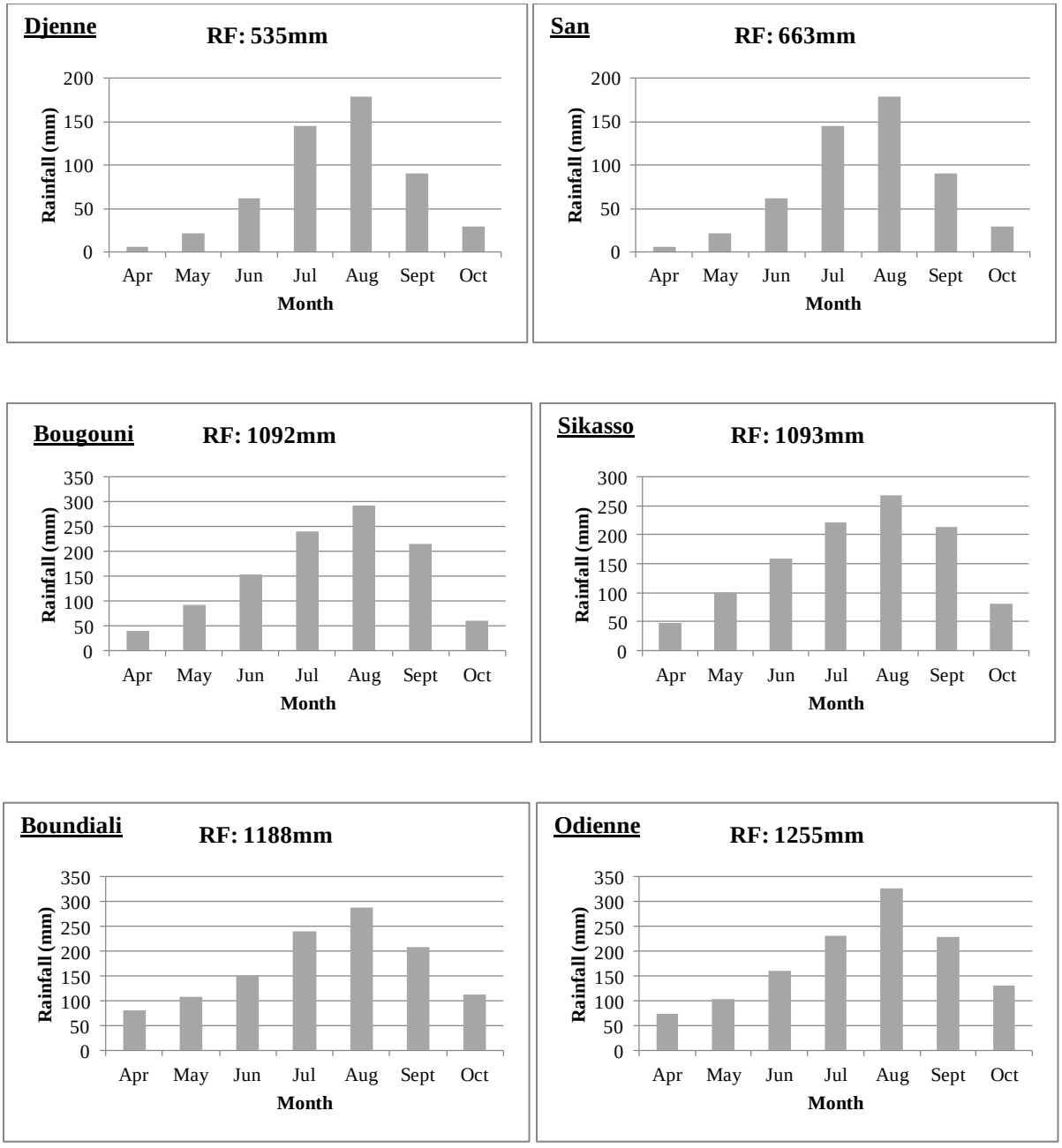

Figure 10: Distribution of rainfall in the growing season for the period 1982-2011 for the Sahel (Djenne and San), Sudanian (Bougouni and Sikasso) and Sudano-Guinean (Boundiali and Odienne).

5.3. Statistical analysis of rainfall data

5.3.1. The inter-seasonal variability of precipitation

The arid and semi-arid climates are characterized by high variability of climate parameters from one year to another, especially high rainfall variability. The high variability in precipitation causes high variability of ecosystem conditions and is the main cause for the difficulties of vegetation and animal survival in the dryland. The variability of rainfall is illustrated with the aid of standard deviation (STD) and coefficient of variation (CoV). In this study, standard deviation and coefficient of variation were computed for precipitation data for each station. The spatial distributions of these parameters are shown in Figure 11 and Table 4 for the station level statistic. Throughout the area, the variability in precipitations differs from one area to another.

Table 4: Rainfall STD and CoV at station level (only stations completely inside the basin are presented here)

Station	Pays	STD	CoV	Station	Pays	STD	CoV
Bougouni	ML	151.71	0.15	Misseni	ML	108.67	0.1
Kadiolo	ML	124.88	0.14	Cinzana	ML	26.91	0.04
N'tarla	ML	118.66	0.18	Manakoro	ML	86.92	0.09
Sikasso	ML	94.8	0.1	Kolondieba	ML	12.38	0.01
Koutiala	ML	135.8	0.19	Bla	ML	91.06	0.16
San	ML	95.79	0.18	Klela	ML	14.66	0.01
Dioila	ML	26.29	0.03	Odienne	CI	232.78	0.18
Djenne	ML	49.46	0.13	Dogo B.	ML	80.96	0.08
Mahou	ML	102.3	0.16	Koumantou	ML	57.86	0.06
Beleko	ML	75.21	0.11	Boundiali	CI	92.43	0.1
Kimparana	ML	30.04	0.05	Farako	ML	82.07	0.09
Dionkele N.	BF	109.74	0.13	Filamena	ML	47.82	0.03
Kignan	ML	106.14	0.11	Tengrela	CI	118.77	0.11
Bobola Z.	ML	86.08	0.12	Kouto	CI	104.08	0.11
Fana	ML	12.25	0.02	Minignan	CI	22.93	0.02

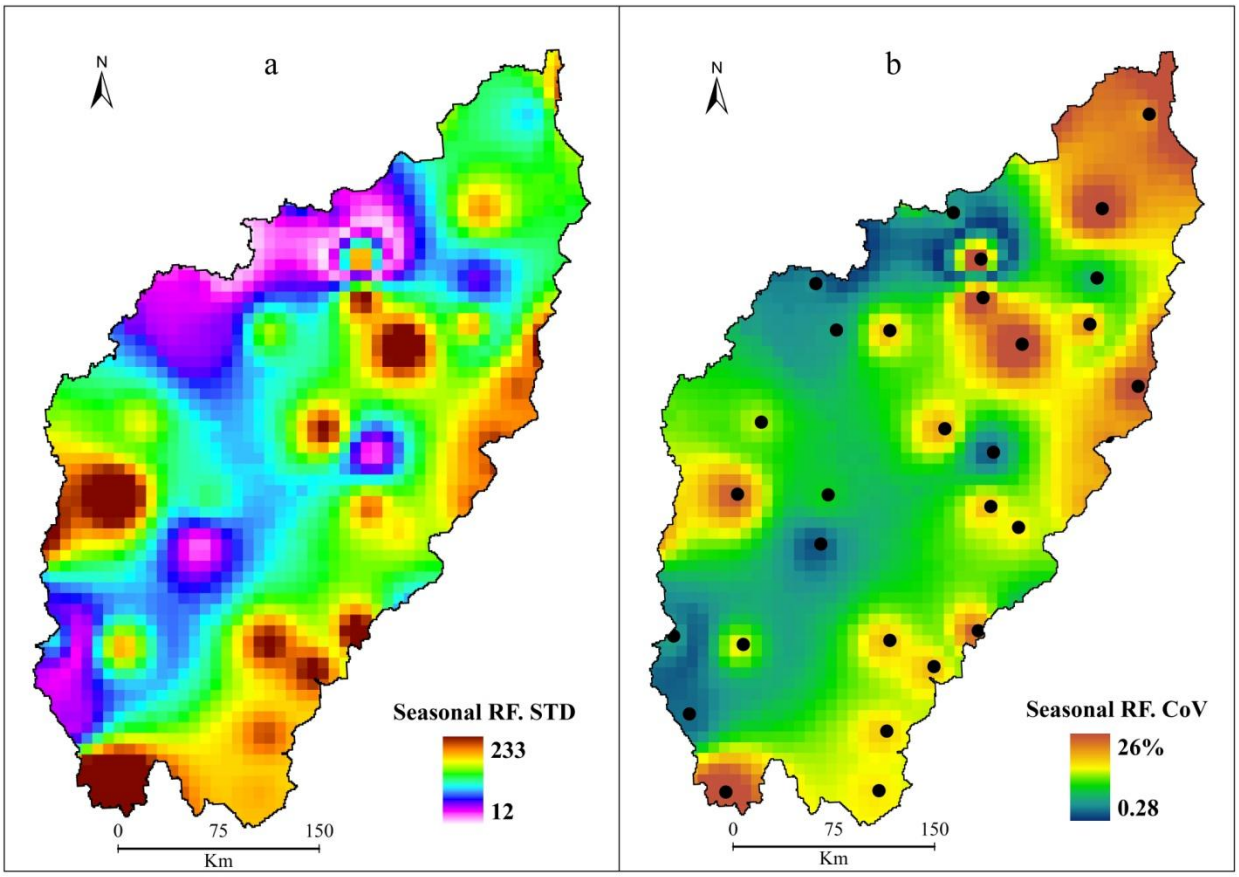

Figure 11: (a) Standard deviation of Rainfall and (b) coefficient of variation of seasonal rainfall (RF) for the period from 1982 to 2011

The coefficient of variation of the growing season across the study area is spatially shown in Figure 11-b. Throughout, the study region the variability in precipitation is mixed. It decreases from a mean value of 25% mainly from the North to 0.03% in West and South West. From 30 stations considered in this analysis only seven exhibit a high variability. Most of them are located in the northern part, except the station of Odienne in South.

5.3.2. Change in decadal rainfall

The rainfall time-series for the period from 1982 to 2011 (30 years) is divided into the following three sub-sets: 1982-1991 (P1), 1992-2001(P2) and 2002-2011 (P3). These sub-sets are not

following any particular climatic period, even though each include years with above and below normal rainfall condition. The mean rainfall for the period (in mm), the standard deviation and the coefficient of variation is computed using the total seasonal rainfall (Table 5).

Table 5: Differences in the mean and coefficient of variation of annual rainfall

Stations*	Mean RF P1	CoV	P2-P1	Mean RF P2	CoV	P3-P2	Mean RF P3	CoV	P3-P1
Bougouni	1093.24	16.12	-12.66	1080.58	19.31	-26.78	1053.80	18.44	-39.44
Kadiolo	931.24	14.60	132.95	1064.19	16.12	72.93	1137.12	9.83	205.88
Ntarla	679.10	14.97	176.85	855.96	24.03	-8.81	847.15	19.38	168.05
Sikasso	978.75	13.97	75.75	1054.50	20.09	75.49	1129.99	12.48	151.25
Koutiala	762.29	18.88	75.97	838.25	26.05	17.75	856.00	21.23	93.71
San	618.43	21.84	7.21	625.64	25.37	46.88	672.52	21.23	54.09
Dioila	746.79	17.46	25.73	772.53	27.86	47.09	819.62	23.10	72.82
Djenne	448.61	21.48	86.73	535.34	22.26	53.57	588.91	24.63	140.30
Mahou	734.05	16.09	127.55	861.60	19.05	39.31	900.92	17.32	166.87
Beleko	666.79	9.68	108.49	775.28	22.69	9.79	785.07	23.20	118.28
Kimparana	667.16	15.51	56.37	723.52	27.57	41.91	765.44	19.67	98.28
Kignan	881.01	10.29	30.18	911.19	26.14	-42.63	868.56	16.44	-12.45
Bobola Z.	720.35	15.45	99.12	819.46	22.40	56.78	876.24	17.14	155.89
Fana	713.80	10.09	57.97	771.77	26.94	33.24	805.01	21.02	91.21
Misseni	1060.62	9.71	45.81	1106.44	16.56	-91.52	1014.92	12.67	-45.71
Cinzana	601.50	11.89	89.55	691.05	22.28	-52.27	638.78	21.41	37.28
Manakoro	1058.71	11.83	76.92	1135.63	17.86	-105.99	1029.63	19.37	-29.08
Kolondieba	965.87	14.16	69.74	1035.61	15.64	50.38	1085.99	14.58	120.12
Bla	610.57	14.49	117.11	727.68	17.13	-10.75	716.93	15.74	106.36
Klela	846.48	12.02	85.96	932.44	11.97	32.96	965.39	14.42	118.91
Odienne	1163.61	15.77	67.32	1230.93	15.73	94.66	1325.59	10.62	161.98
Dogo B.	947.34	10.01	61.54	1008.88	15.83	17.40	1026.28	25.35	78.94
Koumantou	977.43	11.81	-55.86	921.57	19.74	135.43	1057.00	16.89	79.57
Boundiali	1121.51	16.77	108.85	1230.37	19.77	-64.08	1166.28	14.38	44.77
Farako	951.18	11.52	95.55	1046.73	12.68	106.68	1153.41	12.59	202.23
Filamena	1203.20	5.78	174.77	1377.97	15.75	-65.11	1312.86	20.61	109.66
Tengrela	923.84	12.36	99.53	1023.37	24.60	163.06	1186.43	15.60	262.60
Kouto	1070.10	11.61	34.04	1104.14	18.57	-43.45	1060.69	10.96	-9.41
Minignan	1178.50	10.38	78.89	1257.39	12.75	-157.85	1099.54	20.02	-78.96

* Only Stations located within the catchment are presented here.

Comparing the periods P1 and P2, the seasonal rainfall amount showed an increase for all of the stations used except of Koumantou and Bougouni station where a decrease of 56 mm and 12 mm respectively where recorded. Between the second period P2 and the third period P3, the rainfall amount in 11 stations showed a decline in their seasonal total.

5.3.3. Trends in rainfall time-series

The seasonal precipitations over the study area for the period from 1982-2011 include drought year, normal years and to some extend also extremely dry condition. The seasonal series include the rainfall for the months April to October. The Mann Kendall test was applied to seasonal rainfall time-series for trend test and p-value was used for the strongly trend significance estimation. The spatial distribution of the Kendall tau (MK-z) and p-value of significance is shown in Figure 12. As shown in the result (Figure 12-a), the rainfall spatial pattern exhibits an increase for the majority of the area.

The precipitation amount increased for about 17 mm during the study period for most of the rainfall station used. In contrast the results of significance test applied reveal only a few portions in the study area with a significant positive trend (p-value < 0.7) (Figure 12-b). These areas are the Northern, Eastern and Odienne area in the Southern corner.

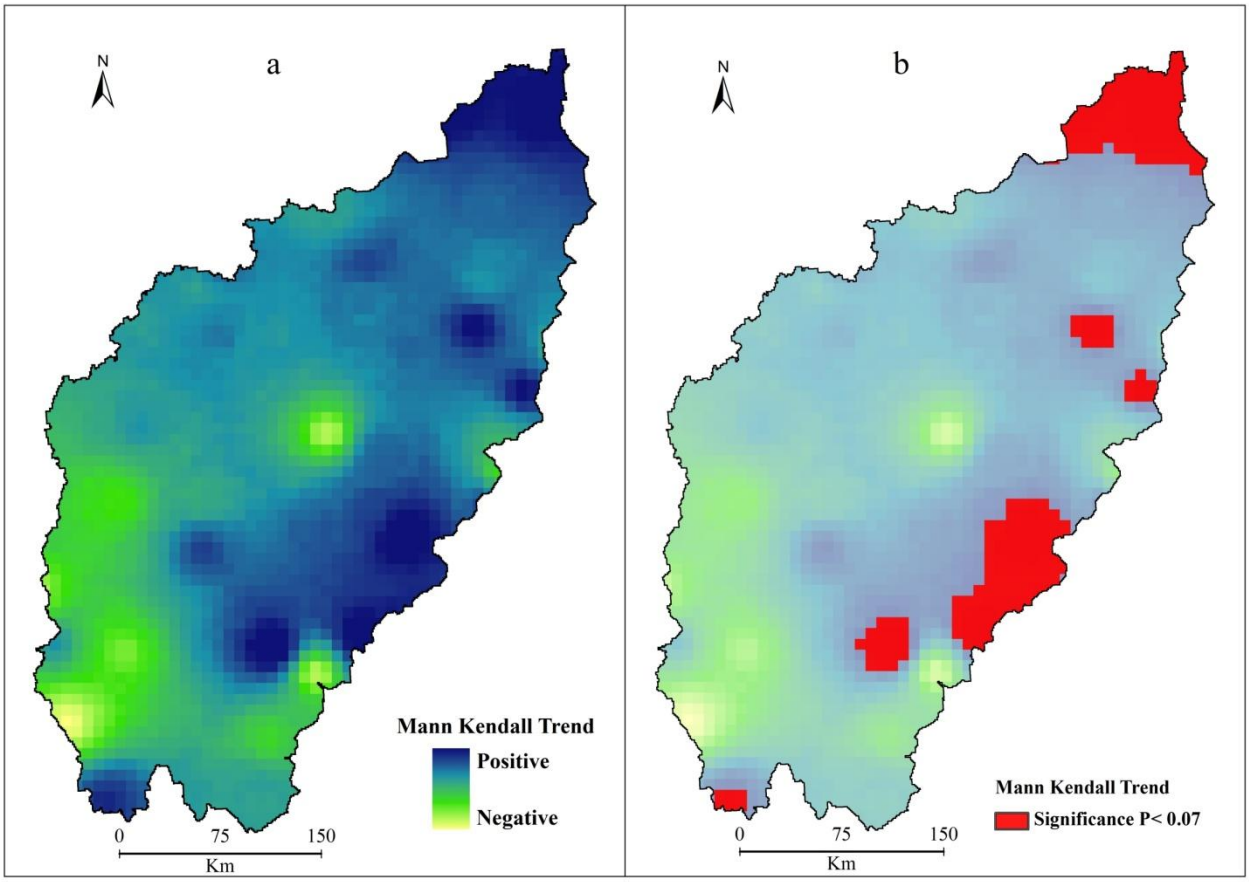

Figure 12: (a) Mann Kendall trend in growing season rainfall and (b) Areas showing significant trend at $p<0.07$

5.4. Discussion

Climate is the most important determinant of vegetation density and dynamics within semi-arid ecosystems which are characterised by high inter-annual variability. The most important climate variable over West Africa is rainfall, and hence many sectors of the economy depend on water as a resource. The high variability and change in African and especially West African rainfall have been investigated in several research studies (Le Barbé *et al.*, 2002; Nicholson *et al.*, 2000; Nicholson, 2013). This section examined the rainfall time-series in the study area and creates a

basis for further analysis of vegetation dynamic and its relationship with climatic factors represented by rainfall in this study. The spatial rainfall distribution, variability and trend over the 30-year have been investigated using an 8 km gridded rainfall time-series data for the study area.

The precipitation is characterized by the seasonal movement of the Intertropical Convergence Zone (ICTZ) and the main factors influencing it distribution are associated with the sea surface temperature and the El Nino-Southern Oscillation (ENSO) (Koumare, 2014). The rain band resides offshore the Guinean coast during December to February when it is the weakest of the year. During the spring, as its moves onshore and strengthens, this rain band becomes part of the West African Monsoon (WAM). The evolution of the WAM rainfall undergoes several stages (Le Barbé *et al.*, 2002). The first is the intensification of a quasi-stationary rain band along the Guinean coast during April to June. This is followed by a sudden change of the rain band northwards to the Sahelian region in late June and July (Sultan and Janicot, 2000), where it becomes quasi-stationary again until October. After that, the rain band weakens gradually while, in contrast to the sudden northward change in July, moving southwards smoothly to its weakest position offshore in the boreal winter.

Rainfall in the study area is seasonal with most of the rain falling between April and October with the maximum occurring in August. The total rainfall varies across the catchment with the Southern area receiving 1200 mm per year while the Northern area receiving only 480 mm year for the period 1982-2011. For the spatial pattern of the entire study area, the variability in growing season precipitation amounts to 26%. For the individual station, the coefficient of variation ranged from 1% (Kolondieba station) to 19% (Koutiala station).

The results of trend analysis in rainfall time-series exhibited low statistic inference of trend for most for the area. Although all stations exhibited upward trend in growing season precipitation, only a few portion showed a trend, which were significant at p-value less than 0.07. These results are in agreement with Bégué *et al.* (2011), who observed a similar no significant rainfall trend in the same area during the period from 1982 to 2005 for almost the whole catchment.

6. TREND ANALYSIS IN NDVI TIME-SERIES DATA

6.1. Introduction

Trend is the overall temporal trajectory of an indicator. Time-trends are reference points that are easily understood by stakeholders and generally are not biased in an obvious way (O'Malley and Wing, 2006). The direction of trend can be increasing, decreasing, or stable. However, if a trend is not considered in regards to a reference, the results may be misleading (O'Malley and Wing, 2006). The establishment of a benchmark and the subsequent analysis of trend allow assessment of ecological resilience i.e. the response and recovery of an ecosystem in relation to a disturbance (Westman, 1985). A time-series of data allows examination of specific characteristics of resilience including for example, elasticity (time to recovery) and amplitude (the magnitude of the initial departure of a measurement indicator from the benchmark state). Roughly 30-year duration of NDVI data is good to discriminate between significant changes due to variation caused by seasonal and interannual climatic variation. In this regard, the following sections investigates the long-term trend in vegetation dynamic in Bani river basin using a 30-year (1982-2011) NDVI time-series data.

There are many methods to investigate time-series data. The details were introduced in Chapter 4. Considering the larger dataset, the study employs a MK trend test on monthly and annual NDVI time-series for the study period.

6.2. Comparison of GIMMS and SPOT VGT dataset for 1998-2006

The linear modelling between the GIMMS and the SPOT VGT datasets using some reference land use / land cover types showed good relationship between the two dataset (Figure 13) with a mean correlation coefficient of 0.83 for the study area. The highest correlation ($r \geq 0.9$) between GIMMS and SPOT VGT NDVI was found in savannah, whereas the lowest correlation ($r \leq 0.75$) was found in forest and Shrublands.

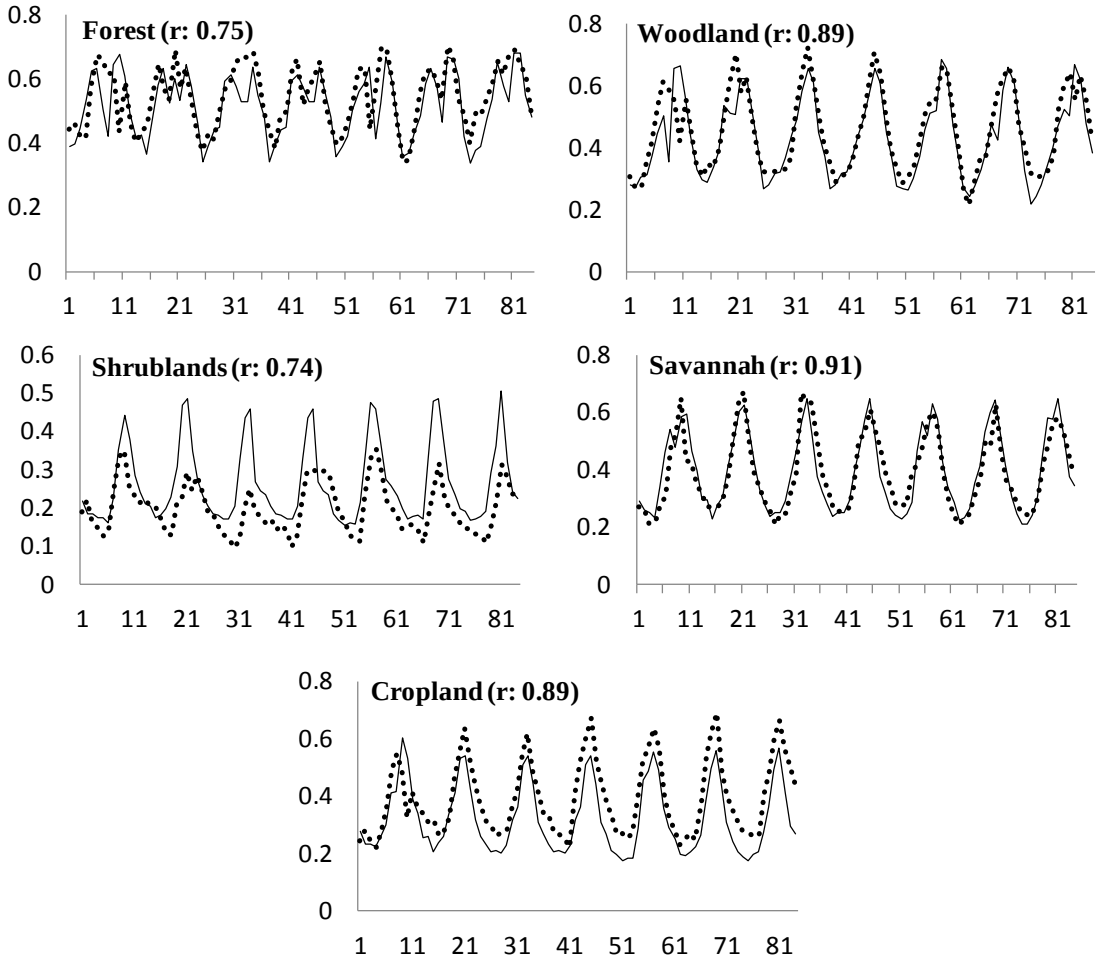

Figure 13: NDVI seasonal profile of VGT (solid line) and GIMMS (dotted line) and correlation coefficient.

The GIMMS data explains about 79 to 85 % of the variance in SPOT VGT in very high correlation areas (Woodland, Savannah and Cropland) and about 55% in high correlation areas (Forest and Shrublands).

6.3. Trends in monthly NDVI

The Mann Kendall trend of long-term monthly NDVI value for the period 1982-2011 is shown in Figure 14. It can be seen from the map patches with increasing NDVI representing greening trend and patches with negative trend as a browning trend. Greening trend are mainly located in central parts as well as the Northern corner, whereas browning trend are sparse and located mainly in the North Western part.

The Northern area of the catchment is characterised by an accumulation of pixels displaying significant negative trends, which might be triggered by two different processes: expansion of agricultural land and high population densities. The concentration of population and economic activities in this area has severely impacted local ecosystems. NDVI values are influenced by the loss of vegetation cover due to large clearing of vegetation for agricultural expansion. The region's main agricultural products are cotton, sorghum, millet and maize.

In contrast the Central part of the catchment is characterised by large patches of positive trend. Three types of land cover changes can be used to explain NDVI increases from Cropland or sparsely vegetated area to natural vegetation or from sparsely vegetated area to Cropland with a presence of an important number of trees in the agro-ecological system.

Comparing the spatial trend patterns (Figure.14-a) with the aggregated land cover map (Figure 14-b), reveals that most of pixels with browning trend are related to Woodland zone and or

mosaic of Cropland and savannah, while the pixels showing negative trend are located in areas dominated by Cropland for more than 70% of the area and with sparse vegetation. The general trends of LULC change between 2000 and 2009 are shown in Table 6. These are extracted from moderate satellite data from the whole study area and as can be seen from Table 6, showing a 30 % increase in Cropland the initial area and 89% increase in grassland increased for 89%. On the contrary the mosaic of savannah with Croplands, woodland and forest area decreased respectively by 11%; 8%; and 20% during the same period.

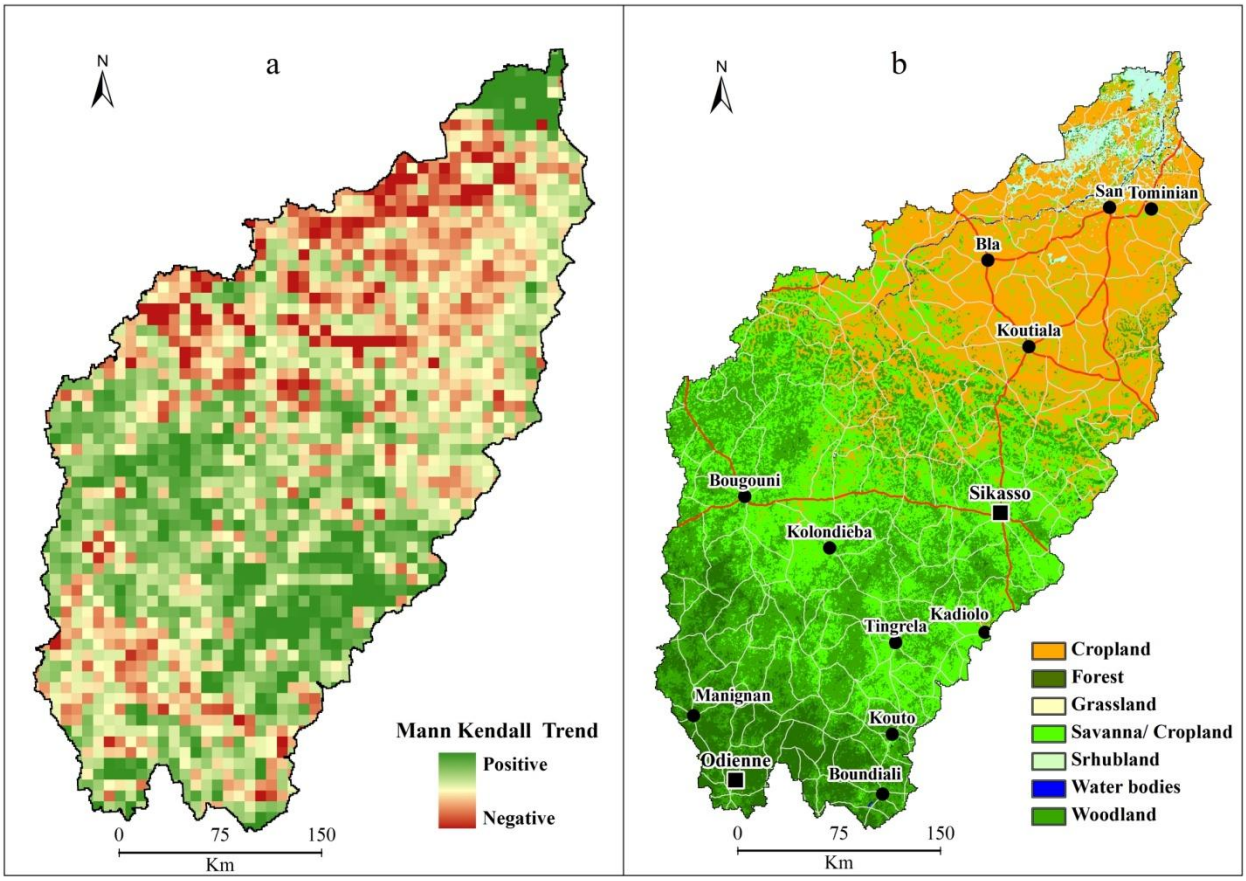

Figure 14: (a) Mann Kendall Monthly NDVI and (b) Modified Globcover LULC map 2009 for the study area.

Table 6: LULC change from medium resolution data for the whole watershed

	Bare area (ha)	Cropland (ha)	Forest (ha)	Grassland (ha)	Mosaic Sav-Crp* (ha)	Water (ha)	Woodland (ha)
2000	-	2956607.72	1192057.62	197261.52	4498913.06	3183.19	4129276.80
2009	9113.64	3829951.04	948611.86	372333.00	4011439.98	1320.76	3790506.22
Change (%)	-	**29.54**	**-20.42**	**88.75**	**-10.84**	**-58.51**	**-8.20**

* Savannah-Cropland

6.4. Trend in annual integral NDVI

The long-term inter-annual trend analyses of annual summed NDVI values for the same period (Figure 15-a) shows similar patterns as the monthly time-series. Greening is the dominant process in the central parts, as well as in the Northern corner, whereas the North-Western of the basin is characterized by browning, i.e., a decrease in NDVI values.

The values of the Theil-Sen slope (Figure 15-b) are given in total units of annually accumulated NDVI change per year and range between -0.025 and +0.024 with a mean slope of 0.0209. However, the 95% confidence interval spreads very tight around the mean from 0.0205 to 0.0213 per year. The Theil-Sen slope showed a similar pattern as the Kendall tau.

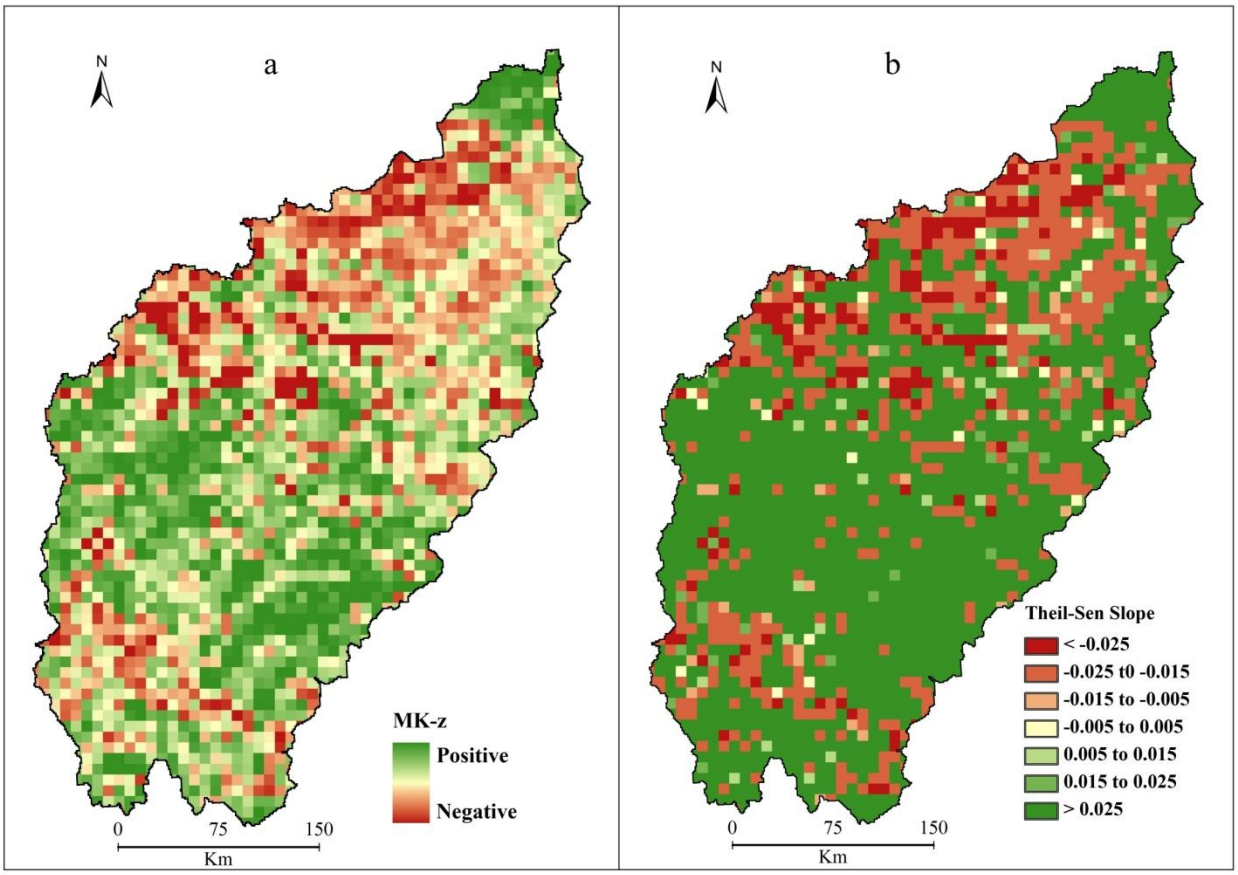

Figure 15: (a) Mann Kendall monotonic trend and (b) Theil-Sen slope in annual NDVI time-series 1982-2011

6.5. Significance in monthly NDVI time-series 1982-2011

The Figure 16 showed (a) the Mann Kendall z significance and (b) the p-value of monthly NDVI time-series. The Mann-Kendall significance (MK-*z*) expresses the significance of a Mann-Kendall trend, also used as a trend test for the Theil-Sen median slope operator as well. As mentioned earlier, the significance α and the *Z*-scores of trend test are: $Z = \pm 2.576$ refers to $\alpha = 0.01$, $Z = \pm 1.960$ refers to $\alpha = 0.05$ and $Z = \pm 1.645$ refers to $\alpha = 0.1$. For example, if a certain region expresses a MK-*z* of +2.576, it means that the calculated Mann-Kendall trend is positive

and with a significance level α of 0.01. In the following, areas with a MK-z between -1.960 and +1.960 (corresponds to $\alpha \geq 0.05$) are referred to as no trend areas. The p-value significance less than 0.07 was used as a threshold of significance for the monotonic trend, thus, the areas with p-value higher than this threshold were masked.

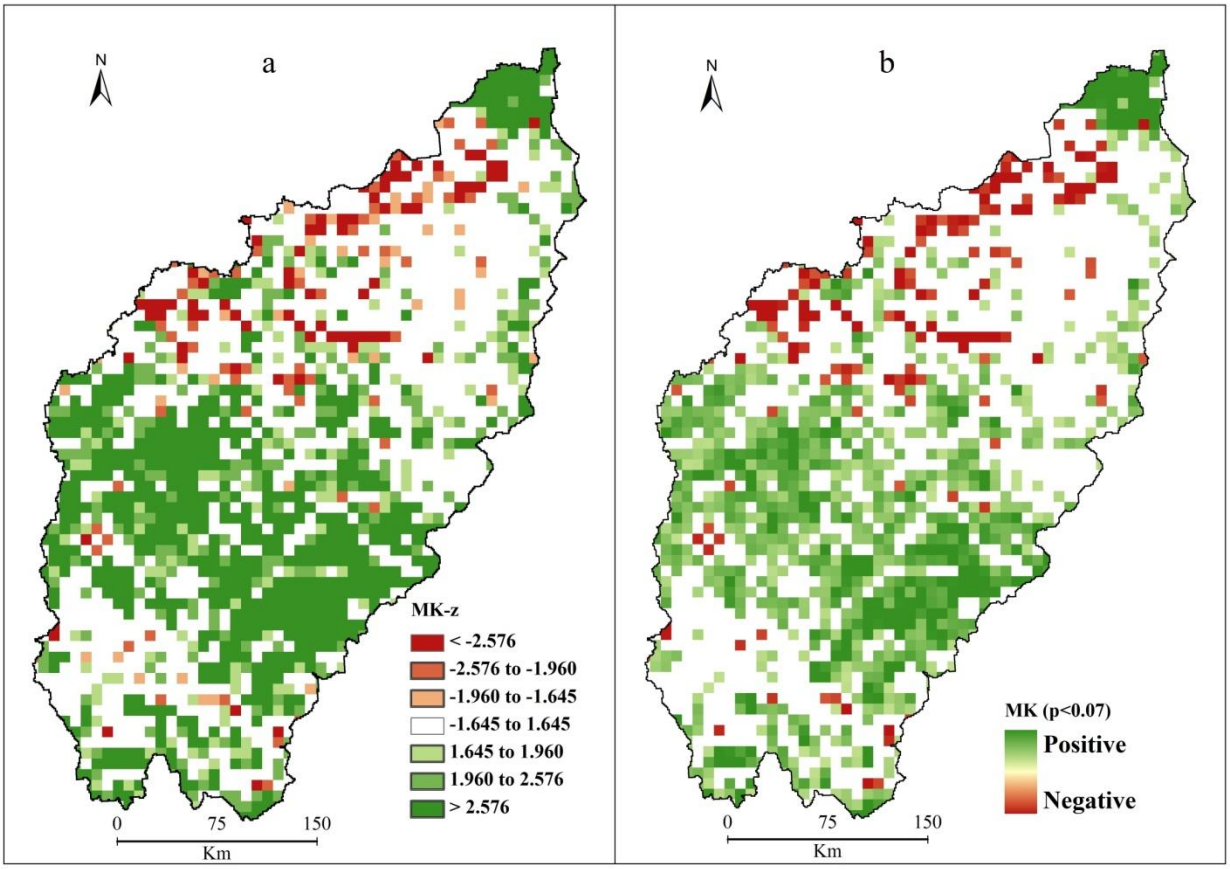

Figure 16: Mann-Kendall significance (a) and p-value (b) of monthly NDVI time-series.

All these two tests of significance confirm the trend associated in these areas for the period of study. The total pixels affected by significant decrease in monotonic trend at p-value less than 0.07 is 155 while 934 pixels showed a significant positive trend at the same threshold. The Z-estimator revealed that 79 pixels were associated with negative trend and 651 pixels with

positive trend at significant at α= 0.01; 138 pixels were associated with negative trend and 866 pixels with positive trend significant at α= 0.05, while 180 pixels were associated with negative trend and 1016 pixels with positive trend significant at α= 0.1.

6.6. Relationship between NDVI trends and Precipitation

One of the key limiting factors of vegetation growth in tropical semi arid regions is precipitation. Consequently, the inter-annual trends in vegetation greenness, as described above, are mainly explained by the availability and spatio-temporal variability of rainfall. This assumption was computed using a linear correlation coefficient at pixel level for monthly rainfall and NDVI series for the growing season from 1982 to 2011. The strength of this relation between rainfall as independent variable and NDVI the dependant variable is shown in Figure 17.

Results from the Pearson correlation showed a positive correlation between NDVI and rainfall indicating the major role of rainfall in vegetation productivity. In most of the basin, the positive correlation indicated that productivity is mostly limited by rainfall even though only a few areas show significant positive correlation. However, the low r coefficient can be explained by many factors, such as the time lag in the response of the vegetation to changes in rainfall, seasonal rainfall distribution (Martiny *et al.,* 2006) or low signal-to-noise ratio (Camberlin *et al.*, 2007) or a lack of sensitivity of the NDVI to variations in rainfall. The non-significance of the Pearson correlation can be explained by the lack of sensitivity of NDVI to variation of rainfall at a certain stage. In the Southern part of the catchment, negative correlation between rainfall and the NDVI could be due to signal saturation above certain biomass values, to a deficit of solar radiation used

for the photosynthesis because of cloud (Camberlin *et al.*, 2007), or due to residual atmospheric contamination of the images (Li *et al.*, 2004).

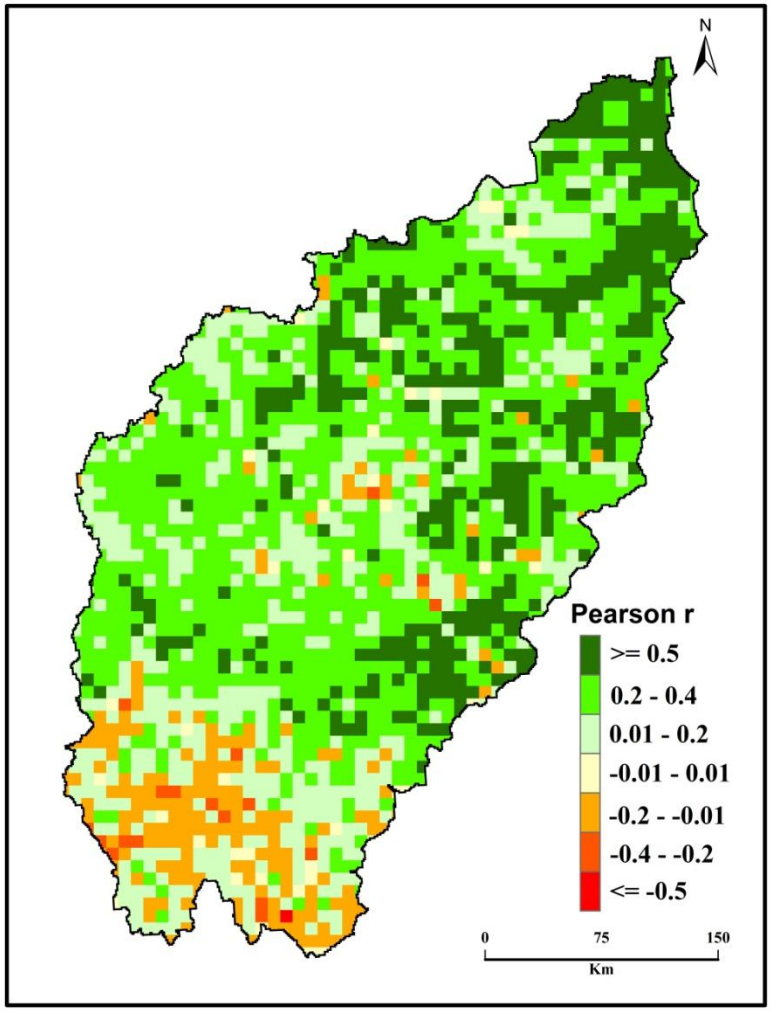

Figure 17: Pearson correlation coefficient between integrated seasonal rainfall and mean NDVI

6.7. Discussion

In this chapter the long-term trend of NDVI have been analysed using a Mann Kendall test. The suitability of Mann Kendall analysis to detect long-term trend in time-series data has been well documented by scientific communities (e.g. De Beurs and Henebry, 2004a, Neeti *et al.*, 2012).

The method allows computing the long-term trend and its significance. The response of seasonal NDVI to rainfall were by computing a correlation coefficient between rainfall and NDVI. Some previous studies indicated a different time lag between rainfall and vegetation, here only the 0 time lag were considered for the analysis.

The results showed a large band with significance positive trend located in the central area of the catchment while the Northern presented significant negative trend. The comparison of this result with land cover data demonstrated that the trend was significant in areas where the natural vegetation was still well represented. The major land cover classes identified in this area were mixed Cropland - savannah and woodland. In contrast to the area showing significant negative trend, the land cover was dominated by Cropland (> 70%) and mixed grassland/shrublands.

Even though rainfall controls a large part of spatial and temporal variation of vegetation dynamic at regional scale, the results showed that there is a considerable variation in response of vegetation to rainfall at local scale. According to Diouf and Lambin (2001), this could be explained by the soil type, the inter-annual variation in rain-use efficiency, the vegetation communities and floristic composition, land use practices and seasonal distribution of rainfall. The Pearson correlation indicated a good relationship between NDVI and rainfall at monthly time scale for the same month, but only a few pixels showed a strong correlation. However, strong relationships between NDVI and rainfall over different regions have been reported from earlier studies (Hermann *et al.*, 2005). Hermann *et al.*, (2005) studied the relationship between NDVI and rainfall over the Sahel for the period from 1981-2000 and reported a positive and significant average correlation coefficient of 0.78 between precipitation and vegetation response. The absence of such strong relationship over the study area as reported in this chapter could be

explained by some negative factors that influence negatively the correlation between NDVI and rainfall. Among these factors are severe changes in rainfall time pattern where for most of the time a large volume of monthly rainfall is obtained in a short time and the resulting floods exit rapidly from the regions (Hashemi, 2011).

7. INTER SEASONAL PATTERN AND CHANGE IN NDVI AND ITS RELATION TO CLIMATE

7.1. Introduction

For the past few decades, the Sudano-Sahelian regions have experienced a lasting drought, which started at the end of 1960s and culminated in 1980s with a rainfall deficit of 15-30% compared to the 1950-1960s (Nicholson *et al.*, 1998; Le Barbé *et al.*, 2002). This might have had a strong impact on the vegetation dynamic in the area. In this Chapter, the changes in inter seasonal vegetation activity were assessed using the 8-km NDVI time-series. Spatially averaged time-series of mean NDVI, and total precipitation over the growing season (April to October), were generated for all pixels. Correlation between growing season NDVI and precipitation were computed to investigate climate effects on inter-seasonal change in vegetation activities. In order to quantify the inter-annual variability, the average NDVI value for the growing season has been computed for each year. From this the NDVI standard deviation ($NDVI_{std}$) and coefficient of variation ($NDVI_{CoV}$) have been calculated for each pixel.

7.2. Spatio temporal patterns in NDVI and rainfall

The spatial NDVI anomaly patterns for the study area are shown in Figure 18. The spatial data were binned into moderate ($|\sigma(i) \leq 1$: AM+ for positive moderate anomaly and AM- for negative moderate anomaly), large ($\sigma(i) > 1$; AL+ for positive large anomaly and AL- for negative large anomaly) and extreme ($\sigma(i) > 2$; AE+ for positive extreme anomaly and AE- for negative extreme anomaly) deviation (Xu *et al*, 2012). These series of maps show the NDVI deviation from the long-term mean.

In 1982 the majority of the study area (Figure 18) showed above-normal condition overall, indicating widespread greenness, the below-normal vegetation condition is observed in the South-Eastern part indicating stress condition. In contrast, most of the area from 1983-1984 showed below-normal vegetation conditions, with some departure from moderate negative anomaly to negative large anomaly. These years are associated with lowest rainfall condition during the period of study. In 1985 a slightly positive anomaly contrast is observed in the Eastern and Central part, whereas the Northern and Southern showed a relative negative condition. The vegetation situation in 1986 changed greatly compared to the last three years, especially showing a substantial above-normal condition. In 1987, only the Western portion showed a below-normal condition which stretched over most of the Western part in 1988. The year 1989 was marked by an above-normal vegetation condition in the Northern part, and stretched over the whole study area in 1990 and 1991 with below-normal in the South in 1991. This above-normal in vegetation condition is showed for the whole area in 1992 and 1993. In 1994 the Southern part highlights an extreme negative condition whereas the Northern showed the opposite. From 1995 to 1999, the general condition showed a positive condition for most of the area. It is generally observed that the period from 2000 to 2010 highlighted a moderate below-normal condition in mostly the Southern and Northern part and a moderate to extreme above normal condition for the rest of the study area. The situation in 2011 was mixed with the below-normal condition in the Western part and above normal in the Eastern part. According to the rainfall anomaly (Figure 19), the years 1984, 2001 and 2002 were associated with dry to very dry condition in the study area.

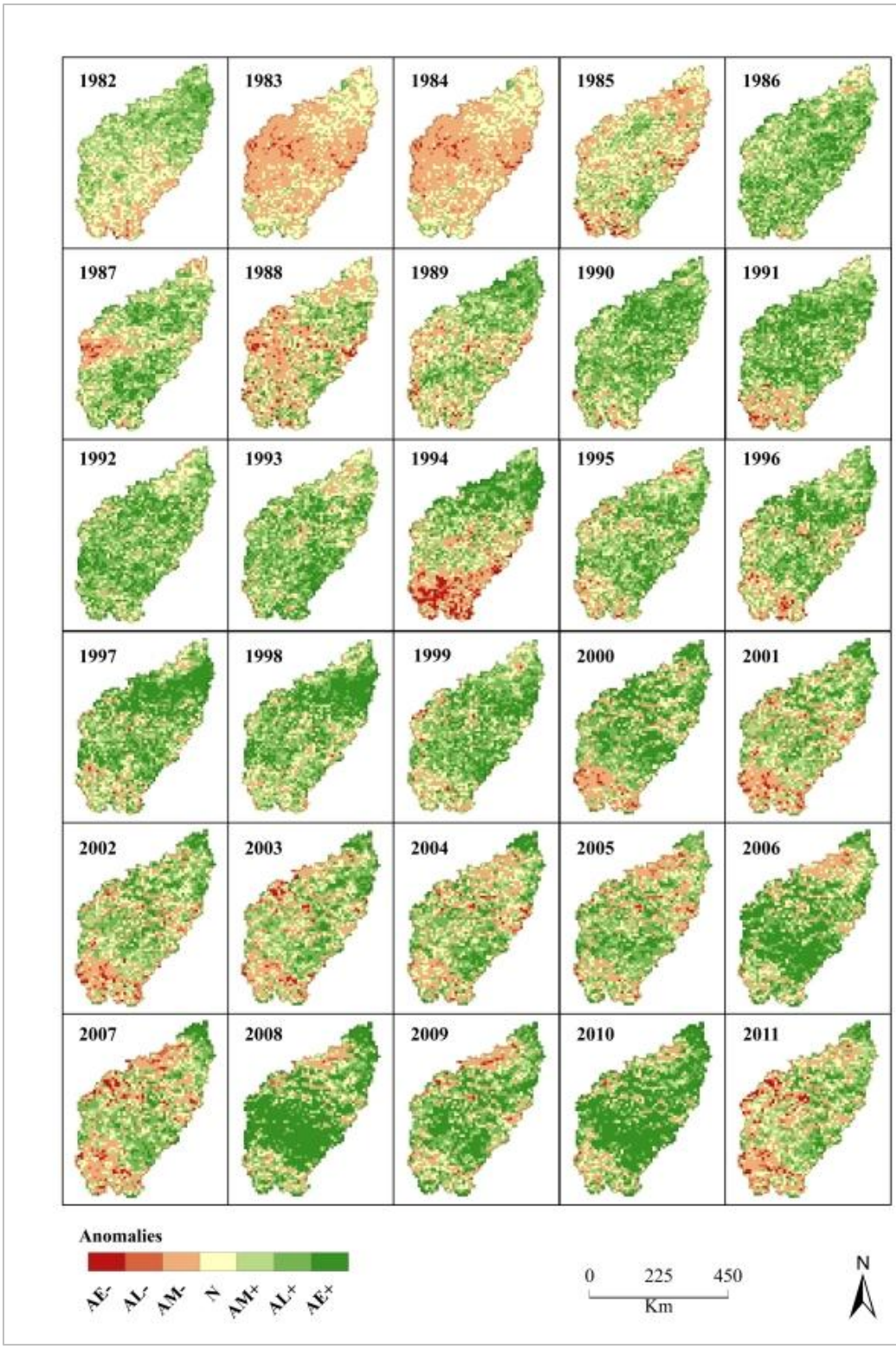

Figure 18: Evolution of vegetation condition in the in the study area during 1982-2011 using rowing season NDVI anomaly patterns.

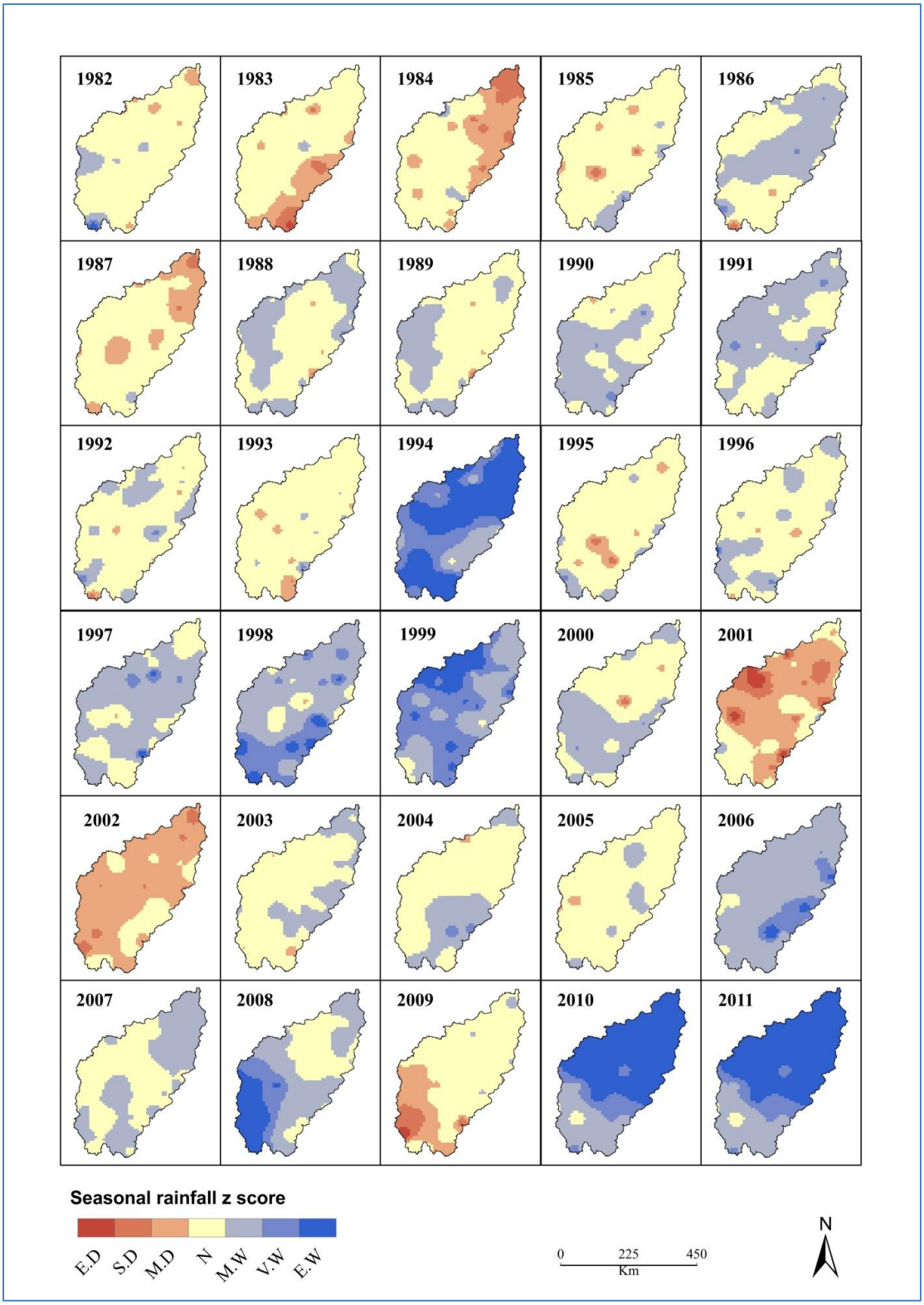

Figure 19: Standardized anomalies in precipitation in the study area for 1981-2011 using integrated precipitation for the growing season (April-October).

7.3. Inter-annual relationship between NDVI and rainfall

7.3.1. Analysis of spatially averaged NDVI versus precipitation

The correlation result shows strong linear relationship between NDVI and rainfall in the region with an r value of 0.98 and a residual standard error of 0.000002 for the period from 1982 to 2011. The scatter plot, as seen in Figure 20, indicated that the correlation between precipitation and NDVI are positive and exhibits a clear spatial pattern. Precipitation and temperature directly influence water balance, causing changes in soil moisture regime which, in turn, influences plant growth. The coefficient of determination R^2 indicated that 96.92% of the variation in vegetation productivity is explained by rainfall in most of the period.

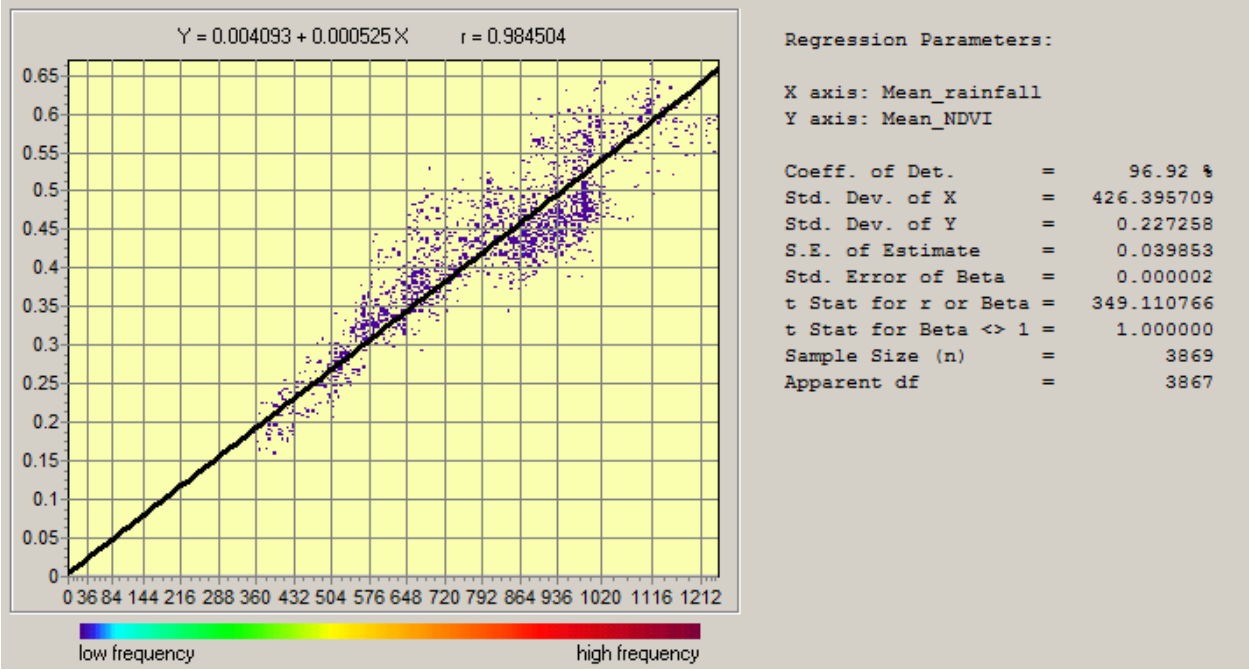

Figure 20: Overall correlation between NDVI and rainfall for the rainy season (mean 1982-2011)

7.3.2. Spatial patterns in inter-annual NDVI-rainfall relationship

Figure 21 showed the mean annual evolution of NDVI and rainfall respectively. The illustration provides a generalized overview of annual evolution of the study area rainy season. Approximately between 90 to 95% of annual rainfall falls between April and October.

The spatial pattern of NDVI study area seems to be influenced by the South-North direction of rainfall due to ITCZ movement.

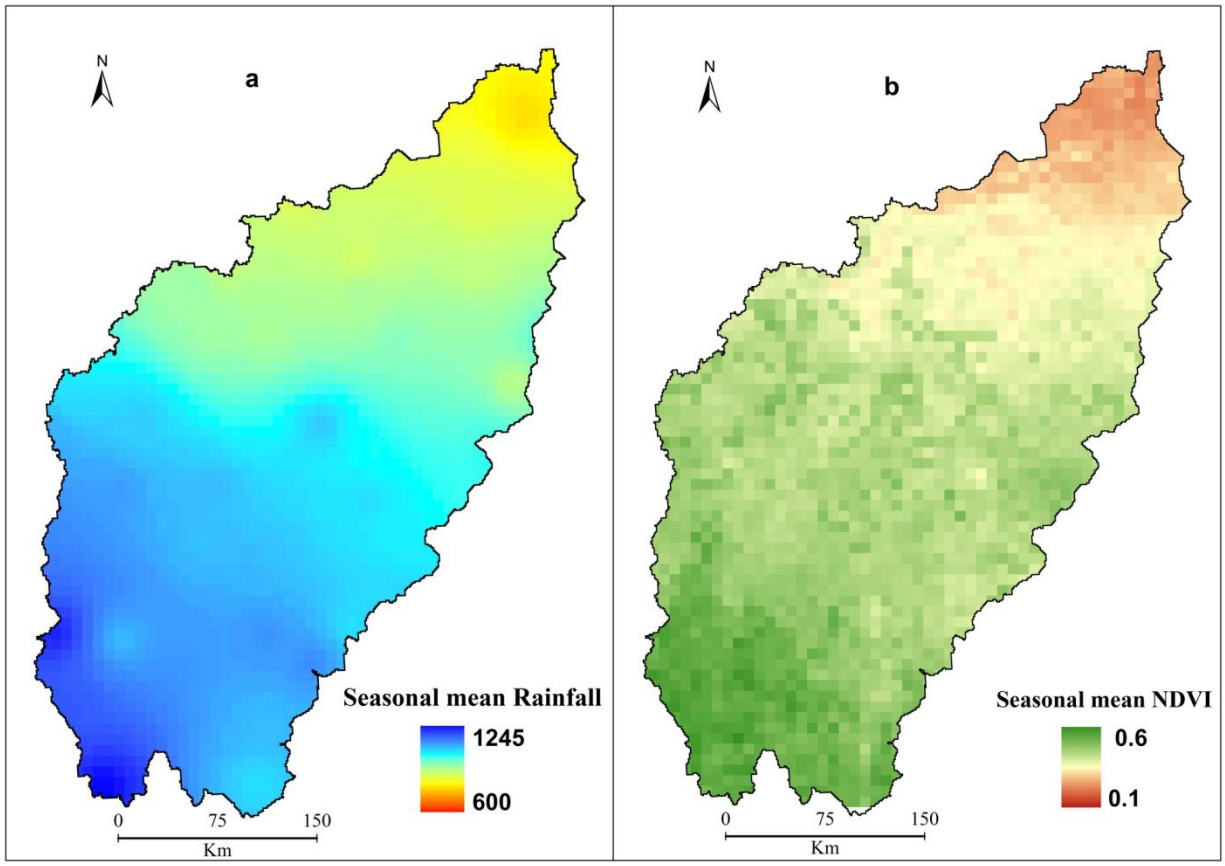

Figure 21: Averaged (a) Rainfall and (b) NDVI for the growing season (1982-2011)

Considering the average season rainfall and NDVI pattern for the entire area for the period from 1982 to 2011, it can be seen from the Figure 21, that there exist a good relationship between

NDVI and rainfall. As rainfall increases to 1245 mm (Figure 21-a), NDVI increases and reaches up to a range of 0.6 (Figure 21-b).

7.4. Quantifying temporal variability in vegetation conditions

7.4.1. NDVI Standard deviation

The standard deviation is one of the simplest methods to characterize a time-series of data and to estimate variability of these data through the time. The standard deviation of NDVI values displays the scope of values calculated for individual years from the mean value having been calculated for the whole period. Low $NDVI_{std}$ indicates a good density of values of individual years around the mean value. On the contrary, high value of $NDVI_{std}$ is associated with a wide scattering of the year values from the mean value. This means a higher variability of NDVI over the time.

The results of the spatial variability of NDVI across the study area are presented in Figure 22-a. The Southern West corner of the study area displayed the highest value of NDVI standard deviation (0.05-0.13) while the low values are displayed in the central part. The standard deviation is good to estimate the variability of a temporal over a time period data but is less accurate for comparison between vegetation classes. The value of the standard deviation is strongly dependant on NDVI value, which is individually determined as a 'lumped' ratio for each pixel. Therefore it is not helpful to make some comparison using NDVI standard deviation. Therefore the coefficient of variation was used to compare variability for the study area between individual pixels. The coefficient of variation is discussed in the next section.

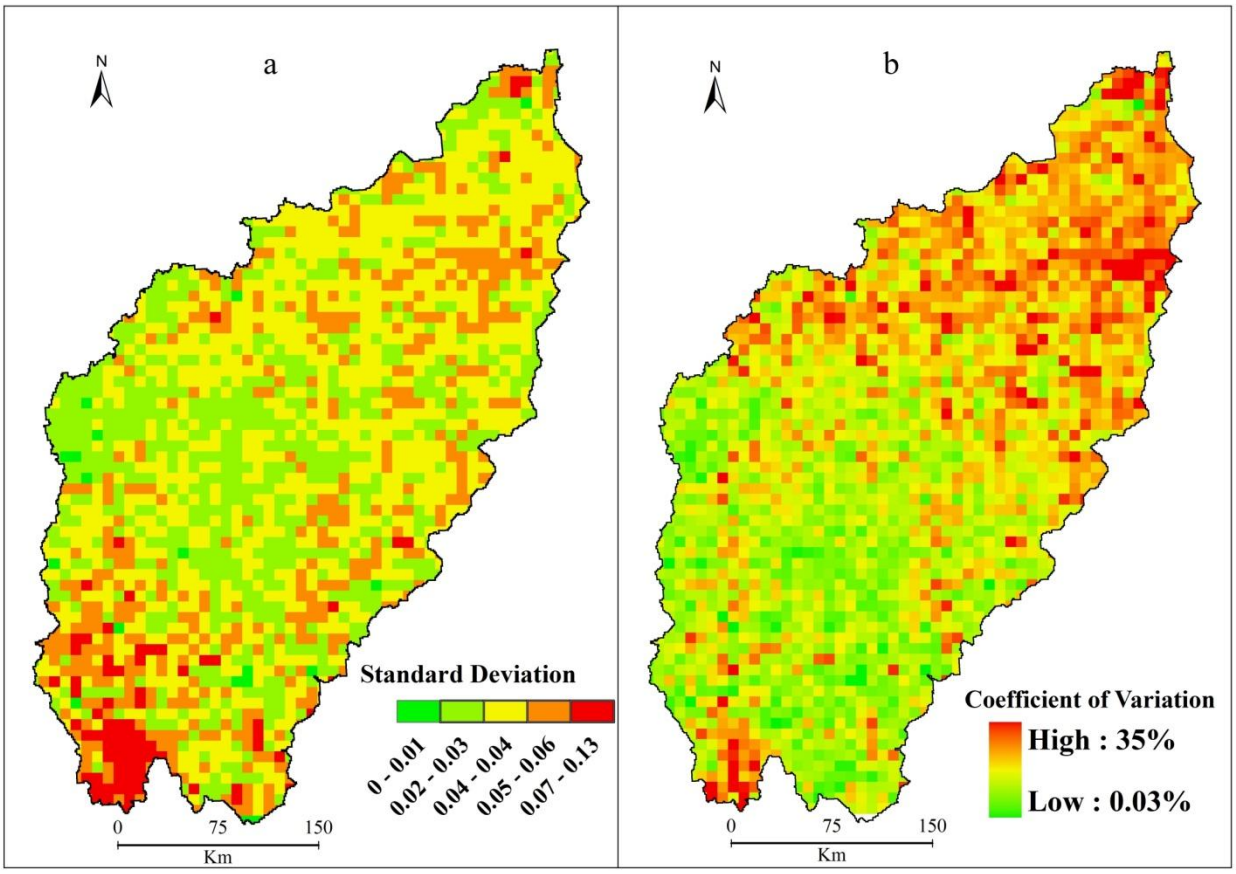

Figure 22: Map showing the NDVI (a) standard deviation and (b) coefficient of variation

7.4.2. Variance of NDVI value over the study period

NDVI interannual coefficient of variation (CoV) has been used to assess vegetation activities and changes in arid and semi-arid regions (Tucker *et al.*, 1991, Weiss and Milich 1997, Vicente-Serrano *et al.* 2006). Milich and Weiss (2000) reported that high CoV embedded among larger areas of much lower CoV may be associated with rapid, dynamic and irreversible (on human timescales) land degradation. Therefore the NDVI CoV was computed and compared with the results of vegetation dynamics.

In order to investigate the variability of vegetation through the entire study period the coefficient of variation for the spatially averaged growing season NDVI values over the period 1982-2011 have been calculated (Figure 22), as well as these values for every pixel in the study area. Coefficient of variation is commonly calculated to compare the amounts of variation (in % from the mean value) in different sets of data and enables the evaluation of the robustness of vegetation to variability in climatic predictors. Thus, the coefficient of variation have been calculated for inter-annual time-series of growing season, which also indicate the response of vegetation cover to inter-annual climate variability. The lower the variation coefficient of NDVI, the lesser the sensitivity of vegetation covers to climatic variations.

7.5. Discussion

In this Chapter the inter-annual change in NDVI and its relationship with rainfall was examined for the period 1982-2011 for the whole catchment. Low to strong temporal correspondence between anomalies in rainfall and vegetation were observed. The correlation between aggregated NDVI (Figure 20) with rainfall was found to be higher than the correlation using monthly NDVI and rainfall for the growing season (Figure 17) at time lag 0.

As mentioned previously, climate in general and rainfall particularly is an environmental factor determining vegetation production and growth in an area. Aggregated rainfall amount and its impact on vegetation covers were quantified by statistical analysis. The results indicate a high correlation between aggregated mean seasonal NDVI and rainfall during the study period 1982-2011.

Temporal variation in NDVI value over the period 1982-2011 has been studied using simple techniques of descriptive statistic. The results showed high variability of NDVI in the study area.

The coefficient of variation (CoV) for the monthly NDVI varied between 0.03 to 35%. The highest CoV was observed in the Northern part of the study area where the rainfall variability is also high. This study concluded that the high variability of NDVI in the study area is explained by climate using rainfall data. The results presented high strong correlation between CoV for NDVI and CoV for rainfall (Figures: 12 and 22).

However, it can be noted that at around 750 mm of rainfall NDVI almost saturates and there is no further increase in NDVI, despite rainfall increase up to a range of 2450 mm that eventually occurs in the South. NDVI does not respond well to these rainfall events and still remain below (0.5). Since most of the rainfall (83%) occurs between July-October with the maximum in August, therefore averaging NDVI data for these months fairly represents the growing season for the region (Anyamba and Tucker, 2005).

8. ANALYSIS OF LULC CHANGE FROM 1980s TO 2010 IN SELECTED AREAS

8.1. Introduction

This study uses multi-temporal imageries to monitor the dynamic of LULC in some selected pixels. Therefore comparisons of LULC classification using multi-temporal datasets are often found to improve the accuracy of classification (Chen *et al.*, 2008). It offers more opportunities for complete description of LULC classes than what could be achieved with single date imagery. Most of the images used in this study were acquired in the end of the growing season, considered as the suited period for distinguishing various LULC classes in the study area (Ruelland *et al.*, 2009). The study was conducted in four (4) selected pixels of 8-km by 8-km, used as reference subset within the study area. The basis of selection of these references subsets is described in the following section.

8.2. Hot spots pixels selection

Several pixels with the same general trend (positive or negative) can be identified in the trend maps on which four subset pixel (8-km × 8-km) were selected for the study of land cover change. The spatial location of the selected subset is shown in Figure 23. Table 7 shows the selection criteria.

These were: negative NDVI and RF trend (subset #1), positive NDVI and negative RF trend (subset #2), negative NDVI and positive RF trend (subset #3) and at last positive NDVI and RF trend (subset #4). These hot spots were analysed with high resolution satellite data to evaluate the reliability of identified anomalous behaviour and provide an interpretation of these hot spots.

Table 7: NDVI and RF characteristics for the subsets selected and underlying hypothesis

Subset #	NDVI trend ($p<0.07$)	Rainfall trend	NDVI CoV	NDVI Departure	
1	-	+	15%	Negative	Human
2	+	-	12%	Positive	
3	-	-	6%	Negative	Climate
4	+	+	12%	Positive	

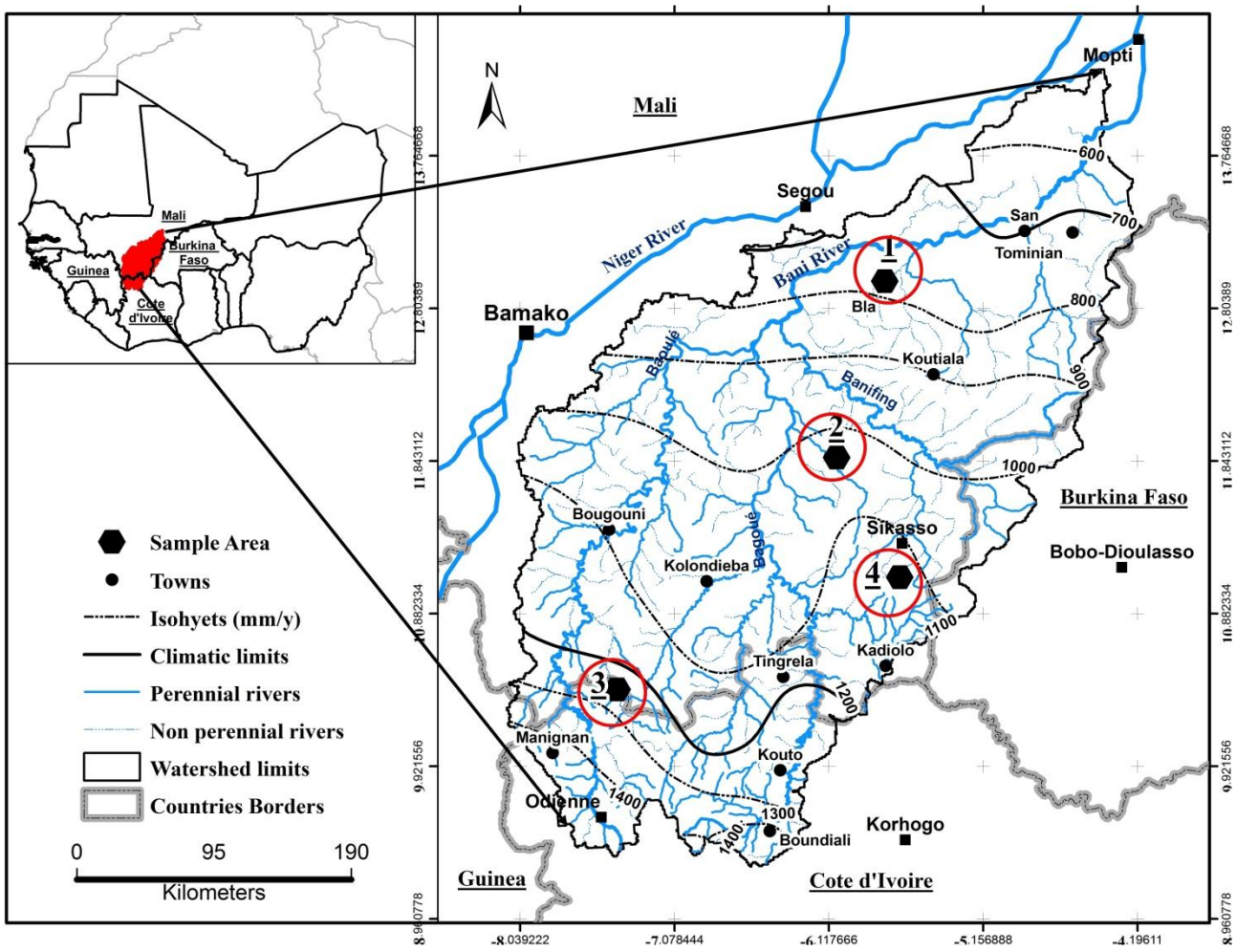

Figure 23: Map showing the reference subsets for LULC change detection within the study area

8.3. Accuracy Assessment Reports

The Kappa statistics, as mentioned previously, provides a statistically valid assessment of the quality of classification and was used to assess overall class accuracy (Tottrup and Rasmussen, 2004). According to Pontius (2000), a Kappa value higher than 0.5 can be considered as satisfactory for modelling of LULC change. Landis and Koch (1977) characterised agreement for the Kappa coefficients as follows: values greater than 0.79 are excellent, values between 0.6 and 0.79 are substantial and values of 0.59 or less indicate moderate or poor agreement.

The overall classification accuracy is the percentage of correctly classified samples of an error matrix. It is computed by dividing the total number of correctly classified samples by the total number of reference samples. It can be expressed by

$$Overall - accuracy = \frac{1}{N}\sum_{k=1}^{n} a_{kk} \qquad (13)$$

Where: "***a"*** is the individual cell values, "***k+a***" is the total row, "***k a+"*** is the column total, "***n***" the number of classes and "***N***" the total number of samples.

The mapping accuracy of each LULC class was derived from the calculated producer's accuracy and user's accuracy (Story and Congalton, 1986; Congalton and Green, 1999) using the following equations:

$$producer's - accuracy = \frac{a_{ii}}{\sum_{i=1}^{n} a_{i+}} \qquad (14)$$

$$user's - accuracy = \frac{a_{ii}}{\sum_{i=1}^{n} a_{+i}} \quad (15)$$

Where: "a_{ii}" is the number of sample correctly classified, "a_{i+}" the column total for $class_i$ and "a_{+i}" the row total for $class_i$.

The confusion matrix, the producer's and the user's accuracy are calculated for each class, as well as the overall accuracy and the accuracy estimate that removes the effect of random change on accuracy, referred to as the Kappa statistic (Skidmore, 1999).

Tables 8 to 10 show the complete set of statistics for the categories of LULC classes based on the comparison between the ground truth pixels and the classified pixels in the region of interests (ROI) respectively for subset areas 1 to 4.

For the 1st period, accuracy assessment results showed an overall accuracy of 81.69% and a kappa coefficient of 0.86 with a producer's accuracy and user's accuracy of 88% and 77.6% respectively for subset (1). Subset (2) showed an overall accuracy of 92.95% and a kappa of 0.90 with a producer accuracy of 93.3% and a user accuracy of 86.5%. For subset (3) the kappa was 0.90 and the overall accuracy was 93.08% with a user accuracy and producer accuracy of respectively 87.4% and 90.50%. Subset (4) exhibited a kappa of 0.93 and an overall accuracy of 95.49% with a user and producer accuracy of 85.4% and 94.8% respectively.

During the second period, the kappa and overall accuracy were 0.78 and 86.05% for subset area (1) with a user and producer accuracy of 70.5% and 85%. These values were 0.86 for the kappa, 89.68% for the overall accuracy, 89.9% for the user accuracy and 88.7% for the producer accuracy for subset (2). Subset (3) showed a kappa of 0.95 and an overall accuracy of 97.07%

with user accuracy and producer accuracy of 97% and 97.7% respectively. Subset (4) exhibited a value of 0.86 for the kappa and 89.27% for the overall accuracy while the user and producer accuracy were 84.8% and 91.6% respectively.

Lastly during the third period, the overall accuracy and the kappa were 92.02% and 0.89 for subset (1), while the user and producer accuracy were respectively 97.6% and 98.1%. Subset (2) showed 90.40% for the overall accuracy and 0.86 for kappa statistic, the user and producer accuracy were 85.5% and 92.9%. Subset (3) showed an overall accuracy of 90.34% and a kappa of 0.87; the user and producer accuracy was 99.4% and 97.9% respectively. For subset (4) the kappa was 0.92 and 94.68% for the overall accuracy, while 98.8% and 87.3% were respectively for the user and producer accuracy.

Table 8: Accuracy assessment results of the LULC map produced from Landsat for the subset #1

	1984					1999					2009				
	Ground pixels	Com. %	Om. %	Prod. Acc. %	User Acc.%	Ground pixels	Com. %	Om. %	Prod. Acc. %	User Acc. %	Ground pixels	Com. %	Om. %	Prod. Acc. %	User Acc. %
BL	228	31.1	18.4	81.6	68.9	82	77.2	19.5	80.5	22.8	820	13.1	23.2	76.8	86.9
CRP	1051	1.1	1.3	98.7	99.0	2229	3.3	13.1	86.9	96.7	1289	10.2	4.3	95.7	89.8
ST	1219	4.7	16.7	83.3	95.3	2014	7.9	15.3	84.7	92.1	1052	8.3	5.8	94.2	91.7
OT	524	9.2	15.1	84.9	90.8	727	29.6	12.2	87.8	70.4	1031	3.0	4.9	95.2	97.0
Shr	587	18.9	6.1	93.9	81.2										
WT	29	69.8	10.3	89.7	30.2						367	2.4	1.9	98.1	97.6
O.Acc.	89.61					86.05					92.02				
Kappa	0.86					0.78					0.89				

BL: Bare Land, CRP: Cropland, WT: Water bodies, OT: Open Trees, SHB: Shrublands, ST: Steppes.

Table 9 : Accuracy assessment results of the LULC map produced from Landsat for the subset #2

	1984					1999					2010				
	Ground pixels	Com. %	Om. %	Prod. Acc. %	User Acc.%	Ground pixels	Com. %	Om. %	Prod. Acc. %	User Acc. %	Ground pixels	Com. %	Om. %	Prod. Acc. %	User Acc. %
BL	100	46.6	7.0	93.0	53.5	230	6.4	23.9	76.1	93.6	285	21.6	11.9	88.1	78.4
BA	398	5.5	5.0	95.0	94.5	488	6.7	5.5	94.5	93.3	200	0.5	1.5	98.5	99.5
CRP	1181	1.0	6.9	93.1	99.0	404	17.4	5.0	95.1	82.6	1593	2.2	2.9	97.1	97.9
OT	1059	4.6	11.0	89.1	95.5	905	11.5	9.8	90.2	88.5	597	14.3	31.5	68.5	85.7
CT	991	9.8	3.8	96.2	90.2	1045	8.5	12.1	87.9	91.5	645	19.5	7.1	92.9	80.5
O.Acc.	92.95					89.68					90.45				
Kappa	0.9					0.86					0.86				

BL: Bare Band, BA: Burn Area, CRP: Cropland, OT: Open Trees, CT: Closed Trees.

Table 10: Accuracy assessment results of the LULC map produced from Landsat for the subset #3

	1986					1999					2010				
	Ground pixels	Com. %	Om. %	Prod. Acc. %	User Acc.%	Ground pixels	Com. %	Om. %	Prod. Acc. %	User Acc. %	Ground pixels	Com. %	Om. %	Prod. Acc. %	User Acc. %
BL	55	41.9	21.8	78.2	58.1	116	0.9	1.7	98.3	99.1	120	32.8	0.8	99.2	67.2
BA	794	0.1	0.9	99.1	99.9	1581	1.3	1.4	98.6	98.7	469	21.1	14.7	85.3	78.9
CRP	798	3.8	18.4	81.6	96.2	662	8.3	0.3	99.7	91.7	613	1.7	4.9	95.1	98.3
OT	910	14.4	5.6	94.4	85.6	1156	2.2	7.6	92.4	97.8	805	8.9	16.5	83.5	91.1
CT	638	2.8	0.6	99.4	97.2	405	2.4	0.3	99.8	97.6	520	0.6	2.1	97.9	99.4
O. Acc.	93.08					97.07					90.34				
Kappa	0.9					0.95					0.87				

BL: Bare Land, BA: Burn Area, CRP: Cropland, OT: Open Trees, CT: Closed Trees.

Table 11: Accuracy assessment results of the LULC map produced from Landsat for the subset #4.

	1984					2000					2010				
	Ground pixels	Com. %	Om. %	Prod. Acc. %	User Acc.%	Ground pixels	Com. %	Om. %	Prod. Acc. %	User Acc. %	Ground pixels	Com. %	Om. %	Prod. Acc. %	User Acc. %
GRS	642	0.2	1.6	98.4	99.8	86	21.2	4.7	95.4	78.9	31	74.5	22.6	77.4	25.5
OT	146	8.3	2.1	98.0	91.7	268	5.5	10.1	89.9	94.5	303	9.6	0.3	99.7	90.4
CT	181	15.4	0.0	100.0	84.6	780	1.7	1.0	99.0	98.3	1070	0.7	6.6	93.4	99.3
BA	259	0.0	11.2	88.8	100.0	838	1.9	24.0	76.0	98.2	1157	3.4	2.0	98.0	96.6
CRP	896	0.9	5.8	94.2	99.1	297	31.1	3.0	97.0	68.9	450	6.1	6.9	93.1	94.0
BL	28	62.7	10.7	89.3	37.3	181	30.1	7.7	92.3	69.9	370	1.2	12.7	87.3	98.8
O. Acc.	95.49					89.27					94.68				
Kappa	0.93					0.86					0.92				

GRS: Grassland, BL: Bare Land, BA: Burn Area, CRP: Cropland, OT: Open Trees, CT: Closed Trees.

8.4. Land Use/ Land Cover (LULC) change

The LULC class or categories refer to the dominant class in the delineated polygon. The following seven (7) classes presented in Table 12 were used as reference nomenclature for this study.

Table 12: Description of LULC classes used in this study.

Land cover types	Description	Code
1. Bare Land	Areas with sparse or no vegetation cover due to prolonged drought or degradation (This class also encompassed roads and build up areas)	BL
2.Cropland	Cultivated formations with or without scattered trees (canopy coverage 20%) These areas are characterized by annual crops (mainly millet and sorghum), harvested in October–November, followed by a period of bare soil with crop residues	CRP
3.Shrublands	Land covered with approximately > 20% herbaceous vegetation and with woody vegetation covering approximately < 20% of the delineated polygon.	Shr
4.Steppe	Discontinuous grassy formations (10–40% plant cover year-round) with or without scattered bushes/tall shrubs (canopy coverage, 10%). The rest of the land cover consists of erosional surfaces of indurated gravelly ferralitic clay-silt soils with almost no vegetation	ST
5.Open Trees with herbaceous vegetation	Mixed class. Land with herbaceous vegetation and woody cover covering approximately > 20% and < 70% of the delineated polygon	OT
6.Closed Trees / woodland	Mixed class. Land with herbaceous vegetation and a woody cover covering. Land with a dense cover of trees covering approximately >70% of the delineated polygon.	CT
7.Water bodies	Permanent or temporary water bodies, rivers or streams	WT

In subset 1, six LULC categories were identified and mapped (Figure 26); these classes were Bare Land, Cropland, Shrublands, Steppe, Open Trees and Water. Figure 24 showed that the most extent area in 1984 for this area was Cropland with 3280.81 ha (50.77%). This is followed by Shrublands with 1679.10 ha (25.98%), Steppe with 813.17 ha (12.58%), Open Trees with 487.76 ha (7.55%) and Bare Land with 201.80 ha (3.12%).

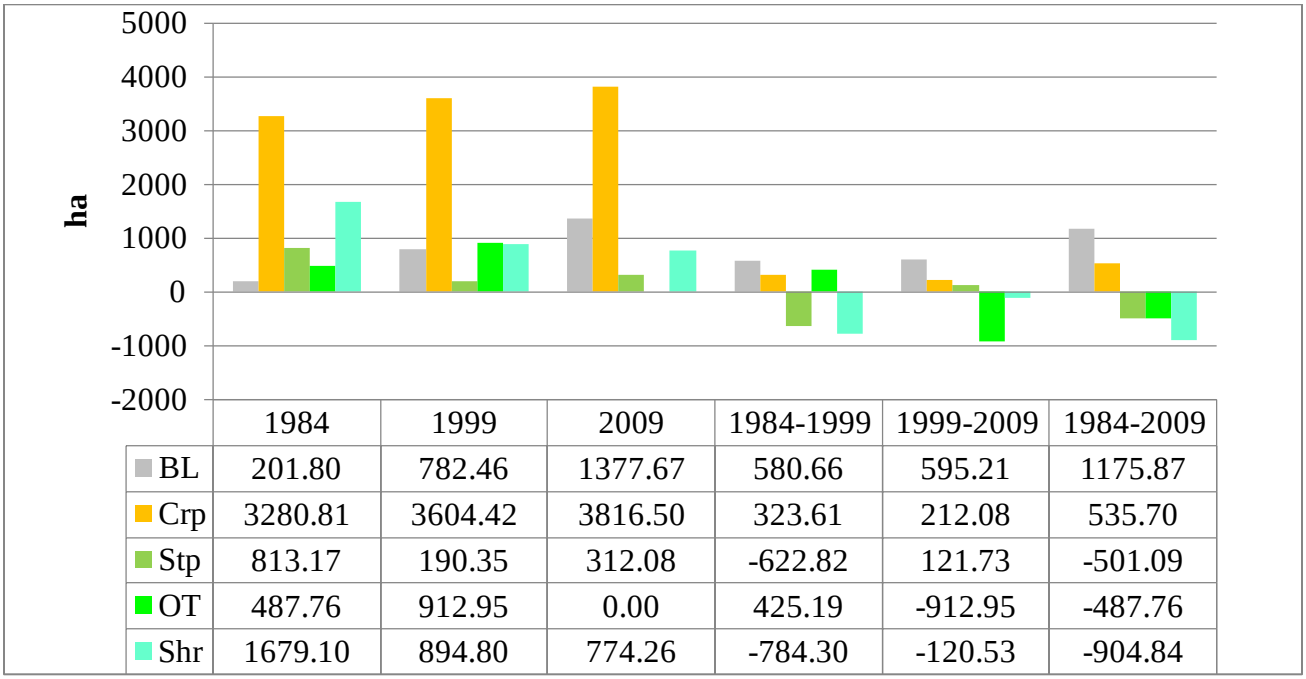

	1984	1999	2009	1984-1999	1999-2009	1984-2009
BL	201.80	782.46	1377.67	580.66	595.21	1175.87
Crp	3280.81	3604.42	3816.50	323.61	212.08	535.70
Stp	813.17	190.35	312.08	-622.82	121.73	-501.09
OT	487.76	912.95	0.00	425.19	-912.95	-487.76
Shr	1679.10	894.80	774.26	-784.30	-120.53	-904.84

Figure 24: Result of LULC classification and change area for the subset # 1

The Cropland was the dominant LULC class in 1999 with 3604.42 ha (55.78%) followed by Open Trees with 912.95 ha (14.13%), Shrublands with 894.80 ha (13.85%), Bare Land 782.46 ha (12.11%), and Steppes 190.35 ha (2.95). In 2009 the dominant LULC class was Cropland with 3816.50 ha (59.05%), followed by Bare Land 1377.67 ha (21.32%), Shrublands 774.26 ha (11.98 ha) and Steppes 312.08 ha (4.83%). The changes in coverage for these LULC classes during the three intervals were presented in Figure 24. It showed that Bare Land and Cropland increased for 1175.87 ha and 535.70 ha while Open Trees disappeared, steppe and Shrublands were decreased

for 501.09 ha and 904.84 ha from 1984 to 2009. The area covered by one of the Settlement in the study area (Bla), were 80.23 ha, 289.07 ha and 485 ha for 1984, 1999 and 2009. There are added to Bare Land statistics for the respective years.

In subset area (2), four LULC classes were identified and mapped (Figure 27) for the years 1984, 1999 and 2010; these were Bare Land, Cropland, Open Trees and Closed Trees. Figure 25 showed that the most extensive LULC category of this subset as at 1986 was Open Trees which covered about 2458.52 ha (38.03%). The second most extensive LULC category was Cropland which 2163.45 ha (33.47%). Closed Trees covered about 1709.15 ha (26.44%), followed by the Bare Land, which covered 79.98 ha (1.24%) of the total area of study.

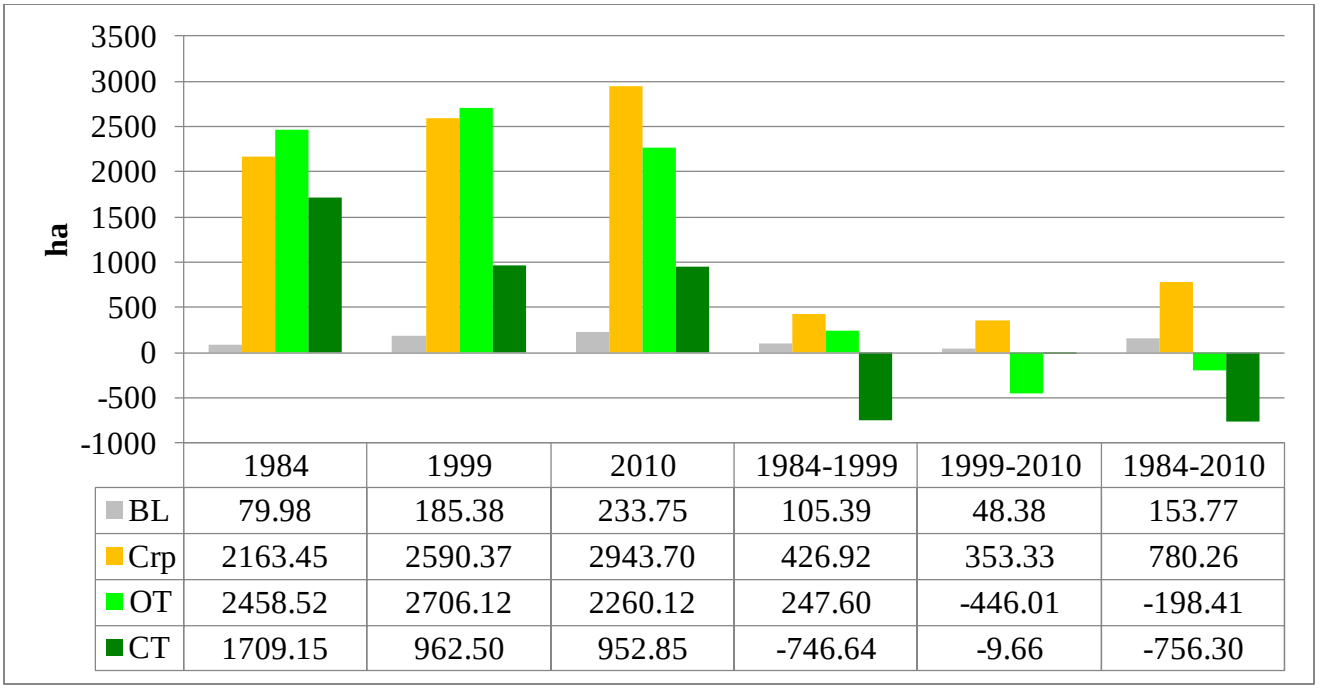

	1984	1999	2010	1984-1999	1999-2010	1984-2010
BL	79.98	185.38	233.75	105.39	48.38	153.77
Crp	2163.45	2590.37	2943.70	426.92	353.33	780.26
OT	2458.52	2706.12	2260.12	247.60	-446.01	-198.41
CT	1709.15	962.50	952.85	-746.64	-9.66	-756.30

Figure 25: Result of LULC classification and change area for subset # 2

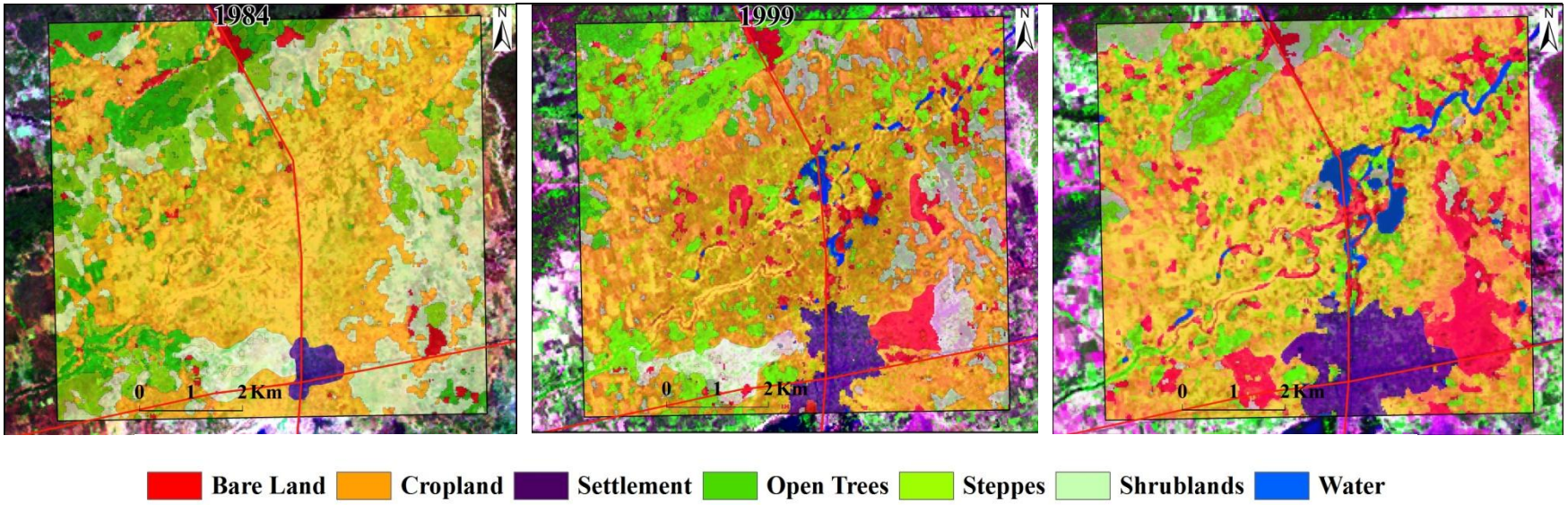

Figure 26: LULC change maps for subset area #1

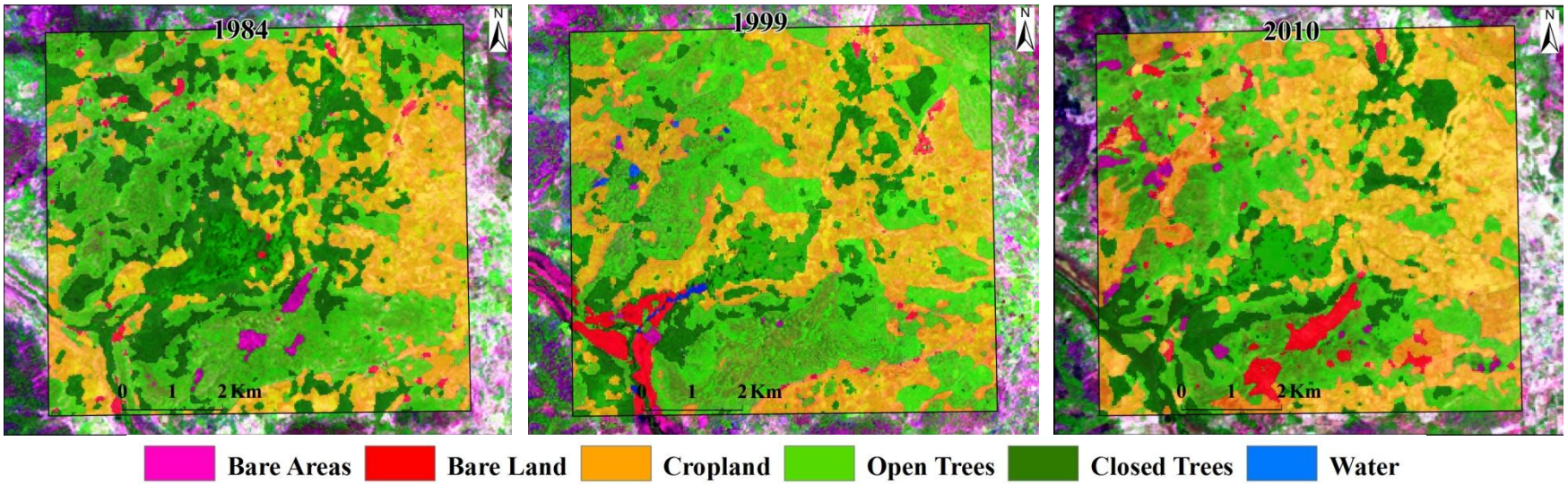

Figure 27: LULC change maps for subset #2

Moreover as shown in Figure 25 the order of magnitude of the spatial extent of the LULC categories in 1984 was almost the same for 1999. In 1999 the most extensive LULC was consistently Open Trees with 2706.12 ha (41.87%). It is followed by Cropland which covered around 2590.37 ha (40.07%). The Closed Trees and Bare Land covered respectively 962.50 ha (14.89%) and 185.38 ha (2.87%). The order of magnitude of the extent of coverage of the LULC changed a bit in 2010, with the most extensive cover being Cropland, which covered 2943.70 ha (45.54%), followed by Open Trees with 2260.12 ha (34.97%), Closed Trees with 952.85 ha (14.74%) and Bare Land with 233.75 ha (3.62%). Figure 25 also summarizes the overall change between LULC classes from 1984 to 2010. It can be seen from Figure 25 that Open Trees and Closed Trees decreased for 198.41 ha and 756.30 ha respectively between 1984 and 2010 while the Cropland and Bare Land increased for 780.26 ha and 153.77 ha.

Figure 29 shows the LULC change maps for the years 1986, 1999 and 2010 for the third subset area. As in subset 2, the LULC classes identified and mapped were Cropland, Bare Land, Open Trees and Closed Trees. Figure 28 shows that the most extensive LULC class in 1984 was Open Trees with 2968.47 ha (46.27%). This is followed by Closed Trees with 1409.59 ha (21.97%), Cropland with 323.33 ha (5.04%) and Bare Land with 102.95 ha (1.60%). 25.11 % of the area was burned representing 1610.85 ha so excluded from the statistics.

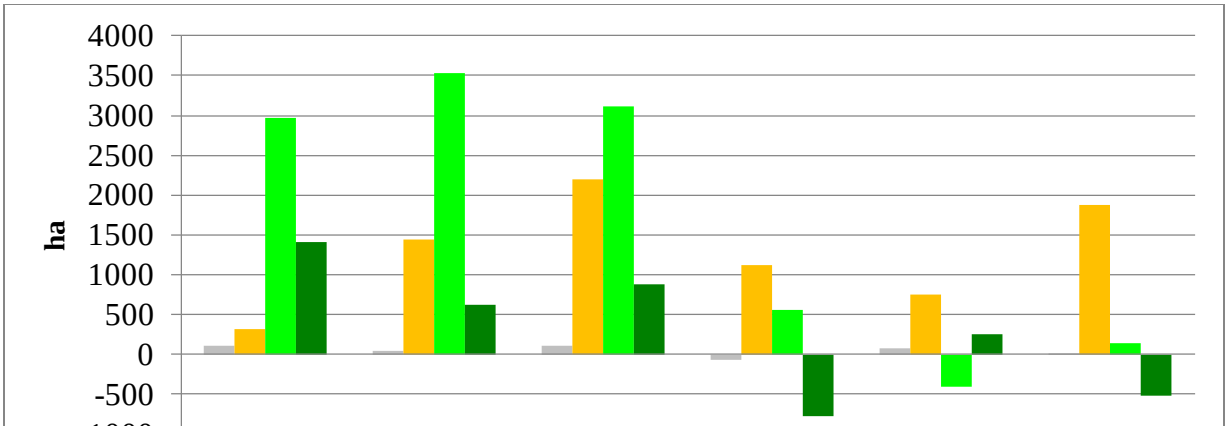

	1986	1999	2010	1986-1999	1999-2010	1986-2010
BL	102.95	35.34	111.90	-67.61	76.56	8.95
Crp	323.33	1437.04	2190.58	1113.71	753.54	1867.25
OT	2968.47	3529.59	3115.36	561.13	-414.24	146.89
CT	1409.59	628.69	886.17	-780.89	257.47	-523.42

Figure 28: Result of LULC classification and change area for the subset # 3

The spatial extent of LULC classes in 1986 was different from that in 1999. In 1999, the most extensive was always Open Trees with 3529.59 ha (55.02%). It was followed by the Cropland with 1437.04 ha (22.40%), the Closed Trees with 628.69 ha (9.80%) and Bare Land with 35.34 ha (0.55%) and 784.51 Burned (12.23%). The order and magnitude of the extent of coverage of the LULC in 1999 was different from 2010. The most extensive LULC class in 2010 remained Open Trees with 3115.36 ha (48.56%), followed by Cropland with 2190.58 ha (34.15%), Closed Trees 886.17 ha (13.81%) and Bare Land with 111.90 ha (1.74%). The overall change from 1986 to 2010 showed that Closed Trees lost 523.42 ha from its initial area in 1984. The Cropland increased for about 1987.25 ha and the Open Trees for 146.89 ha.

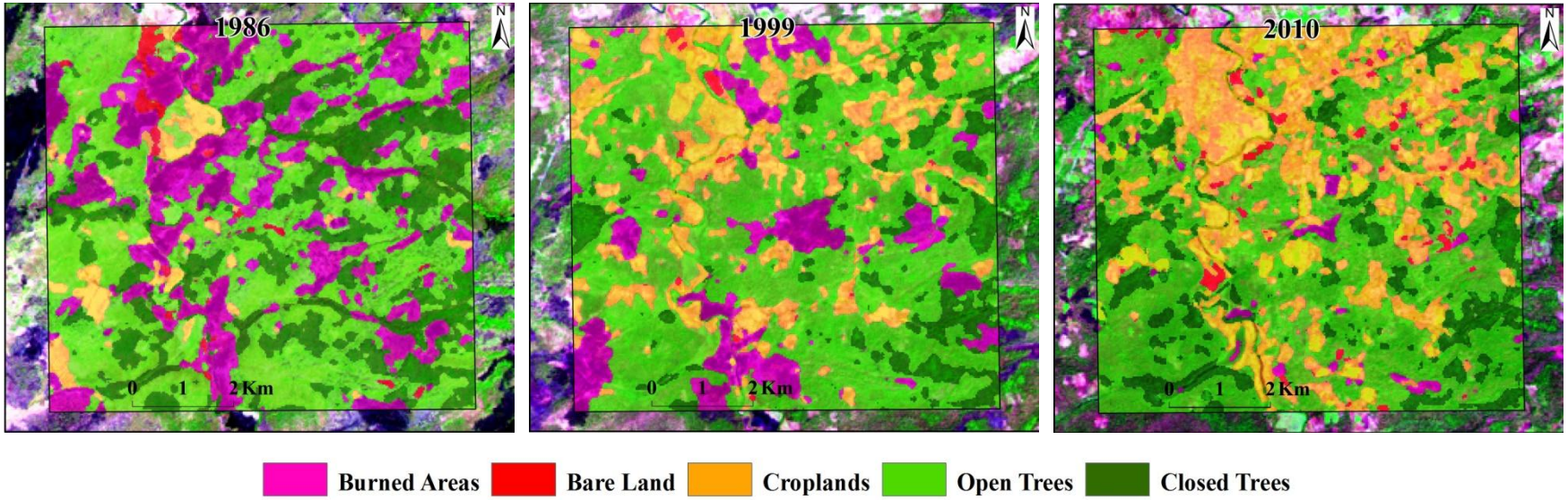

Figure 29: LULC changes maps for subset area #3

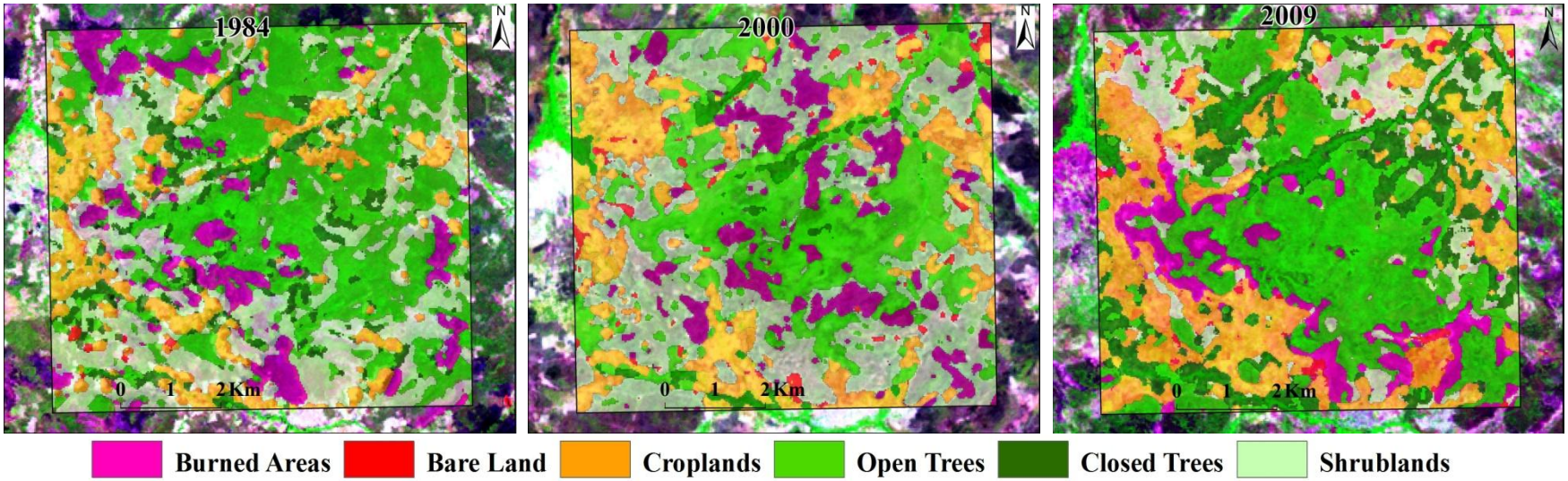

Figure 30: LULC changes maps for subset area #4

The result of LULC classification for subset (4) from 1984 to 2009 is presented in Figure 30. In this area five LULC categories were identified and mapped. These were Bare Land, Cropland, Open Trees, Closed Trees and Shrublands. Figure 31 showed that the most extensive LULC class in 1984 was Open Trees with 2224.53 ha (34.77%) followed by Shrublands with 1999.77 ha (31.26%), Cropland with 1004.28 ha (15.70%), Closed Trees with 541.40 ha (8.46%) and Bare Land with 16.20 ha (0.25%).

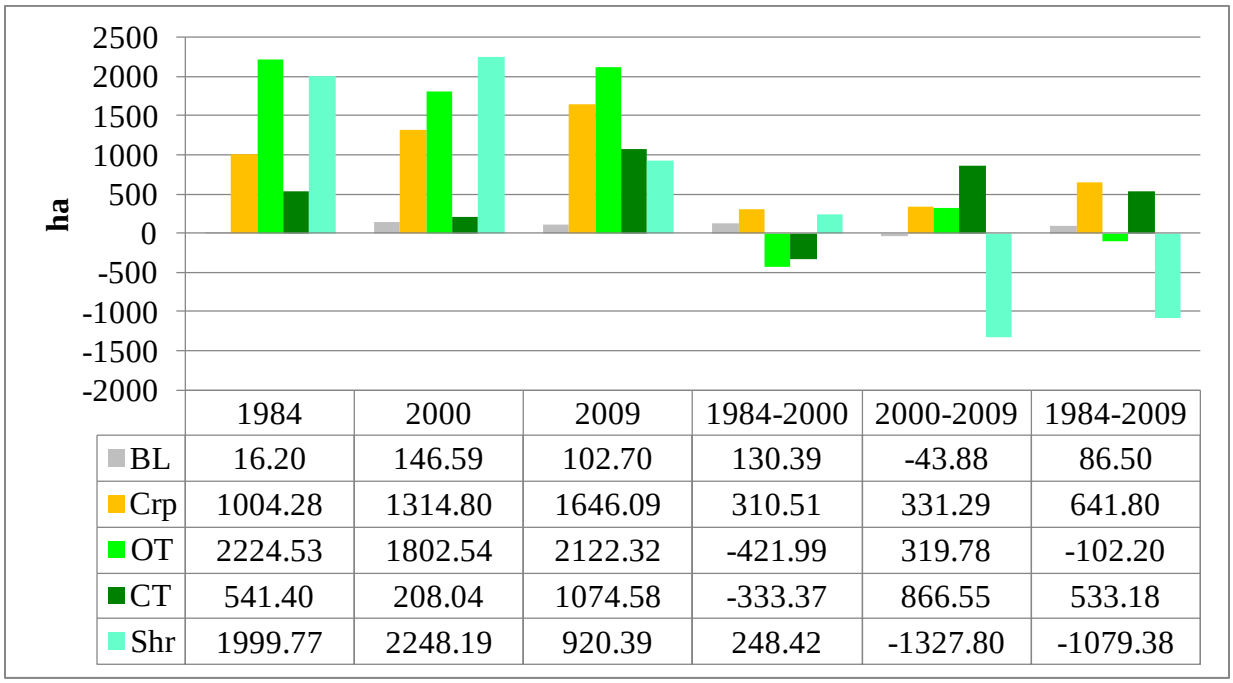

	1984	2000	2009	1984-2000	2000-2009	1984-2009
BL	16.20	146.59	102.70	130.39	-43.88	86.50
Crp	1004.28	1314.80	1646.09	310.51	331.29	641.80
OT	2224.53	1802.54	2122.32	-421.99	319.78	-102.20
CT	541.40	208.04	1074.58	-333.37	866.55	533.18
Shr	1999.77	2248.19	920.39	248.42	-1327.80	-1079.38

Figure 31: Result of LULC classification and change area for the subset #4

In 2000, the most dominant LULC class was Shrublands with 2248.19 ha (35.14%), followed by Open Trees with 1802.54 ha (28.18%), Cropland with 1314.80 ha (20.55%), Closed Trees with 208.04 ha (3.25%), and Bare Land with 146.59 ha (2.29%). 11.58% of the area (676.80 ha) was Burned (removed for the statistic). In 2009 Open Trees was the most dominant LULC with 2122.32 ha (33.18%) followed by Cropland with 1646.09 ha (25.73%), Closed Trees with

1074.58 ha (16.80%), Shrublands with 920.39 ha (14.39%), and Bare Land with 102.70ha (1.61%). Burned Area covered 530.86 ha (8.30%). The overall change from 1984 to 2009 showed that the Closed Trees and Open Trees classes decreased by 1079.38 ha and 102.20 ha respectively from their initial spatial extent of 1984.

8.5. Discussion

The rate of LULC changes in the references subset pixels within the Bani River Basin were determined using 30-meter Landsat data for 30-year monitoring period (1984/86 to 2009/10). The results confirm the potential of multi-temporal Landsat data to provide accurate and economical analyses of land cover change over time that can be used as input to land management, hydrological modelling as well policy decisions. Across subset common LULC change features include Cropland expansion, deforestation in all subsets, and urbanization.

Pattern and dynamics of LULC change differed markedly between the four subset areas. In subset 1, Cropland increased subsequently and occupied 59.5% of the subset in 2009. The second dominant land cover class was Bare Lands which include also Settlement covering 21.32% of the area in the same date. At the same time, Steppe and Shrublands decreased by respectively 501.09 ha and 904.84 from their initial value while Open Trees disappeared completely in 2009. In Subset 2, Cropland was the most dominant LULC class covering 45.54% of the box in 2010. Open Trees and Closed Trees formations decreased respectively by 199.41 ha and 756.30 ha between 1984 and 2010. In Subset 3, Open Trees was the dominant LULC class in 2010 and occupied 48.56 % of the total area in 2010. Cropland increased for 1867.25 ha, while Closed Trees decreased for 523.42 ha during the period 1986-2010. In subset 4, the major LULC class was Open Trees and occupied 33.18% of the total area, even though this class decreased by

102.20 ha between1984 and 2009. Cropland displayed an increase and occupied 25.73% of the total area in 2009. Closed Trees decreased for 533.18 ha while Shrublands decreased by 1069.38 ha during the same period.

The results indicated a general decrease in areas under natural vegetation and an increase in areas under agricultural land. These results are in conformity with Tappan and McGahuey, (2007) and Ruelland *et al.*, (2009). Ruelland *et al.*, (2009) observed that area under agricultural land increased over the last decades in the area. This increase in Cropland is in response to the increased demand of land to produce more food for the increasing human population.

According to Boakye *et al.*, (2008) changes in LULC are related to population growth and rainfall decline. It is highly unlikely that rainfall decline plays any major role in LULC change over the study area for the [1984/86-2009/10] period considered, which coincides with a fairly monotonic positive rainfall trend across West Africa. In contrast, there is considerable evidence that increasing anthropogenic pressure leads to significant impacts, both negative and positive, on terrestrial agro-ecosystems of the region.

9. LINKING CHANGE IN VEGETATION PRODUCTIVITY TO CLIMATE AND LULC CHANGES

9.1.Introduction

Vegetation productivity and land degradation are of global concern and have far reaching consequences for agricultural yields, biodiversity and as a whole the ability of a landscape to sustain ecosystem service provisions (Le *et al.*, 2012; Fensholt and Proud, 2012). Satellite derived vegetation productivity observations have a long heritage in global change studies (Le *et al.*, 2012; Lambin and Ehrlich., 1997). By linking the remote sensing phenology trend to concurrently available data metrics on rainfall and rate of LULC change, integrative assessments of vegetation responses to climate and anthropogenic activities can be effectively performed. In this section, statistical agreement between long-term trend in vegetation productivity, corresponding rainfall and rate of LULC change from Landsat time-series were used to discern and explain climate versus human induced vegetation cover change.

9.2. Quantification of land conversion

The land cover classes as defined in Chapter 8 were grouped to Cropland, natural vegetation, settlement and others. The Cropland represent the formations with or without scattered trees (canopy coverage 20%). These areas are characterized by annual crops (mainly millet, cotton and sorghum), harvested in October-November, followed by a period of bare soil with crop residues. Natural vegetation category regroups all areas with perennial or temporal vegetation cover that would have been growing in the absence of man. The categories “others” include area identified as burn area, water bodies/stream or bare land from the original classification. The settlement was not considered in subset 2; 3 and 4 because this class covered less than 1% of these areas.

To assess the change from one date to another, each raster cell from 1980/1986 was compared with the corresponding cell in the 1999/2000, the 1999/2000 with the 2009/2010 and the 1984/1986 with the 2009/2010 for the overall period. This procedure creates a table showing the initial value of each cell of 1984/1986 and the final value of each cell of 1999/2000 for the first period, and 1999/2000 to 2009/2010 for the second period. Similarly for the overall period, the initial value is 1984/1986 cell value and the final value is the 2009/2010 cell value (Table 13 to 15). Also a change matrix with initial year data in the rows and the final year data in the columns was created for the three periods (1984/1986-1999/2000); (1999/2000-2009/2010) and (1999/2000-2009/2010). In the matrix Tables the total at the beginning indicates the initial stage image total area of each LULC classes and the total end represents the final stage area of LULC classes. The difference is the total net change of the two time images. The negative image difference indicates that a certain LULC is in a state of decrement and the positive value indicates increment. The change indicates the total areas of each LULC classes that were transformed to other land cover types. In Tables 13 to 15, the values on the diagonal are the areas that had not changed during the period.

Table 13 showed the transformation of LULC types between 1984 and 2000. The image difference indicated that the vegetation decreased by 994.36 ha; 518.67ha; 219.97 ha and 499.79 ha respectively in subset 1 to 4 during this period. Settlement increased by 152.58 ha for subset 1 where it has been considered as a major LULC class. Cropland increased by 333.16 ha; 424.48 ha; 1114.21 ha and 298.30 ha respectively in subset 1 to 4. During this period in subset 1, vegetation cover lost 1375.59 ha in the profit of Cropland, 11.08 ha for settlement and 246.32 for the class ‘others’, the remaining unchanged area covered 1354.23 ha. It could be seen in the result that 554.05 ha have been converted from Cropland to vegetation cover, 144.67 ha for

settlement and 368.15ha for the class ‘others’. From the total area of vegetation cover in subset 2 during the same period, 1142.67 ha were converted to Cropland and 143.48 ha to ‘others’.

On the other hand the vegetation cover class and the ‘others’ class gained respectively 672.71 ha and 60.93 ha from Cropland. In subset 3; 782.98 ha from vegetation cover were converted to Cropland and 532.15 ha to others. From the Cropland initial area, 146.42 ha were converted to vegetation cover and 37.34 ha to ‘others’. In subset 4, the stable area for Cropland and vegetation were respectively 474.04 ha and 3343.14 ha. From vegetation covered initial area, 786.38 ha were converted to Cropland and 637.79 ha to ‘others’ while 454.47 ha and 84.08 ha were converted from Cropland to respectively vegetation cover and ‘others’.

Table 13: Conversion matrix of LULC types in the 4 subsets between 1984/1986 and 1999/2000 (ha).

Subset #1 (1984-1999)							Subset #2 (1984-1999)					
	Others	SETT	CRP	VG	Total. Beg.	Rate (%)	Others	SETT	CRP	VG	Total. Beg.	Rate (%)
Others	16.61	0.20	20.17	84.45	121.43	419.71	22.98	‘’	15.45	94.77	133.21	70.70
SETT	0.00	77.13	3.26	0.10	80.49	189.56	‘’	‘’	‘’	‘’	‘’	‘’
CRP	368.15	144.67	2207.91	554.05	3274.78	10.14	60.93	‘’	1431.10	672.71	2164.75	19.61
VG	246.32	11.08	1375.59	1354.23	2987.22	-33.29	143.48	‘’	1142.67	2880.58	4166.74	-12.45
Total End.	631.09	233.07	3606.94	1992.83	6463.93		227.40	‘’	2589.22	3648.08	6464.70	
Change	614.47	155.94	1399.09	638.60			204.42		1158.12	767.49		
Difference	509.65	152.58	332.16	-994.39			94.19		424.48	-518.67		

Subset #3 (1986-1999)							Subset #4 (1984-2000)					
Others	252.07	‘’	515.00	948.74	1715.81	-52.12	104.30	‘’	50.47	469.92	624.69	32.25
SETT	‘’	‘’	‘’	‘’	‘’	‘’	‘’	‘’	‘’	‘’	‘’	
CRP	37.34	‘’	139.37	146.42	323.14	344.81	84.08	‘’	474.04	454.47	1012.59	29.46
VG	532.15	‘’	782.98	3061.89	4377.02	-3.86	637.79	‘’	786.38	3343.17	4767.34	-10.48
Total End.	821.56	‘’	1437.35	4157.05	6415.96		826.17	‘’	1310.88	4267.56	6404.62	
Change	569.49		1297.98	1095.16			721.87		836.85	924.39		
Difference	-894.25		1114.21	-219.97			201.49		298.30	-499.79		

Table 14 showed the transformation of LULC types between 1999 and 2010. Vegetation decreased by 902.12 ha for the subset 1; 449.91 ha for the subset 2; 160.33 ha for the subset 3; 138.48 ha for the subset 4 respectively. Cropland increased by 240 ha for subset 1; 396.32 ha for subset 2; 758.50 ha for the subset 3 and 331.26 ha for subset 4. The increasing demand for cultivation of land must have contributed to the deterioration of natural vegetation.

Looking at the conversion matrix given in Table 13, of total areas under vegetation cover, 903.22 ha were transformed to Cropland, 36.19 ha to settlement and 323.55 to others, while 729.87 ha remained unchanged in subset 1 from 1999 to 2009. During the same period, 308.03 ha; 158.91 ha and 483.15 ha initially Cropland were converted respectively to vegetation cover, settlement and 'others'. In subset 2, of a total of vegetation cover in 1999, 1143 ha were converted to Cropland and 221.14 ha to 'others' while 2283.19 remained stable. In other hand the vegetation cover and others gained respectively 757.61 ha and 64.64 from Cropland initial area. From the initial area of vegetation cover in subset 3, 985.70 ha were converted to Cropland and 91.93 ha to others while the stable area covered 3079.42 ha. Cropland lost 386.39 ha to vegetation cover and 45.44 ha for others. For subset 4, the unchanged area for vegetation cover and Cropland were 3091.69 ha and 765.88 ha respectively. From the initial total of vegetation in 2000; 703.24 ha were converted to Cropland and 472.63 ha to others. Vegetation cover and others gained respectively 460.37 ha and 84.64 ha from Cropland initial area.

Table 14: Conversion matrix of LULC in the 4 subsets between 1999/2000 and 2009/2010 (area in ha).

Subset #1 (1999-2009)							Subset #2 (1999-2010)					
	Others	SETT	CRP	VG	Total. Beg.	Rate (%)	Others	SETT	CRP	VG	Total. Beg.	Rate (%)
Others	266.69	63.58	248.30	52.51	631.09	70.60	22.20	‘’	47.83	157.37	227.40	35.44
SETT	3.26	226.94	2.57	0.30	233.07	108.36	‘’	‘’	‘’	‘’	‘’	‘’
CRP	483.15	158.91	2656.85	308.03	3606.94	5.66	64.65	‘’	1766.97	757.61	2589.22	14.26
VG	323.55	36.19	903.22	729.87	1992.83	-45.27	221.14	‘’	1143.75	2283.19	3648.08	-12.33
Total End.	1076.66	485.63	3810.94	1090.70	6463.93		307.99	‘’	2958.54	3198.17	6464.70	
Change	809.97	258.68	1154.09	360.83			285.79		1191.57	914.98		
Difference	445.58	252.55	204.00	-902.13			80.59		396.32	-449.91		

Subset #3 (1999-2010)							Subset #4 (2000-2009)					
Others	86.02	‘’	204.63	530.91	821.56	-72.81	76.12	‘’	173.02	577.03	826.17	-23.33
SETT	‘’	‘’	‘’	‘’	‘’	‘’	‘’	‘’	‘’	‘’	‘’	‘’
CRP	45.44	‘’	1005.52	386.39	1437.35	52.77	84.64	‘’	765.88	460.37	1310.88	25.27
VG	91.93	‘’	985.70	3079.42	4157.05	-3.86	472.63	‘’	703.24	3091.69	4267.56	-3.24
Total End.	223.40	‘’	2195.84	3996.72	6415.96		633.39	‘’	1642.14	4129.08	6404.62	
Change	137.37		1190.33	917.30			557.27		876.26	1037.40		
Difference	-598.17		758.50	-160.33			-192.78		331.26	-138.48		

From the year 1984/86 to 2009/10 the LULC structure in the 4 reference areas obviously changed and reciprocal conversion between different types of LULC took place frequently. The dynamic of LULC in the subsets is characterised mainly by decrease of vegetation cover, increase of Cropland in all the subsets and increase of residential (settlement) in subset 1. The natural vegetation decreased from 2979.81 ha to 1088.46 ha for subset 1; from 4167.81 ha to 3216.6 ha for subset 2; from 4362.84 ha to 3998.52 ha for subset 3 and 4767.34 ha to 4129.08 ha for subset 4 (Table 15).

It could be observed from Table 15 that about 407.46 ha of vegetation were converted to Cropland, and settlement in subset 1. Out of the total 2979.81 ha, only 681.39 ha remained unchanged, 1708.38 ha converted to Cropland, 442.26 ha to others and 147.78 ha to settlement. Looking into Cropland, 2079.9 ha remained unchanged while 370.08 ha have been transformed to vegetation cover as a process of recovery, 576.81 ha to 'others' and 255.24 ha to settlement. In subset 2, of the total area of vegetation cover (4167.81 ha), 2593.08 ha remained unchanged, while 1357.38 ha have been converted to Cropland, and 217.35 ha to 'others'. From an initial total of 2165.31 ha, the unchanged area for Cropland covered 1548.63 ha, while 571.95 ha were converted to vegetation cover and 44.73 ha to 'others'. In subset 3, Cropland and 'others' gained respectively 1262.56 ha and 132.84 ha from vegetation cover, while 2962.44 ha remained unchanged. In subset 4, the unchanged area of vegetation cover was 3368.36 ha, while 1015.02 have been converted to Cropland and 383.97 ha to 'others'. From the total Cropland area at the initial stage (1012.29 ha), 410.65 have been converted to vegetation cover and 56.93 ha to 'others'.

Table 15: Overall (1980s-2009/10) matrix and rate of LULC conversion for the 4 subsets pixels

Subset #1 (1984-2009)							Subset #2 (1984-2010)					
	Others	SETT	CRP	VG	Total. Beg.	Rate (%)	Others	SETT	CRP	VG	Total. Beg.	Rate (%)
Others	55.35	0.63	27.54	36.99	120.51	791.56	45.18	‘’	34.47	51.57	131.22	134.15
SETT	0	80.55	0	0	80.55	501.12	‘’	‘’	‘’	‘’	‘’	‘’
CRP	576.81	255.24	2079.9	370.08	3282.03	16.22	44.73	‘’	1548.63	571.95	2165.31	35.79
VG	442.26	147.78	1708.38	681.39	2979.81	-63.47	217.35	‘’	1357.38	2593.08	4167.81	-22.82
Total End.	1074.42	484.2	3815.82	1088.46	6462.9		307.26	‘’	2940.48	3216.6	6464.34	
Change	1019.07	403.65	1735.92	407.07			262.08		1391.85	623.52		
Difference	282.86	403.65	533.79	-1891.35			176.04		775.17	-951.21		

Subset #3 (1986-2010)							Subset #4 (1984-2009)					
Others	79.74	‘’	793.08	850.41	1723.23	-87.01	192.50	‘’	82.11	350.07	624.69	1.39
SETT	‘’	‘’	‘’	‘’	‘’	‘’	‘’	‘’	‘’	‘'	‘’	‘’
CRP	11.25	‘’	133.02	185.67	329.94	564.86	56.93	‘’	545.01	410.65	1012.59	62.17
VG	132.84	‘’	1267.56	2962.44	4362.84	-8.35	383.97	‘’	1015.02	3368.36	4767.34	-13.39
Total End.	223.83	‘’	2193.66	3998.52	6416.01		633.39	‘’	1642.14	4129.08	6404.62	
Change	144.09		2060.64	1036.08			440.89		1097.13	760.72		
Difference	-1499.4		1863.72	-364.32			8.7		629.55	-638.27		

9.3. Overall rate of land conversion

Table 16 shows the rate of land conversion for the entire period of study. The vegetation index (NDVI) and the rainfall (RF) for the subset pixels were scored following their positive or negative trend**.** The general picture showed a decrease of vegetation cover in the 4 subsets pixel. The total area lost in natural vegetation cover was about 63.47% and 22.83% for subset 1 and 2 while it was 8.35% for the subset 3 and the subset 4 for 13.39%. The Cropland showed an increase pattern in all the areas. This was estimated as 564.86% for subset 3; 62.17% for subset 4; 35.79% for subset 2 and 16.22% for the subset 1. Except for the subset 3 where the class 'others' decreased for 87.01%, it increased for 791.12% for subset 1; 134.15% for subset 2 and only 1.39% for subset 4.

Table 16: NDVI and Rainfall trend associated with rate of LULC change in the 4 references area

			Land cover change in % (1984/86-2009/10)			
Sites #	NDVI	Rainfall	Others	Settlement	Cropland	Vegetation
Subset 1	-2	-2	791.56	501.12	16.22	-63.47
Subset 2	2	-2	134.15	0	35.79	-22.82
Subset 3	-2	2	-87.01	0	564.86	-8.35
Subset 4	2	2	1.39	0	62.17	-13.39

9.4. Development of statistical agreement between NDVI, Rainfall and LULC conversion

Spearman's rank correlation coefficients were generated between the long-term vegetation indexes (NDVI), rainfall (RF) and rate of LULC conversion during the study period to test the hypotheses that there exist associations between them. The rank correlation coefficient was used

because the data did not satisfy the normal distribution assumption. The values for the rank correlation coefficient range between -1 and +1, where -1 and +1 indicate a perfect negative and positive linear relationship between the ranks of the two variables. The vegetation and rainfall indexes for the subset pixels were scored following their positive or negative trend. Table 17 shows the statistical distribution of variables used in spearman rank correlation. The observation data consisted of the 4 subsets. Table 18 summarized the spearman correlation matrix between NDVI, RF and rate of LULC change for the selected subsets.

Table 17: Basic statistic of parameter used for correlation

Variables	Obs. without missing data	Minimum	Maximum	Mean	Std. deviation
NDVI	4	-2.000	2.000	0.000	2.309
Rainfall	4	-2.000	2.000	0.000	2.309
Others	4	-87.010	791.560	210.023	398.203
Settlement	4	0.000	501.120	125.280	250.560
Cropland	4	16.220	564.860	169.761	264.072
Vegetation	4	-63.470	-8.350	-27.007	25.038

Table 18: Spearman rank correlation matrix between NDVI, RF and rate of land cover change

Variables	NDVI	Rainfall
NDVI	1	0.000
Rainfall	0.000	1
Others (Bare land and Burn Area)	0.000	-0.894
Settlement	-0.577	-0.577
Cropland	0.000	0.894
Vegetation	0.000	0.894

According to Table 17, the spearman correlation confirmed a negative correlation but not significant at 0.05 between vegetation trend and increase in urbanisation. This suggested that an increase of human settlement impact negatively on vegetation production. The analysis

confirmed also a better correlation between Cropland and natural vegetation with rainfall trend. This means, an increase in rainfall was accompanied by an increase of vegetation productivity and Cropland area.

9.4 Discussion

In Subset 1, (negative NDVI anomaly), the general trend of human-induced change involve shifts from natural vegetation types to cultivation area and urban area. This subset is located along the national road Segou-Mopti or Segou Sikasso [x; y:-5.769163; 12.986464]. Vegetation is characterised by Steppes interspersed with annual herbaceous species. These Steppe areas are in general degraded. Locally Open Trees can be observed along the area. Agricultural activities are dense and concerns Cotton, the main cash crop, Sorghum, Millet and Maize. It should be noted that Bla, the main town of the area with 21915 habitants (RGPH, 2009) occupies a sizeable portion of this reference area. This city located at the junction of the national road Segou-Mopti and Segou-Sikasso, significantly increased in both size and population because of its strategic position. The statistics of temporal trajectories (Table 14), showed that 45% (2897.19 ha) in subset 1 did not change and 6% (407.07 ha) was changed by natural forces to vegetation between 1984 and 2009. The human-induced change occupied 49% (3158.6 ha), including cultivation (1735.92 ha) and urbanisation (403.65 ha), thus a case of human-induced vegetation productivity decline. This result is in agreement with Defries *et al.*, (2010), who mentioned urbanisation as one of the poles of vegetation degradation and more specifically of deforestation. Therefore, the decrease in vegetation cover and increase in agricultural land and urban area was consistent with the long-term trend in vegetation productivity for this subset, confirmed by the spearman rank of -0.57 on Table 18.

The subset 2 (positive NDVI trend) is located around Kignan, the main town in the area [x; y: -6.072697; 11.868181] and drained by the *Wenye* river, a tributary of Bani. The vegetation cover is mostly dominated by Open Trees (Open Woodland with shrubs) and Closed Trees (Woody Savannah). Agricultural activities are concentred on cash crop (cotton) and food cropping (sorghum, millet, maize and rice) in the rainy season. The particularity of this subset is the presence of an inland valley (about 328.28 ha) which is intensively used by the local people for Rice production during the season and Potato/ Sweet Potato in the dry season. From the statistic of conversion trajectories (Table 14), the non-change areas represent 64.8% (4186.83 ha); 9.7% (623.52 ha) were changed by natural forces to vegetation cover. The human-induced changes concerned about 25.5% (1653.93 ha in which 1391.85 ha to agricultural land). The intensive use of the valley land allowed having an important quantity of green biomass that might have influenced the long-term value of NDVI in the pixel, considered as a human-induced greening, confirmed with the spearman rank value of 0.89 (Table 18).

The subset 3, [x; y: -7.435937; 10.409089], a negative NDVI anomaly hot spot, is located along the border between Mali and Cote d'Ivoire and drained by the *Degou* river. Vegetation is characterised by Open Trees (Open Woodland with shrubs) and Closed Trees (Closed Woodland/ Woody Savannah or Open Forest). The agricultural activities are focussed on cereal production during the uni-modal rainy season. From the statistics on Table 14; 49.5% (3175.2 ha) of the total area have not changed during the period of study. The vegetation area recovery by natural process represents 16% (1036.08 ha). The human-induced change concerned 34.5% (2212.73 ha) in which 2060.64 ha have been converted to Cropland. Ruelland *et al.*, (2009) mentioned a decrease of the proportion of woody formation in the same agro climatic zone for about 55% during the period 1986-2007. The same authors reported a high dynamic of Cropland

caused by deforestation of new field and abandonment of old field. Most of the plots farmed in 1986 were no longer being formed in 2007. The decline in rainfall trend in the area during the last 30-year can be an explanation for such negative anomaly hot spot.

In subset 4, positive NDVI anomaly hot spot **[**x; y: -5.678636; 11.122660], the main vegetation cover are Open Trees (Open Woodland with shrubs) and Closed Trees (Closed Woodland/ Woody Savannah or Open Forest) and shrublands with various herbaceous species. Cotton, Maize, Sorghum and Millet are the main crop in the area. The results showed that the areas which have been unchanged during the study period represent 64% (4105.87 ha) of this reference area. The vegetation recovery area represent 11.90% (760.72 ha) while 24% (1538.02 ha) have been modified by human action (1097.13 ha converted to Cropland). Considering the rainfall trend (Chapter 5), this subset has experienced a significant positive trend that may impact the vegetation dynamic in the area.

10. CONCLUSIONS AND RECOMMENDATIONS

10.1. Conclusions

Analysis and monitoring of long-term vegetation dynamics still represents a challenge from the remote sensing point of view. Presence of clouds, high humidity and the particular dynamics of the land cover of such areas are challenging for mapping. Anthropogenic activities that modify the dynamics of these areas make comprehensive analysis more complex. As a result of the importance of vegetation cover in the carbon cycle and the high population pressures which impact it, it is important to have better methods to evaluate and monitor vegetation over a long period.

Long-term trend in NDVI and rainfall have been characterized using a MK trend test and the p-value for strongly significance estimation. The results showed a large area with positive NDVI trend mostly located in the central zone of the study area while areas with negative NDVI trend were observed in the Northern zone where natural vegetation has been significantly affected by human activities. Generally the rainfall pattern showed a positive trend for almost the entire study area but, only a few portions showed a significant positive trend. The study demonstrated that satellite based vegetation reflectance data can serve as a good proxy for studying variability and change of vegetation cover.

The relationships between NDVI and rainfall have been assessed by computing a Pearson correlation using monthly and long-term mean datasets. The study highlighted a high temporal variability of vegetation and rainfall in the study area during the last three decades. The phenology of vegetation is closely reflected by the seasonal cycle of rainfall. At monthly time

scale the results showed a good but not significant relationship between the two datasets at zero (0) time lag for the entire study area. The aggregated datasets showed a high correlation. The per-pixel based interannual anomaly of NDVI versus annual precipitation showed some similar pattern. The NDVI data revealed substantial sensitivity to the climatic signal both in time and space and allowed the investigation of the influence of climate and human activity.

Based on a supervised classification with maximum likelihood algorithm, multi-temporal Landsat images for 1984/86; 1999/00 and 2009/10 were classified to determine LULC change. The images were chosen for four (4) reference areas according to their long-term trend in both NDVI and rainfall. These areas were checked carefully to prove their anthropogenic or climatic cause. A multi-temporal post classification change detection algorithm was used to determine change in LULC for the three periods and a kappa statistic for accuracy assessment. The common LULC change features include Cropland expansion, urbanization and decrease in natural vegetation. The rate of change is different from one class to other and from one site to another.

Statistical agreements between long-term trends in vegetation productivity, corresponding rainfall and rate of LULC change from Landsat time-series imagery was used to discern climate versus human-induced vegetation cover change. Spearman correlation was used to assess the relationship between metrics of vegetation, rainfall trends and LULC categories. Human impact was seen to be a major driving force for changes in vegetation cover for some reference areas during the study period. As shown, the negative trends can be linked to conversion of vegetation cover to settlement and cultivated land as well. Changes in vegetation cover for other subsets are assumed to be a climate influenced vegetation cover changes. The positive trend in rainfall

condition during the past years has positively impacted these areas where the natural vegetation is still well represented. The study results improve the understanding of the nature and mechanisms of the ecosystem dynamics in the Bani River Basin and provide the basis for predicting changes in productivity that accompany changes in climate and human activity.

10.2. Recommendations

In the course of this research some issues were not addressed mainly due to resource and time constraints. A few of these issues are presented below for future research:

- The approaches used in this study showed usefulness and applicability, but require further validation and refinement, and ideally the inclusion of additional climatic and landscape components like temperature and soil types and soil degradation information.
- Earth observation can considerably contribute to the monitoring of vegetation conditions over time. The obtained remote sensing based results highlighted hotspots of significant change that need subsequent detailed investigation on the ground.
- Although the generation of NDVI time-series data using the MVC techniques was able to minimize the effect of clouds, the images can still be affected by the presence of clouds. It is possible to expect that the cloud free data over the long-term period would provide more stronger and realistic relationships between variables.
- It will be good to integrate population dataset into the analysis for in depth analysis of the role of population dynamics and pressure as drivers of vegetation conditions indicated by the NDVI.

REFERENCES

Abdi, H., (2007). Z-scores-In: N.J., Salkind (Ed): Encyclopedia of Measurement and Statistics. Sage, Thousand Oaks, pp 1057-1058.

Ahmedou, O.C.A., Nagasawa, R., Osman, A.E., Hattori, K., (2008). Rainfall variability and vegetation dynamics in the Mauritanian Sahel. Climate Research, 38, 78-81. doi: 10.3354/cr0077.

Almazroui, M., (2011), Calibration of TRMM rainfall climatology over Saudi Arabia during 1998–2009, Atmospheric Research, 99. 400-414.

Anyamba, A., and Tucker, C.J., (2005). Analysis of Sahelian vegetation dynamics using NOAA-AVHRR NDVI data from 1981-2003. Journal of Arid Environments 63, 596-614

Anyamba, A., Tucker, C.J., and Eastman, J.R. (2001). NDVI anomaly patterns over Africa during the 1997/98 ENSO warm event. International Journal of Remote Sensing, 22, 1847-1859.

Bajgiran, P.R., Darvishsefat, A.A., Khalili, A., Makhdoum, M.F., (2008). Using AVHRR-based vegetation indices for drought monitoring in the Northwest of Iran, Journal of Arid Environments 72, 1086-1096. doi:10.1016/j.jaridenv.2007.12.004.

Bartholome, E., and Belward, A.S., (2005). GLC2000: A new approach to global land cover mapping from Earth Observation data. International Journal of Remote Sensing, 26(9), 1959–1977.

Bayarjargal, Y., Karnieli, A., Bayasgalan, M., Khudulmur, S., Gandush, C., Tucker, C. J., (2006). A comparative study of NOAA-AVHRR derived drought indices using change vector analysis, Remote Sensing of Environment 105, 9-22, doi:10.1016/j.rse.2006.06.003.

Bégué, A., Vintrou, E., Ruelland, D., Claden, M., Dessay, N., (2011). Can a 25-year trend in Soudano-Sahelian vegetation dynamics be interpreted in terms of land use change? A remote sensing approach. Global Environmental Change, 21, 423-420.

Binns, T., (1990). Is Desertification a Muth? Geography, 75, 106-113.

Boakye, E., Odai, S.N., Adjei, K.A., Annor, F.O., (2008). Landsat Images for Assessment of the Impact of Land Use and Land Cover Changes on the Barekese Catchment in Ghana, European Journal of Scientific Research 22(2):269-278.

Broodryk, N.L., (2010). Long-term monitoring of vegetation dynamics in the Goegap Nature Reserve, Namaqualand, South Africa, Doctoral Thesis, University of Pretoria.

Brunet-Moret, Y., Chaperon, P., Lamagat, J.P., and Molinier, M. (1986). Monographie hydrologique du fleuve Niger. Niger Supérieur, Tome 1, ORSTOM Ed. Collection monographies hydrologiques 8, Paris, France. 260p.

Burgan, R.E., Hartford, R. A., Eidenshink, J.C., (1996). Using NDVI to assess departure from average greenness and its relation to fire business. General Technical Report INT-GTR-333.Ogden, UT: U.S. 12p.

Burt, T.P., (1994). Long-term study of the natural environment-perspective science of mindless monitoring? Progress in Physical Geography, 18, 475-496.

Butt, B., and Olson J.M., (2002). An approach to dual land use and land cover interpretation of 2001 satellite imagery of the eastern slopes of Mt. Kenya. Land use Change Impacts and Dynamics (LUCID) Project Working Paper 16. International Livestock Research Institute (ILRI), Nairobi, Kenya.

Camberlin, P., Martiny, N., Philippon, N., Richard, Y., (2007). Determinants of the interannual relationships between remote sensed photosynthetic activity and rainfall in tropical Africa, Remote Sensing of Environment, 106, 199-216.

Campbell, J.B., (1996). Introduction to remote sensing, 2nd edition, Taylor & Francis, London.

Chen, S. and Ravallion, M., (2004). How have the worlds poorest fared since the early 1980s? Policy Research Working Paper 3341. World Bank, Washington, DC:

Chen, Z., Ren, L. J., Gong, P., Zhang M., Wang L., Xiao S. and Jiang, D. (2008). Monitoring and management of agriculture with remote sensing. In; Shunlin L. (ed). Advances in Land Remote Sensing. Springer Science and Business Media B.V., USA 397-493.

Collet, L., (2010). Flow evolution in a large Sudano-Sahelian catchment under the constrain of climatic scenarios for the 21st century, Msc Thesis, Université Pierre et Marie Curie, Ecole des Mine de Paris et Ecole Nationale du Génie Rural des Eaux et Forets.

Congalton, R. G. and Green, K. (1999). Assessing the accuracy of remotely sensed data: Principles and Practices. Lewis Publishers.

Crawford, T., (2001). "Patterns of Change in Land Use, Land Cover, and Plant Biomass: Separating Intra- and Inter-annual Signals in Monsoon-driven Northeast Thailand". In: GIS and Remote Sensing and Applications in Biogeography and Ecology, Dordrecht: Kluwer Academic Publishers.

De Beurs, K.M., (2005). A statistical framework for the analysis of long image time series: the effect of anthropogenic change on land surface phenology, PhD dissertation, Faculty of The Graduate College, University of Nebraska.

De Beurs, K.M., and Henebry, G.M., (2004a). Land surface phenology, climatic variation, and institutional change: Analyzing agricultural land cover change in Kazakhstan, Remote Sensing of Environment, 89, 497-509.

De Beurs, K.M., and Henebry, G.M., (2004b). Trend Analysis of the Pathfinder AVHRR Land (PAL) NDVI Data for the deserts of Central Asia, IEEE Geosciences and Remote Sensing Letters, 1, No. 4, October 2004.

De Beurs, K.M., and Henebry, G.M., (2005a). A statistical framework for the analysis of long image time series, International Journal of Remote Sensing, 2005, 26(8), 1551-1573.

De Beurs, K.M., and Henebry, G.M., (2005b). Land surface phenology and temperature variation in the International Geosphere-Biosphere Program high latitude transects, Global Change Biology, (2005) 11, 779-790.

De Blij H.J., and Miller. P.O., (1996). Physical Geography of the Global Environment. John Wiley, New York. Pp. 290. :http://www.physicalgeography.net/fundamentals/9k.html. (Assessed the 18th Dec. 2014).

De Sherbinin, A., (2002). A CIESIN thematic guide to Land Use/ Land Cover change (LULC). Center for International Earth Science Information Network (CIESIN) Columbia University Palisades, NY, USA.

Defries, R.S., and Townshend, J.R., (1999). Global land cover characterization from satellite data: from research to operational implementation. Global Ecology and Biogeography, 8(5), 367-379.

Defries, R.S., Rudel, T., Uriarte, M., Hansen, M., (2010). Deforestation driven by urban population growth and agricultural trade in the twenty-first century, Nature Geosciences 3, 178-181.

Di Gregorio, A., (2005). Land Cover Classification System - Classification concepts and user manual for Software version 2. FAO, Rome, Italy.

Dietz, E.J., and Killeen, T.J., (1981). A nonparametric multivariate test for monotone trend with pharmaceutical applications, Journal of American Statistical Association, 76, 169-174.

Diouf, A., and Lambin, E.F., (2001). Monitoring land-cover changes in semi-arid regions: remote sensing data and field observations in the Ferlo, Senegal, Journal of Arid Environments, 48, 129-148.

Dirks, K.N., Hay, J.E., Stow, C.D., and Harris, D., (1998). High-resolution of rainfall on Norfolk Island, Part II: Interpolation of rainfall data, Journal of Hydrology 208, 187-193.

Easterling, W.E., Aggarwal, P.K,, Batima, P., Brander, K.M., Erda, L., Howden, S.M., Kirilenko, A., Morton, J., Soussana, J.F., Schmidhuber, J., Tubiello, F.N., (2007) .Chapter 5, Food, fibre and forestproducts". IN: Climate Change (2007): Impacts, Adaptation and Vulnerability. Contribution of Working Group II to the Fourth Assessment Report of the Intergovernmental Panel on Climate Change, M.L. Parry, O.F. Canziani, J.P. Palutikof, P.J. van der Linden and C.E. Hanson, Eds., Cambridge University Press, Cambridge, UK, pp. 273-313.

Ekpoh, I.J., Nsa, E., (2011). Extreme Climatic Variability in North-western Nigeria: An Analysis of Rainfall Trends and Patterns, Journal of Geography and Geology, 3, 1.

Erasmi, S., Schucknecht, A., Barbosa, M. O., Matschullat, J., (2014). Vegetation Greenness in Northeastern Brazil and its Relation to ENSO Warm Events, Remote Sensing, 6, 3041-3058; doi: 10.3390/rs6043041.

Evans, J., and Geerken, R., (2004). Discrimination between climate and human-induced dryland degradation, Journal of Arid Environments, 57, 535-554.

Fensholt R., Proud, S.R., (2012). Evaluation of Earth Observation based global long term vegetation trends - Comparing GIMMS and MODIS global NDVI time series, Remote Sensing of Environment,119, 131-147.

Fensholt, R., Rasmussen, K., Kaspersen P., Huber, S., Horion, S., Swinnen, E., (2013). Assessing Land Degradation/Recovery in the African Sahel from Long-Term Earth Observation based Primary Productivity and Precipitation Relationships, Remote Sensing, 5, 664-686, doi: 10.3390/rs5020664.

Fischer, G., Shah, M., Tubiello, F.N., van Velhuizen, H., (2005). Socio-economic and climate change impacts on agriculture: an integrated assessment, 1990-2080. Philosophical Transactions of the Royal Society B 360, 2067-2073.

Fleming, K., Awange, J.L., Kuhn, M., Featherstone, W.E., (2011). Evaluating the TRMM 3B43 monthly precipitation product using gridded rain gauge data over Australia, Australian Meteorological and Oceanographic Journal, 61, 171-184.

Forkuo, E.K., and Frimpong A., (2012). Analysis of Forest Cover Change Detection, International Journal of Remote Sensing Applications, 2(4), 82-92.

Franklin, J.F., (1989). Importance and justification of long-term studies in ecology. In: G.E Likens (ed.) Long-term studies in ecology: approaches and alternatives. Pp 3-19. Springer-Verlag, New York.

Friedl, M.A., McIver, D.K., Hodges, J.C.F., Zhang, X.Y., Muchoney, D., Strahler, A.H., Woodcork, C.E., Gopal, S., Schneider, A., Cooper, A., Baccini, F., Gao, F., Shaaf, C., (2002). Global land cover mapping from MODIS: algorithms and early results. Remote Sensing of Environment, 83(1-2), 287–302.

Fritz, S., and Belward, A., (2004). A new land-cover map of Africa for the year 2000. Journal of Biogeography, 31, 861–877.

Fritz, S., Bartholomé, E., Bleward, A., Hartley, A., Stibig, H.J., Eva, H., Mayaux, P., Bartalev, S., Latifovic, R., Kolmert, S., Roy, P., Agrawal, S., Bingfang, W., Wenting, X., Ledwith, M., Pekel, F.J., Giri, C., Mücher, S., de Badts, E., Tateishi, R., Champeaux, JL., Defourny, P., (2003). Harmonisation, mosaicing and production of the Global Land Cover 2000 database (Beta version). Office for official publications of the European communities, Luxembourg, EUR 20849 EN, 41 pp., ISBN 92-894-6332-5.

Getahun., Y.S., (2012). Spatial-temporal Analyses of Climate Elements, Vegetation Characteristics and Sea Surface Temperature Anomaly. A Case study in Gojam, Ethiopia. Master Thesis, University of Nova.

Globcover, 2009. Product description and validation report. 53 p

Goosse H., Barriat, P.Y., Lefebvre, W., Loutre, M.F., Zunz, V., (2010). Introduction to climate dynamics and climate modelling. Online textbook available at http://www.climate.be/textbook.

Hammond, R., McCullagh. P.S., (1982). Quantitative techniques in Geography-Clarendon Press, Oxford ISBN 0198740670, 364 pp.

Hansen, M.C., and Reed, B., (2000). A comparison of the IGBP DISCover and University of Maryland 1 km global land cover products. International Journal of Remote Sensing, 21(6), 1365-1373.

Hashemi, S.A., (2011). Investigation of Relationship Between Rainfall and Vegetation Index by Using NOAA/AVHRR Satellite Images, World Applied Sciences Journal, 14(11), 1678-1682.

Havstad, K.M., and Herrick, J.E., (2003). Long-term ecological monitoring. Arid Land Research and Management, 17, 389-400.

Hellden, U., (1991). Desertification – Time for An Assessment? Ambio, 20(8), 372-383.

Herold, M., Mayux, P., Woodcock, C.E., Baccini, A., Schmullius, C., (2008). Some challenges in global land cover mapping: An assessment of agreement and accuracy in existing 1 km datasets. Remote Sensing of Environment, 112, 2538-2556.

Herrmann, S. M., Ayamba, A., Tucker, C.J, (2005). Recent trends in vegetation dynamics in the African Sahel and their relationship to climate. Global Environmental Change 15, 394-404.

Hirsch, R.M., and Slack, J.R., (1984). A nonparametric trend test for seasonal data with serial dependence, Water Resources Research, 20, 727-732.

Hoaglin, D.C., Mosteller, F., and Tukey, J.W., (2000). Understanding Robust and Exploratory Data Analysis, pp. 160-170 (New York: John Wiley).

Hoeffding, W., (1948). A class of statistics with asymptotically normal distribution, Annals of Mathematical Statistics, 19, 293-325.

Holben, B.N., (1986). Characteristics of maximum-value composite images from temporal AVHRR data, International Journal of Remote Sensing, 7, 1417-1434.

Houghton, R.A., (1994). The worldwide extent of land use change, Bioscience, 44, 305-313.

Hountondji, Y, C., Sokpon, N., Ozer, P., (2006). Analysis of the vegetation trends using low resolution remote sensing data in Burkina Faso (1982-1999) for the monitoring of desertification, International Journal of Remote Sensing, 27(5), 871-884, doi: 10.1080/01431160500382782.

Huffman, G., Adler, R., Bolvin, D., Gu, G., Nelkin, E., Bowman, K., Hong, Y., Stocker, E., and Wolff, D,. (2007). The TRMM Multisatellite Precipitation Analysis (TMPA): Quasi-global, multiyear, combined-sensor precipitation estimates at fine scales, Journal of Hydrometeorology, 8(1), 38-55, doi:10.1175/JHM560.1.

Huffman, G., Adler, R., Rudolf, B., Schneider, U., and Keehn, P., (1995). Global precipitation estimates based on a technique for combining satellite based estimates, rain gauge analysis, and NWP model precipitation information, Journal of Climate, 8(5), 1284-1295.

Hulme, M., and Kelly, P.M., (1993). Exploring the linkages between climate change and desertification. Environment, 35: 4-11 and 39-45.

Jensen, J.R., (2005). Introductory digital image processing: a remote sensing perspective (third edition*)*. Prentice-Hall, Englewood Cliffs.

Justice, C. O., Townshend, J.R.G., Holben, B.N., Tucker, C.J., (1985). Analysis of the phenology of global vegetation using meteorological satellite data, International Journal of Remote Sensing, 6, 1271-1318.

Kendall, M.G., (1975). Rank Correlation Methods, Charles Griffin, London.

Kerr, J.T., and Ostrovsky, M., (2003). From space to species: ecological applications for remote sensing, TRENS in Ecology and Evolution, 18(6), 299-305.

Kogan, F.N., (1997). Global drought watch from space, Bulletin of the American Meteorological Society, 78: 621-636.

Koumare, I., (2014). Temporal/Spatial Distribution of Rainfall and Associated Circulation Anomalies over West Africa, Pakistan Journal of Meteorology, Vol.10.

Kowabata A., Ichi, K., Yamaguchi, Y., (2001). Global Monitoring of Inter-annual Changes in Vegetation Activities Using NDVI and its Relationship to Temperature and Precipitation. International Journal of Remote Sensing, 22, 1377-1382.

Kraus, E.B., (1977). Subtropical droughts and cross-equatorial energy transports. Monthly Weather Review, 105: 1009-1018.

Kulawardhana, R.W., (2008), Determination of spatio-temporal variations of vegetation cover, land surface temperature and rainfall and their relationships over Sri Lanka using NOAA AVHRR data. Master's Thesis, University of Peradeniya, Department of Agricultural Engineering, Sri Lanka.

Kummerow, C., Barnes, W., Kozu, T., Shiue, J., Simpson, J., (1998). The Tropical Rainfall Measuring Mission (TRMM) sensor package, Journal of Atmospheric and Oceanic Technology 15, 809-817.

Kummerow, C., Simpson, J., Thiele, O., Barnes, W., Chang, A.T.C., (2000). The status of the Tropical Rainfall Measuring Mission (TRMM) after two years in orbit, Journal of Applied Meteorology, 39, 1965-1982.

Lacaze, B., Toulouse, B., (2011). Green vegetation cover trends in Sahelian Western Africa observed from SPOT VGT 2001-2010, Geophysical Research Abstracts, 13, EGU2011-4043.

Lamb, P.J., (1979). Large-scale tropical Atlantic surface circulation patterns associated with sub-Saharan weather anomalies, Tellus, 30, 240-251.

Lambin E.F., Ehrlich, D., (1997). Land-cover Changes in Sub-Saharan Africa (1982-1991): Application of a Change Index Based on Remotely Sensed Surface Temperature and Vegetation Indices at a Continental Scale, Remote Sensing of Environment, 61, 181-200.

Landis, J. R. and Koch, G. G. (1977). The measurement of observer agreement for categorical data. Biometrics, 33, 159-174.

Landmann, T., Dubovyk, O., (2014). Spatial analysis of human-induced vegetation productivity decline over eastern Africa using a decade (2001–2011) of medium resolution MODIS time-series data, International Journal of Applied Earth Observation and Geoinformation 33, 76-82. http://dx.doi.org/10.1016/j.jag.2014.04.020

Latifovic, R., Zhu, Z-L., Cihlar, J., Giri, C., Olthof, I., (2004). Land cover mapping of North and Central America: Global land cover 2000, Remote Sensing of Environment, 89(1), 116-127.

Le Barbé, L., Lebel, T., Tapsoba, D., (2002). Rainfall Variability in West Africa during the Years 1950-90, Journal of Climate,15(2), 187-202.

Le, Q.B., Tamene, L., Vlek, P.L.G., (2012). Multi-pronged assessment of land degradation in West Africa to assess the importance of atmospheric fertilization in masking the processes involved, Global and Planetary Change, 92-93,71-81.

Li, B., Tao, S., Dawson R., W., (2002). Relations between AVHRR NDVI and ecoclimatic parameters in China, International Journal of Remote Sensing, 23(5), 989-999, doi: 10.1080/014311602753474192.

Li, J., Lewis, J., Rowland, J., Tappan, G., Tieszen, L.L., (2004). Evaluation of land performance in Senegal using multi-temporal NDVI and rainfall series, Journal of Arid Environments 59, 463-480.

Libiseller, C., and Grimvall, A., (2002). Performance of partial Mann-Kendall test for trend detection in the presence of covariates, Environmetrics, 13, 71-84.

Lillesand, T.M., Kiefer, R.W., (1994). Remote sensing and Image Interpretation. Third Edition, John Wiley and Sons, Inc., 750 pp.

Lloyd, C. D., (2005). Assessing the effect of integrating elevation data into the estimation of monthly precipitation in Great Britain, Journal of Hydrology, 308, 128-150.

Loveland, T.R., Reed, B.C., Brown, J.F., Ohlen, D.O., Shu, Z., Yang, L., Merchant, J.W., (2000). Development of a global land cover characteristics database and IGBP DISCover from 1 km AVHRR data, International Journal of Remote Sensing, 21(6), 1303-1330.

Lu, D., and Weng, Q., (2007). A survey of image classification methods and techniques for improving classification performance, International Journal of Remote Sensing, 28(5), 823-870

Lu, G.Y., and Wong, D.W., (2008). An adaptive inverse-distance weighting spatial interpolation technique, Computer and Geosciences 34, 1044-1055.

Lusch, D.P., (1999). Introduction to Environmental Remote Sensing, Centre for Remote Sensing and GIS, Michigan State University.

Ly, S., Charles, C., Degré, A., (2011) Geostatistical interpolation of daily rainfall at catchment scale: the use of several variogram models in the Ourthe and Ambleve catchments, Belgium, Hydrology and Earth System Sciences, 15, 2259-2274.

Manandhar, R., Odeh, I.O.A., Ancev, T., (2009). Improving the Accuracy of Land Use and Land Cover Classification of Landsat Data using Post-classification Enhancement. Remote Sensing, 1(3), 330-344.

Mann, H.B., (1945). Nonparametric Tests Against Trend, Econometrica, 13, 245-259.

Maley, J., (1980). Les changements climatiques de la fin du Tertiaire en Afrique : leur conséquence sur l'apparition du Sahara et de sa végétation, ORSTON Fonds Documentaire, 29(105), 63-86.

Martiny, N., Camberlin, P., Richard, Y., Philippon, N., (2006). Compared regimes of NDVI and rainfall in semi-arid regions of Africa. International Journal of Remote Sensing, 27, 5210-5223.

Masek J.G., Honzak M.M Goward S.N, Liu P., Pak E., (2001). Landsat-7 ETM+ as an observatory for land cover initial radiometric and geometric comparisons with Landsat-5 Thematic Mapper, Remote Sensing of Environment, 78, 118-130.

Mayaux, P., Bartholomé, E., Massart, M., VanCutSem, C., Cabral, A., Nonguierma, A., Diallo, O., Pretorius, C., Thompson, M., Cherlet, M., Pekel, J.F., Defourny, P., Vasconcelos, M., DiGregorio, A., Fritz, S., DeGrandi, G., Elvidge C., Vogt, E., Belward, A., (2003). A land cover map of Africa/Carte de l´occupation du sol de l´Afrique, Luxembourg, European Commission Joint Research Centre.

Milich, L., Weiss, E., (2000). GAC-NDVI interannual coefficient of–variation (CoV) images: ground truth sampling of the Sahel along north–south transects, International Journal of Remote Sensing, 21, 235-260.

Nellemann, C., MacDevette, M., Mander, T., Eickhout, B., Svihus, B., Prins, A.G., Kaltenborn, B.P., (2009). The Environmental Food Crisis. The Environment's Role in Averting Future Food Crises. A UNEP rapid response assessment. Norway, United Nations Environment Programme, GRID-Arendal.

Nemani, R., and Steve R., (1997). Land covers characterization using multi temporal red, near – IR and thermal-IR data from NOAA/AVHRR. Ecological applications, 7(1), 79-90.

Neeti, N., Rogan, J., Christman, Z., Easteman, R.J., Millones, M., Schneider, L.,Nickl, E., Schmook, B., Turner II, B.L., (2012). Mapping seasonal trends in vegetation using AVHRR-NDVI time series in the Yucatán Peninsula, Mexico, Remote Sensing Letters, 3(5), 433-442.

Nicholson, S., Some, B., McCollum, J., Nelkin, E., Klotter, D., Berte, Y., Diallo, B., Gaye, I., Kpabeba, G., Ndiaye, O., Noukpozounkou, J., Tanu, A., Thiam, A., Toure, A.A. and Traore, A., (2003). Validation of TRMM and other rainfall estimates with a high-density gauge dataset for West Africa: Part II: Validation of TRMM rainfall products, Journal of Applied Meteorology, 42(10), 1355-1368.

Nicholson, S.E., (2013). The West African Sahel: A review of Recent Studies on the Rainfall Regime and Its Interannual Variability, ISRN Meteorology, 2013, 32p. http://dx.doi.org/10.1155/2013/453521

Nicholson, S.E., and Farrar, T.J., (1994). The influence of soil type on the relationships between NDVI, rainfall and soil moisture in Semiarid Botswana. I. NDVI response to rainfall. Remote Sensing of Environment, 50: 107-120.

Nicholson, S.E., Some, B., Kone, B., (2000). An analysis of recent rainfall conditions in West Africa, including the rainy seasons of the 1997 E1 Nino and the 1998 La Nina years, Journal of Climate, 13, 2628-2640.

Nicholson, S.E., Tucker, C.J., Ba, M.B., (1998). Desertification, drought, and surface vegetation: an example from the West African Sahel, Bulletin of the American Meteorological Society, 79, 815-829.

O'Malley, R., and Wink, K., (2000). Forging a new tool for ecosystem reporting, Environment 42:21–31.

Onoz, B., Bayazit, M., (2003). The Power of Statistical Tests for Trend Detection, Turkish Journal of Engineering & Environmental Sciences 27(2003), 247-251.

Pickett, S.T.A., (1989). Long-term studies: past experience and recommendations for the future. In P.G. Risser (ed.) Long-term ecological research: an international perspective, 71-88. Scientific Committee on Problems of the Environment (SCOPE) 47. Wiley, Chichester.

Pidwirny, M., (2006). Characteristics of the Earth's Terrestrial Biomes, In: Fundamentals of Physical Geography, 2nd Edition. Available from: http://www.physicalgeography.net/fundamentals/9k.html

Pontius, R. G. (2000). Quantification error versus location error in comparison of categorical maps, Photogrammetric Engineering and Remote Sensing, 66(8), 1011-1016.

Propastin, P.A., Kappas, M., Muratova, N.R., (2008). A remote sensing based monitoring system for discrimination between climate and human-induced vegetation change in Central Asia, Management of Environmental Quality: An International Journal, 19(5), 579-596 http://dx.doi.org/10.1108/14777830810894256.

Propastin, P.A., Kappas, M., Muratova, N.R., (2006). Temporal Responses of Vegetation to Climatic Factors in Kazakhstan and Middle Asia, Shaping the Change XXIII FIG Congress Munich, Germany, October 8-13, 2006. https://www.fig.net/pub/fig2006/papers/ts65/ts65_03_propastin_etal_0493.pdf.

Qi, J., Cabot, F., Moran, S., Dedieu, G., (1995). Biophysical Parameter Estimations Using Multidirectional Spectral Measurements, Remote Sensing of Environment (54)71-83.

RGPH, (2009). 4eme Recensement Général de la Population et de l'Habitat, Mali, Résultats Définitifs Tome 0 : Répertoire des villages, 318p.

Richard, J., and Jia, X., (1999). Remote Sensing Digital Image Analysis. An Introduction, Third Revised Enlarged Edition, Springer-Verlag. Chapter 9, 229-244.

Richard, Y., and Poccard, I., (1998). A statistical study of NDVI sensitivity to seasonal and inter-annual rainfall variations in southern Africa, International Journal of Remote Sensing, 19: 2907-2920.

Richards, J., and Jia, X., (2006). Remote Sensing Digital Image Processing, An Introduction. 4th Edition, Heidelberg Springer-Verlag.

Ruelland, D., Ardoin-Bardin, S., Billen, G., Servat E., (2008a). Sensitivity of a lumped and semi-distributed hydrological model to several methods of rainfall interpolation on a large basin in West Africa, Journal of Hydrology, 361(1-2), 96-117.

Ruelland, D., Dezetter, A., Puech, C., Ardoin-Bardin, S., (2008b). Long-term monitoring of land cover changes based on Landsat imagery to improve hydrological modelling in West Africa. International Journal of Remote Sensing, 29(12), 3533-3551.

Ruelland, D., Levavasseur F., Tribotté, A., (2009). Patterns and dynamics of land-cover changes since the 1960s over three experimental areas in Mali. International Journal of Applied Earth Observation and Geoinformation, 12, 11-17 doi:10.1016/j.jag.2009.10.006.

Ruelland, D., Tribotte, A., Puech, C., Dieulin, C., (2011). Comparison of methods for LUCC monitoring over 50 years from aerial photographs and satellite images in a Sahelian catchment. International Journal of Remote Sensing 32(6), 1747-1777, doi: 10.1080/01431161003623433.

Salim, H.A., Chen, X., Gong, J., (2008). Analysis of Sudan vegetation dynamics using NOAA-AVRR NDVI data from 1982-1993, Asian Journal of Earth Sciences, 1, 1-15.

Schultz, P.A., and Halpert, M.S., (1995). Global analysis of the relationships among a vegetation index, precipitation and land surface temperature, International Journal of Remote Sensing, 16, 2755-2776.

Shiferaw, A., (2011), Evaluating the land use and land cover dynamics in Borena Woreda of South Wollo highlands, Ethiopia, Journal of Sustainable Development in Africa 13(1), 87-107.

Shige, S., Sasaki, H., Okamoto, K., Iguchi, T., (2006). Validation of rainfall estimates from the TRMM precipitation radar and microwave imager using a radiative transfer model: 1. Comparison of the version- 5 and -6 products, Geophysical Research Letters, 33(L13803), doi: 10.1029/2006GL026350.

Shrestha, R.P., (2008). Land use and climate change. API seminar series on Climate, Energy and Food Security in the Asia Pacific, Asian Institute of Technology, Bangkok.

Skidmore, A.K., (1999). Accuracy assessment of spatial information. In: Stein, A. van der Meer, F. and Gorte. B. (ed.). Spatial statistics for remote sensing Dordrecht, Kluwer Academic Publishers, Netherlands.

Snedecor, G.W., Cochran,W.G., (1980). Statistical Methods-Seventh Edition.-The Iowa State University Press, ISBN 0-8138-1560-6, 507 pp.

Solomon, S., Qin, D., Manning, M., Alley, R.B., Berntsen, T., Bindoff, N.L., Chen, Z., Chidthaisong, A., Gregory, J.M., Hegerl, G.C., Heimann, M., Hewitson, B., Hoskins, B.J., Joos, F., Jouzel, J., Kattsov, V., Lohmann, U., Matsuno, T., Molina, M., Nicholls, N., Overpeck, J., Raga, G., Ramaswamy, V., Ren, J., Rusticucci, M., Somerville, R., Stocker, T.F., Whetton, P., Wood R.A., and Wratt, D., (2007): Technical Summary. In: Climate Change 2007: The Physical Science Basis. Contribution of Working Group I to the Fourth Assessment Report of the Intergovernmental Panel on Climate Change [Solomon, S., D. Qin, M. Manning, Z. Chen, M. Marquis, K.B. Averyt, M. Tignor and H.L. Miller (eds.)]. Cambridge University Press, Cambridge, United Kingdom and New York, NY, USA.

Song, X., Saito, G., Kodama, M., Sawada, H., (2004). Early Detection System of Drought in East Asia Using NDVI from NOAA/AVHRR Data. International Journal of Remote Sensing, 25: 3105-3111.

Song, Y., Mingguo, M.A., Veroustraete, F., (2010). Comparison and conversion of AVHRR GIMMS and SPOT VEGETATION NDVI data in China, International Journal of Remote Sensing, 31, 9, 2377-2392.

South African Environmental Observation Network (SAEON). (2004). South African Environmental Observation Network Review: An eye on our changing world, National Research Foundation, Pretoria.

Story, M., and Congalton, R.G., (1986). Accuracy assessment: a user's perspective, Photogrammetric Engineering and Remote Sensing, 52 (3): 397-399.

Sultan, B., and Janicot, S., (2000). An abrupt shift of the ITCZ over West Africa and intra-seasonal variability, Geophysical Research Letters, 2, 3353-3356.

Symeonakis, E., and Drake, N., (2004). Monitoring Desertification and Land Degradation Over Sub-Saharan Africa, International Journal of Remote Sensing, 25, 573-592.

Tabari, H., Marofi, S., Aeini, A., Talaee, P.H., Mohammadi, K., (2011). Trend Analysis of Reference Evapotranspiration in the Western half of Iran, Agricultural and Forest Meteorology 151, 128-136.

Tappan, G., Cushing, M., (2004). Use of SLC-Off Landsat Image Data for Monitoring Land Use/Land Cover Trends in West Africa, USGS, EROS Data Centre, SIOUX Falls, SD, http://www.ga.gov.au/image_cache/GA6007.pdf.

Tappan, G., McGahuey, M., (2007). Tracking environmental dynamics and agricultural intensification in southern Mali, Agricultural Systems, 94, 38-51.

Tateishi, R., and Ebata, M., (2004). Analysis of phonological change patterns using 1982-2000 Advanced Very High Resolution Radiometer (AVHRR) data, International Journal of Remote Sensing, 25: 2287-2300.

Teegavarupu, R. and Chandramouli, V., (2005). Improved weighting methods, deterministic and stochastic data driven models for estimation of missing precipitation records, Journal of Hydrology, 312, 191-206.

TerrAfrica, (2009). The Role of Sustainable Land Management (SLM) for Climate Change Adaptation and Mitigation in Sub-Saharan Africa (SSA), Land and Climate, Issue Paper, A TerrAfrica partnership publication, 127 pp., April.

Tottrup, C. and Rasmussen, M. S. (2004). Mapping long-term changes in savannah crop productivity in Senegal through trend analysis of time series of remote sensing data. Agriculture, Ecosystems and Environment, 103(3), 545-560.

Tucker C.J, Newcomb, W.W., Los S.O, Prince S.D, (1991). Mean and inter-year variation of growing-season normalized difference vegetation index for the Sahel 1981-1989, International Journal of Remote Sensing, 12, 1133-1135.

Tucker C.J., and Sellers. P.J., (1986). Satellite remote sensing of primary vegetation, International Journal of Remote Sensing, 7, 1395-1416.

Tucker, C.J., and Nicholson S.E., 1999. Variations in the size of the Sahara Desert from 1980-1997. Ambio, 28. 587-591.

Vicente-Serrano S.M., Cuadrat-Prats, J.M., Romo, A., (2006). Aridity–influence on vegetation patterns in the middle Ebro-Valley (Spain): evaluation by means of AVHRR images and climate interpolation techniques, Journal of Arid Environ, 66, 353-375.

Vlek, P., Le, Q.B., Tamene, L., (2008). Land decline in Land-Rich Africa- A creeping disaster in the making. Rome, Italy. CGIAR Science Council Secretariat.

Wang J., Rich P. M., Price K.P., (2003). Temporal responses of NDVI to precipitation and temperature in the central Great Plains, USA, International Journal of Remote Sensing, 24, 2345-2364.

Wang, J., Price, K.P., Rich. P.M., (2001). Spatial patterns of NDVI in response to precipitation and temperature in the central Great Plains, International Journal of Remote Sensing, 22, 3827-3844.

Weiss J.L., Gutzler, D.S., Coonrod, J.E.A., Dahm. C.N., (2004). Long-Term Monitoring With NDVI in a Diverse Semi-Arid Setting Central New Mexico, USA, Journal of Arid Environment, 58, 248-274.

Weiss, D.J., and Walsh, S.J., (2008). Remote Sensing of Mountain Environments; University of North Carolina at Chapel Hill: Geography Compass, 3(1), 1-21.

Weiss, E., and Milich, L., (1997). Errors in a standard method for generating interannual NDVI coefficient of variation (CV) images, International Journal of Remote Sensing, 18, 3743-3748.

Wessels, K.J., Prince, S.D., Frost, P.E. and VanZyl, D., (2004). Assessing the effects of human-induced land degradation in the former homelands of northern South Africa with a 1-km AVHRR NDVI time-series, Remote Sensing of Environment, 91, 47-67.

Wessels, K.J., Prince, S.D., Malherbe, J., Small. J., Frost, P.E., and VanZyl, D., (2007). Can human-induced land degradation be distinguished from the effects of rainfall variability? A case study of South Africa, Journal of Arid Environments, 68, 271-297.

Westman, W.E., (1985). Ecology, impact assessment, and environmental planning. New York, NY: John Wiley and Sons. 532 p.

WMO, (2005). Climate and Land Degradation. World Meteorological Organization, WMO-No. 989, Geneva, Switzerland.

WMO., (2011). Frequently Asked Questions (FAQs). World Meteorological Organization, Commission for Climatology. http://www.wmo.int/pages/prog/wcp/ccl/faqs.html (accessed 20/09/2014).

Woodwell, G. M. (ed.). (1984). The Role of Terrestrial Vegetation in the Global Carbon Cycle: Measurement by Remote Sensing, SCOPE 23. John Wiley and Sons, New York.

Xu, X., Piao, S., Wang, W., Chen, A., Ciais, P., Myneni, R.B., (2012). Spatio-temporal patterns of the area experiencing negative vegetation growth anomalies in China over the last three decades, Environmental Research Letters, 7, 035701 (9pp).

Yang, L., Wylie, B., Tieszen, L. L., Reed, B. C., (1998). An analysis of relationships among climate forcing and time-integrated NDVI of grasslands over the U.S. Northern and Central Great Plains, Remote Sensing of the Environment, 65, 25-37.

Yin, H., Udelhoven, T., Fensholt, R., Pflugmacher, D., Hostert, P., (2012). How Normalized Difference Vegetation Index (NDVI) Trends from Advanced Very High Resolution Radiometer (AVHRR) and Système Probatoire d'Observation de la Terre VEGETATION (SPOT VGT) Time Series Differ in Agricultural Areas: An Inner Mongolian Case Study, Remote Sensing, 4, 3364-3389.

Zhang, G., Zhang, Y., Dong, J., Xiao, X., (2013). Green-up dates in the Tibetan Plateau have continuously advanced from 1982 to 2011. Edited by Robert E. Dickinson, The University of Texas at Austin, Austin, TX, and approved February 1, 2013 (received for review June 18, 2012)

Zhang, J., Niu, J., Bao, T., Buyantuyev, A., Zhang, Q., Dong, J., Zhang, X., (2014). Human induced dryland degradation in Ordos Plateau, China, revealed by multilevel statistical modelling of normalized difference vegetation index and rainfall time-series, Journal of Arid Land, 6(2): 219-229. doi: 10.1007/s40333-013-0203-x

Zubair, A. O., (2006). Change detection in land use and land cover using remote sensing data and GIS: A case study of Ilorin and its environs in Kwara State. Master's thesis, Department of Geography, University of Ibadan, Ibadan.

APPENDIX

Assessing Long-Term Trends In Vegetation Productivity Change Over the Bani River Basin in Mali (West Africa)

Journal of Geography and Earth Sciences
December 2014, Vol. 2, No. 2, pp. 01-19
ISSN 2334-2447 (Print) 2334-2455 (Online)

Published by American Research Institute for Policy Development
DOI: 10.15640/jges.v2n2a2
URL: http://dx.doi.org/10.15640/jges.v2n2a2